ผลของเอ็น-(2-ไฮดรอกซีโพรพิล)-3-ไตรเมทิลแอมโมเนียมไคโตซานคลอไรด์ชนิดที่มีมวลโมเลกุลสูงต่อความสมบูรณ์ของผนังกั้นของเซลล์คาโค-2 ที่เพาะเลี้ยงชั้นเดียว

นางสาวรัตน์จิกา วงศ์วนากุล

วิทยานิพนธ์นี้เป็นส่วนหนึ่งของการศึกษาตามหลักสูตรปริญญาวิทยาศาสตรดุษฎีบัณฑิต
สาขาวิชาเภสัชศาสตร์ชีวภาพ ภาควิชาชีวเคมีและจุลชีววิทยา
คณะเภสัชศาสตร์ จุฬาลงกรณ์มหาวิทยาลัย
ปีการศึกษา 2559

EFFECTS OF HIGH MOLECULAR WEIGHT N-(2-HYDROXYPROPYL)-3-TRIMETHYLAMMONIUM CHITOSAN CHLORIDE ON THE BARRIER INTEGRITY OF CACO-2 MONOLAYER

Miss Ratjika Wongwanakul

A Dissertation Submitted in Partial Fulfillment of the Requirements
for the Degree of Doctor of Philosophy Program in Biopharmaceutical Sciences
Department of Biochemistry and Microbiology
Faculty of Pharmaceutical Sciences
Chulalongkorn University
Academic Year 2016

Thesis Title	EFFECTS OF HIGH MOLECULAR WEIGHT N-(2-HYDROXYPROPYL)-3-TRIMETHYLAMMONIUM CHITOSAN CHLORIDE ON THE BARRIER INTEGRITY OF CACO-2 MONOLAYER
By	Miss Ratjika Wongwanakul
Field of Study	Biopharmaceutical Sciences
Thesis Advisor	Associate ProfessorSuree Jianmongkol, Ph.D.
Thesis Co-Advisor	Sasitorn Aueviriyavit, Ph.D.

Accepted by the Faculty of Pharmaceutical Sciences, Chulalongkorn University in Partial Fulfillment of the Requirements for the Doctoral Degree

.....Dean of the Faculty of Pharmaceutical Sciences
(Assistant ProfessorRungpetch Sakulbumrungsil, Ph.D.)

THESIS COMMITTEE

.....Chairman
(Associate ProfessorThongchai Sooksawate, Ph.D.)

.....Thesis Advisor
(Associate ProfessorSuree Jianmongkol, Ph.D.)

.....Thesis Co-Advisor
(Sasitorn Aueviriyavit, Ph.D.)

.....Examiner
(Associate ProfessorManeewan Suksomtip, Ph.D.)

.....Examiner
(Chatchai Chaotham, Ph.D.)

.....External Examiner
(Rawiwan Maniratanachote, Ph.D.)

รัตน์จิกา วงศ์วนากุล : ผลของเอ็น-(2-ไฮดรอกซีโพรพิล)-3-ไตรเมทิลแอมโมเนียมไคโตซานคลอไรด์ชนิดที่มีมวลโมเลกุลสูงต่อความสมบูรณ์ของผนังกั้นของเซลล์คาโค-2 ที่เพาะเลี้ยงชั้นเดียว (EFFECTS OF HIGH MOLECULAR WEIGHT N-(2-HYDROXYPROPYL)-3-TRIMETHYLAMMONIUM CHITOSAN CHLORIDE ON THE BARRIER INTEGRITY OF CACO-2 MONOLAYER) อ.ที่ปรึกษาวิทยานิพนธ์หลัก: รศ. ภญ. ดร.สุรีย์ เจียรณ์มงคล, อ.ที่ปรึกษาวิทยานิพนธ์ร่วม: ภญ. ดร.ศศิธร เอื้อวิริยะวิทย์{, 104 หน้า.

ระบบนำส่งยาถูกนำมาใช้ในการพัฒนาการดูดซึมยาที่มีปัญหาทางด้านการละลายและความไม่เสถียรที่ให้ทางการรับประทาน ในบรรดาพอลิเมอร์สังเคราะห์ที่จะนำมาใช้เป็นตัวนำส่งยา 600-HPTChC มีความน่าสนใจเนื่องจากเป็นไคโตซานที่ผ่านการเปลี่ยนแปลงโครงสร้างโดยกระบวนการ quaternization ให้มีคุณสมบัติเพิ่มการละลายในน้ำโดยยังคงคุณสมบัติการยึดเกาะกับเยื่อเมือก อย่างไรก็ดี คุณสมบัติความเข้ากันได้ของเนื้อเยื่อในร่างกายและ กลไกการแพร่ผ่านในเซลล์และระหว่างเซลล์ลำไส้ของ 600-HPTChC ยังไม่ทราบแน่ชัด ในการศึกษานี้จึงมีวัตถุประสงค์เพื่อศึกษาผลของ 600-HPTChC ต่อ cell proliferation และ differentiation รวมทั้งศึกษาผลและกลไกของ 600-HPTChC ต่อการเพิ่มการดูดซึมทั้งภายในเซลล์และระหว่างเซลล์โดยใช้เซลล์เพาะเลี้ยง Caco-2 ซึ่งเป็นโมเดลของเซลล์ลำไส้เล็กในการทดสอบ

จากผลการทดลองพบว่า 600-HPTChC ที่ถูกแทนที่ด้วย Quat-188 ในอัตราส่วนที่ต่ำมีผลต่อความเป็นพิษและยับยั้ง proliferation ของเซลล์เพาะเลี้ยง Caco-2 น้อยกว่าการแทนที่ Quat-188 ในอัตราส่วนที่สูง โดยผลของสารต่อการยับยั้ง cell proliferation อาจไปรบกวน cell cycle ซึ่งส่งผลต่อเนื่องต่อ differentiation ของเซลล์ Caco-2 เมื่อให้สารติดต่อกันเป็นระยะเวลา 9 วัน แต่เมื่อลดระยะเวลาการให้สารเป็น 4 ชั่วโมงต่อวัน เพื่อเลียนแบบระยะเวลาที่สารอยู่ในลำไส้เล็ก โดยยังให้ต่อเนื่องเป็นระยะเวลา 9 วัน กลับพบว่า 600-HPTChC ไม่มีผลต่อ differentiation ของเซลล์ สำหรับผลของสารต่อการแพร่ผ่านระหว่างเซลล์ พบว่า 600-HPTChC มีประสิทธิภาพเพิ่มการแพร่ผ่านระหว่างเซลล์ได้ดีกว่าไคโตซาน จากระยะเวลาในการเปิดและปิดของ tight junction ที่สั้นกว่า สำหรับผลของสารต่อการแพร่ผ่านในเซลล์ พบว่า 600-HPTChC เพิ่มการดูดซึมยา โดยผลที่เกิดขึ้นมาจากการยับยั้งการทำงานของ P-gp และไม่มีผลต่อการเปลี่ยนแปลงทางด้านการแสดงออกของปริมาณโปรตีนและ mRNA ของ P-gp นอกจากนี้ภาพจาก Immunofluorescence ยืนยันการจับกันระหว่าง 600-HPTChC กับ P-gp ที่แสดงออกบนพื้นผิวทางด้าน apical ซึ่งการจับกันดังกล่าวอาจจะส่งผลกระตุ้นการทำงานของ P-gp ATPase ทำให้เกิดการเปลี่ยนแปลงโครงสร้างของ P-gp และส่งผลลดการขับยาออกจากเซลล์ลำไส้ โดยผลการศึกษานี้สนับสนุนการนำ 600-HPTChC มาพัฒนาต่อเพื่อใช้เป็นตัวนำส่งยาผ่านการรับประทาน

ภาควิชา	ชีวเคมีและจุลชีววิทยา	ลายมือชื่อนิสิต .....
สาขาวิชา	เภสัชศาสตร์ชีวภาพ	ลายมือชื่อ อ.ที่ปรึกษาหลัก .....
ปีการศึกษา	2559	ลายมือชื่อ อ.ที่ปรึกษาร่วม .....

5576456033 : MAJOR BIOPHARMACEUTICAL SCIENCES
KEYWORDS: 600-HPTCHC, CACO-2, BIOCOMPATIBILITY, TIGHT JUNCTION, PERMEABILITY, 104 P-GLYCOPROTEIN

RATJIKA WONGWANAKUL: EFFECTS OF HIGH MOLECULAR WEIGHT N-(2-HYDROXYPROPYL)-3-TRIMETHYLAMMONIUM CHITOSAN CHLORIDE ON THE BARRIER INTEGRITY OF CACO-2 MONOLAYER. ADVISOR: ASSOC. PROF.SUREE JIANMONGKOL, Ph.D., CO-ADVISOR: SASITORN AUEVIRIYAVIT, Ph.D.{, pp.

Development of poorly soluble and unstable peptide drugs using drug delivery system has been introduced to improve drug bioavailability via oral administration. Among the oral drug carriers interested in synthetic polymers, 600-HPTChC is the modified chitosan with quaternization process to improve solubility without any effect on the mucoadhesive property of core chitosan. However, the biocompatibility of 600-HPTChC on human intestine and its mechanism on paracellular and transcellular transport remained to be unknown. The purposes of this study were therefore to determine the effects of 600-HPTChC on intestinal cells in aspects of cell proliferation and cell differentiation and to examine the potential effects of 600-HPTChC on improvement of drug bioavailability through paracellular and transcellular pathway using Caco-2 cells as an *in vitro* intestinal model.

The results demonstrated that lower degree of substitution of 600-HPTChC caused lower cytotoxic and anti-proliferative effect on Caco-2 cells comparing to the higher degree of substitution. In addition, anti-proliferative effect of 600-HPTChC might be involved by cell cycle disturbance further causing differentiation delay of the Caco-2 cells after the continuous exposure for 9 days. However, 4 h/day exposure over 9 days, more realistically mimics the daily intestinal exposure, could attenuate the effect of 600-HPTChC on intestinal differentiation. In paracellular pathway, 600-HPTChC was much more efficient than chitosan in both aspects of opening rate and time recovery of tight junction protein. The results also suggested that the mechanism behind the tight junction opening might result from the direct interaction between 600-HPTChC and tight junction protein rather than via intracellular signaling investigated. In transcellular pathway, 600-HPTChC was able to increase the drug absorption by P-gp inhibition without any change in the expression level. Immunofluorescent images indicated that 600-HPTChC could directly bind to P-gp on plasma membrane. Furthermore, the results of P-gp ATPase assay demonstrated that 600-HPTChC acts as the stimulator of P-gp ATPase that might relate to conformation change of P-gp epitope. Overall data support the usefulness of 600-HPTChC as a drug carrier in development of the oral drug delivery system.

Department:	Biochemistry and Microbiology	Student's Signature	.....
Field of Study:	Biopharmaceutical Sciences	Advisor's Signature	.....
Academic Year:	2016	Co-Advisor's Signature	.....

ACKNOWLEDGEMENTS

I would like to express my deepest gratitude and appreciation to my thesis advisor, Associate Professor Suree Jianmongkol, Ph.D., for her valuable guidance, encouragement, understanding, and contribution throughout this study.

I would like to express my sincere appreciation to my thesis co-advisor, Sasitorn Aueviriyavit, Ph.D., for her assistant, supporting, valuable advice, patience and kindness.

I also would like to thank all thesis committees for their valuable comments, suggestions and helpful discussion.

My appreciation goes to the Pharmaceutical Research Instrument Center, Faculty of Pharmaceutical Sciences, Chulalongkorn University and Nano Safety and Risk Assessment Laboratory, National Nanotechnology Center (NANOTEC) for providing research instruments and supporting chemicals and Dr. Warayuth Sajomsang and Miss Pattarapond Gonil (Nanoengineered Soft Materials for Green Environment Laboratory, NANOTEC) for kindly providing the synthesized chitosan and derivatives.

I also would like to thank Professor Kan Chiba, Assistant Professor Tomomi Furihata and lab members of YAKUBUTSU laboratory, Department of Pharmacology, Graduate School of Medicine, Chiba University, for his assistance during my stay in Japan.

Special thanks are extended to the support and grants from Ratchadaphiseksomphot Endowment Fund of Chulalongkorn University (RES 560530026-AS), the 90th Anniversary of Chulalongkorn University (Ratchadaphiseksomphot Endowment Fund, GCUGR1125582018D), Overseas Research Experience Scholarship for Graduate Student and a Grant-in-Aid from TGIST (TG-55-09-55-050D).

Finally, I would like to express my deeply thank to my family and my friends for their support, love and always besides me throughout my PhD study.

CONTENTS

Page

Page

LIST OF TABLES

Page

LIST OF FIGURES

Page

Page

Page

LIST OF ABBREVIATIONS

3D	= Three dimensional
ABC	= Adenosine triphosphate binding cassette
ADP	= Adenosine diphosphate
ANOVA	= Analysis of variance
ATP	= Adenosine triphosphate
BSA	= Bovine serum albumin
°C	= Degree celsius
Caco-2	= Colorectal adenocarcinoma
CO_2	= Carbon dioxide
CM	= Complete medium
cm^2	= Square centimeter
DMEM	= Dulbecco's modified eagle medium
DMSO	= Dimethyl sulphoxide
DNA	= Deoxyribonucleic acid
DQ	= Degree of quaternization
EDTA	= Ethylenediamine tetraacetic acid
FAK	= Focal adhesion kinase
FBS	= Fetal bovine serum
FITC	= Fluorescein isothiocyanate
GAPDH	= Glyceraldehyde 3-phosphate dehydrogenase
xg	= Times gravity
HBSS	= Hanks' balanced salt solution
HCl	= Hydrochloric acid
HPTChC	= *N*-(2-hydroxypropyl)-3-trimethylammonium chitosan chloride
HRP	= Horseradish peroxidase

h	= Hour
kDa	= Kilodalton
MLC	= Myosin light chain
MLCK	= Myosin light chain kinase
MDR1	= Multidrug resistance protein 1
MTT	= 3-(4, 5-dimethylthiazol-2-yl)-2, 5-diphenyltetrazolium bromide
min	= Minute
mL	= Milliliter
mM	= Millimolar
mRNA	= Messenger ribonucleic acid
MW	= Molecular weight
NaCl	= Sodium chloride
PBS	= Phosphate buffered saline
PKC	= Protein kinase C
PVDF	= Polyvinylidene fluoride
P-gp	= P-glycoprotein
qPCR	= Quantitative real-time polymerase chain reaction
SDS	= Sodium dodecyl sulfate
SEM	= Standard error of mean
sec	= Second
V	= Voltage
w/v	= Weight by volume
µg	= Microgram
µL	= Microliter
µM	= Micromolar
ZO-1	= Zonula occludens-1

CHAPTER I
INTRODUCTION

Delivery systems have been developed to improve the bioavailability of drugs and other compounds, such as nucleic acids, to the target cells with greater efficiency and effectiveness. The employment of such carriers includes within the gastrointestinal tract to overcome the intestinal barrier and to increase the payload drug accessibility to the target and so yield a more effective treatment (Vilar, Tulla-Puche and Albericio, 2012; Dunnhaupt et al., 2015). Among the different drug carriers used, biopolymers have been widely applied due to their typically outstanding biocompatibility, biodegradation and natural abundance (Sonia and Sharma, 2011).

Chitosan is a modified natural polymer derived from chitin. It is widely used as pharmaceutical excipient for drug solid dosage form and recently as drug delivery systems due to its biocompatibility, biodegradation and low toxicity (Thanou, Verhoef, and Junginger, 2001). The cationic character of chitosan facilitates its mucoadhesive properties through an interaction with the negatively charge of cell membrane, consequently drug absorption time can be extended (Rodrigues et al., 2012). However, chitosan is practically insoluble at pH over 6.5, which limits its uses as drug carrier under neutral and basic condition. A number of chitosan derivatives have been synthesized in order to improve the solubility at a neutral pH of 7.4 (Sonia and Sharma, 2011). It is crucial that chemical modification of chitosan should overcome the solubility problem without any effect on the mucoadhesive property (Riva et al., 2011).

N-(2-hydroxypropyl)-3-trimethylammonium chitosan chloride (HPTChC), one of quaternized chitosan, is the new synthetic chitosan derivatives generated from chemical modification of chitosan with 3-chloro-2-hydroxypropyltrimethylammonium

(Quat-188) (Sajomsang et al., 2009). Recently, it was reported that HPTChC derived from medium molecular weight of 200 kDa chitosan (200-HPTChC) reversibly enhanced paracellular permeability across intestinal epithelial cells and increased absorption of hydrophilic compounds (Kowapradit et al., 2010). As shown by previous report, the molecular weight of chitosan may affect its enhancing absorption and mucoadhesive properties (Opanasopit et al., 2007). Chitosan with high molecular weight apparently increased paracellular permeability and mucoadhesive effect better than those with low molecular weight. This might be explained by the long chain and high density of positive charge presented in the high molecular weight chitosans (Schipper, Varum, and Artursson, 1996). Hence, high molecular weight HPTChC prepared from 600 kDa chitosan (600-HPTChC) has been synthesized to improve the permeability and mucoadhesive effects. Although the high cationic property in substitution moiety may increase cytotoxicity of these compounds (Chae, Jang, and Nah, 2005), the preliminary data suggested that the biocompatibility between 600-HPTChC and 200-HPTChC in low substitution of Quat-188 was comparable (Appendix E). Further investigation of the intrinsic biocompatibility and effective properties of 600-HPTChC is needed for further use of this compound in drug delivery application.

Like chitosan, 600-HPTChC may be able to disturb the integrity of tight junction, leading to increase paracellular transport and enhance drug absorption. Previous studies showed that chitosan reversibly opened tight junction and reorganized the tight junction structure (Dodane, Khan, and Merwin, 1999; Smith, Wood, and Dornish, 2004). Exposure Caco-2 cells with chitosan (molecular weight 80 and 128 kDa) at the concentration ranging from 0.05% to 0.5% for 1 h reversibly disrupted the tight junction integrity. It was shown that the loss of tight junction integrity resulted from transient redistribution of occludin and ZO-1 from membrane to cytoskeletal fraction (Smith et al., 2004). However, the tight junction integrity of

the barrier could recover completely within 24 h after removal of chitosan (Smith et al., 2004; Yeh et al., 2011).

The opening of tight junction can occur in the normal physiological condition through several signaling pathways including myosin light chain (MLC) phosphorylation and protein kinase C (PKC) (Deli, 2009). The opening of tight junction structure involves changing formation of tight junction strand and reorganization of tight junction proteins such as occludin and ZO-1 (Weber, 2012). It was reported that inhibition of myosin light chain kinase (MLCK) and PKC in Caco-2 cells prevented change of tight junction organization (Smith et al., 2005; Shen et al., 2006). Furthermore, overexpression of MLCK caused the redistribution of ZO-1 and occludin, which subsequently increased paracellular permeability of mannitol across the monolayers of MDCK cells (Shen et al., 2006).

Since the high molecular weight of chitosan and chitosan derivatives cannot permeate through plasma membrane (Tan et al., 2013; Kim, 2014), it is possible that these compounds may interact with membrane proteins, leading to activation of signaling cascade in tight junction opening such as MLC-MLCK signaling pathway. The activation of membrane integrin was apparently related to several signaling cascades including MLC phosphorylation (Connell and Helfman, 2006). It was also demonstrated that the interaction between chitosan and membrane integrin was able to initiate the signaling of tight junction opening such as phosphorylation of FAK and Src tyrosine kinases (Hsu et al., 2012). However, intracellular signaling of integrin stimulating MLC phosphorylation and regulation of tight junction opening remained unclear.

In addition to paracellular transport, drug efflux pump mediated transcellular transport including P-glycoprotein (P-gp) is well established as hindrance of transcellular drug permeation (Takano, Yumoto and Murakami, 2006). Inhibition of P-gp activity by P-gp inhibitor such as quinidine is able to increase the oral absorption

of P-gp substrate drug (Kharasch et al., 2003). Although small molecule inhibitors have been demonstrated the stronger inhibitory effect on P-gp, their adverse effects such as unknown pharmacological effect, drug-drug interaction and unspecific effect of their P-gp inhibition at various sites of organs still need to overcome (Baumert and Hilgeroth, 2009; Shukla et al., 2009). Interestingly, using polymer as the drug excipient is attractive product to avoid these disadvantages at undesirable organs. Previous study has been shown the inhibitory effect of thiolated chitosan on P-gp function leading to enhance the drug absorption in Caco-2 cells (Chen et al., 2015). Therefore, in order to use 600-HPTChC as drug carrier, its potential effects on P-gp function and inhibitory mechanism are worth to be investigated for providing the biochemical and physiological effects in the *in vitro* study.

Hypothesis

600-HPTChC is able to enhance drug absorption on both paracellular and transcellular transport by reversible opening the tight junction protein and impairing the P-gp function, respectively. Regulation of 600-HPTChC on tight junction opening may involve with activation of MLCK, PKC or tyrosine kinase pathway. In addition, interaction of 600-HPTChC in the transmembrane region of P-gp might cause alteration of P-gp function.

Objectives

The objectives of this study were

1. To assess the non-toxic concentrations of 600-HPTChC in the *in vitro* model of intestinal absorptive barrier

2. To investigate the effects of 600-HPTChC on the intestinal epithelial barriers through paracellular and transcellular pathway as follows:

2.1 Effects on tight junction integrity. The potential of 600-HPTChC to disrupt tight junction involving MLCK, PKC and tyrosine kinase signaling pathway were examined.

2.2 Effects on the activity, protein and mRNA level of P-gp.

Scope of study

This study determined the cytotoxic effect and the intrinsic property of 600-HPTChC on paracelllular and transcellular barriers including tight junction and P-gp, respectively using Caco-2 cells as human intestinal epithelium cells. These findings would provide the information on the property of 600-HPTChC and its mechanism involving to drug absorption enhancer via paracellular and transcellular transport.

Conceptual framework

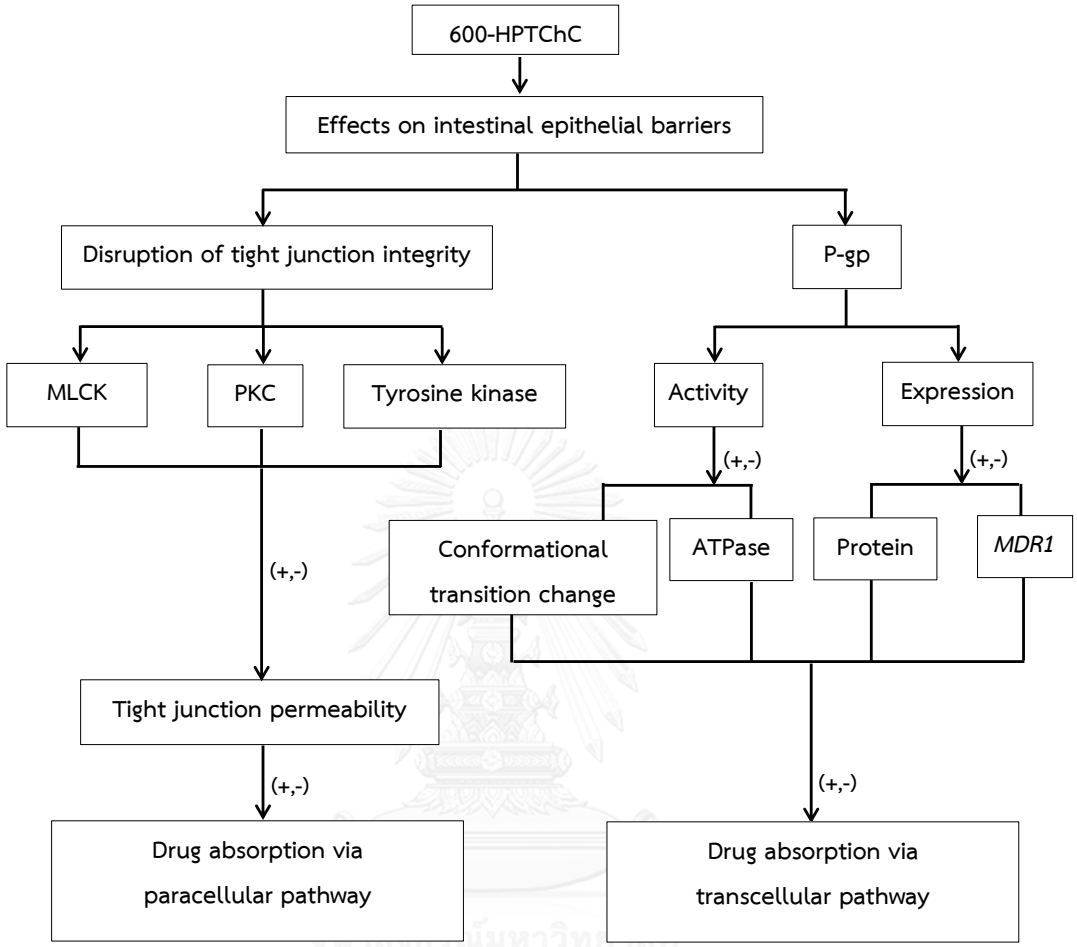

CHAPTER II

LITERATURE REVIEW

Intestinal drug absorption

Generally, most of drugs are favorably taken via oral route due to patients' convenience and accessibility. Orally taken drugs are mostly absorbed in the small intestine through its epithelial barrier (Deli, 2009). The intestinal epithelium is the selective permeable barrier between intestinal lumen and circulatory system (Groschwitz and Hogan, 2009). This barrier contains high villous structures in the apical site in order to increase the absorptive area (Figure 1). Moreover, the intestinal epithelial barrier consists of tight junction complex and various drug influx and efflux transporters (Deli, 2009). Thus, the intestinal barrier is able to restrict the penetration of harmful compound such as microorganism and toxic agents while it allows absorption of dietary nutrient, electrolytes and water.

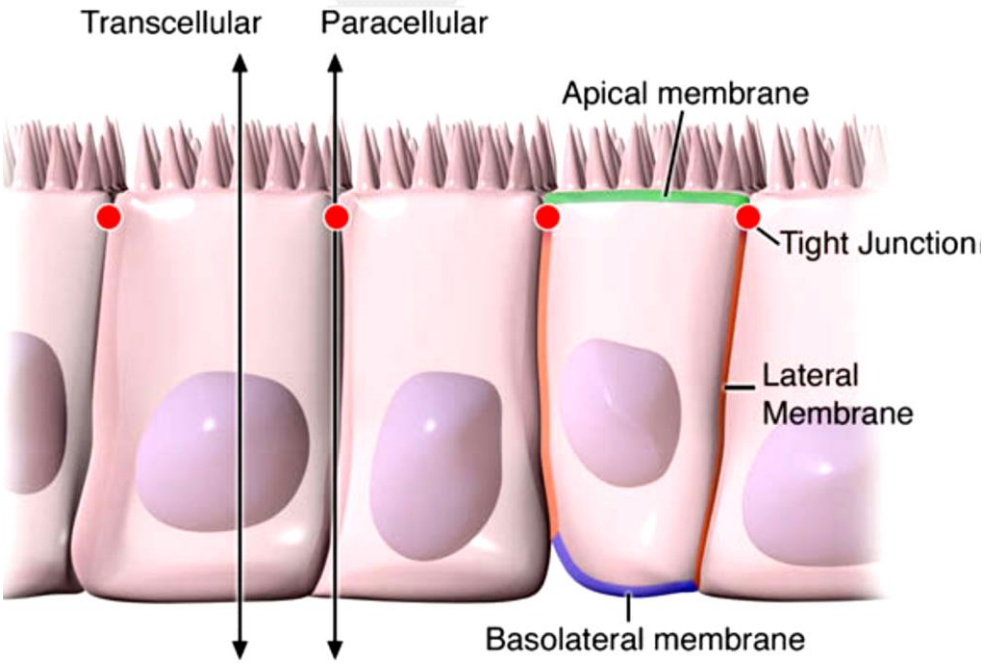

Figure 1. Pathways of intestinal epithelial permeability: transcellular and paracellular route (Groschwitz and Hogan, 2009).

Drug absorption can occur via either transcellular or paracellular pathways (Figure 1). Lipophilic drugs can cross the intestinal epithelium via the transcellular pathway, while hydrophilic drugs permeate passively through the barrier via the paracellular pathway. The paracellular transport is normally limited due to the presence of tight junction structure located at the apical site of the intestinal barrier (Hochman and Artursson, 1994; Groschwitz and Hogan, 2009).

Drug efflux transporter

In the intestine, ATP binding cassette (ABC) transporters such as P-gp, multidrug resistance proteins (MRPs) are transcellular efflux transporters that functions by efflux their substrates from the intestinal cells. Intestinal P-gp, the most studied ABC transporters, is expressed on the apical side. The role of P-gp is responsible for xenobiotic excretion and limiting oral bioavailability caused the drug interactions either in the presence of P-gp inhibitor or inducer (Lin and Yamazaki, 2003; Brand et al., 2006). The function of P-gp is mediated through ATP hydrolysis, converting ATP to ADP by basal P-gp ATPase. P-gp ATPase is activated when molecule binds to the P-gp transmembrane domain (TMD) induced the conformational change in the nucleotide binding domain (NBD) and stimulated the ATP consumption by this enzyme (Linton, 2007; Loo et al., 2012). This ATP catalytic cycle of P-gp leads to drug transport out of the cell membrane (Figure 2).

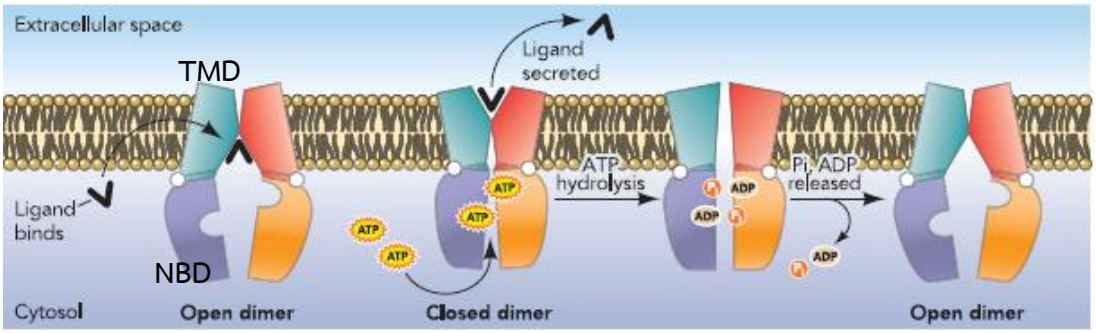

Figure 2. Mechanism of P-gp transport mediated through ATP catalytic cycle (Linton, 2007).

Tight junction structure

Tight junction structure (Figure 3) is formed by tight junction proteins that adhere between the two adjacent cells and function as the gate to control substance diffusion across the paracellular pathway. This structure mainly consists of the cytosolic scaffold and transmembrane proteins including occludin and claudins (Figure 3). Occludin and claudins are tetraspan transmembrane proteins linked to cytoplasmic scaffold proteins in the cytoplasm via the interaction with zonula occluden (ZO) proteins such as ZO-1 (Balda and Matter, 2008). The protein domains of ZO-1, including PDZ1 and GUK domain bind with claudins and occludin, respectively. In addition, ZO-1 links the transmembrane proteins to actin filaments though C terminal domain (Balda and Matter, 2008).

Tight junctions in the intestine are dynamic structures which allow reversible permeation of ions and molecules. Occludin involves in paracellular diffusion of macromolecules and may be responsible for tight junction leakage. Claudin, the structural backbone of tight junction, play a role in selective permeation of ion and small molecules through pore structure (Weber, 2012). The dynamic of structural organization of tight junction proteins can be regulated through signaling processes, leading to an alteration of paracellular permeability (Forster, 2008).

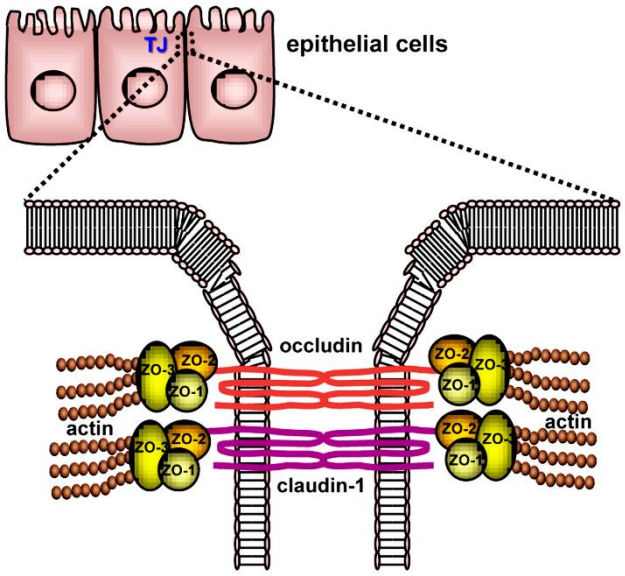

Figure 3. The main component proteins of the tight junction in the epithelial cells forming at the adjacent cell (Betanzos et al., 2013).

Regulation of tight junction complex

Regulation of tight junction permeability has been related to various signaling pathways such as protein kinase C, myosin light chain kinase (MLCK) and tyrosine kinase (Benais-Pont, Matter, and Balda, 2001; Ulluwishewa et al., 2011). It has been reported that the transient and reversible opening of tight junctions can occur in the normal physiological condition via MLC-MLCK signaling pathway (Turner et al., 1997). The MLCK mediated phosphorylation of MLC increased the paracellular permeability across Caco-2 monolayer, leading to a reorganization of actin filament and redistribution of ZO-1 and occludin (Turner et al., 1997; Qasim et al., 2014). After an opening of tight junction complex, tight junction proteins can reassemble physiologically and function normally without any interference on membrane function and integrity (Hayashi et al., 1999).

In case of chitosan and chitosan derivatives, MLC-MLCK signaling pathway may be initially activated through the cell membrane receptor because the large size

of these compounds would limit their crossing through the plasma membrane (Tan et al., 2013; Kim, 2014). The interaction between chitosan and integrin receptor might be take part in tight junction opening, leading to an increase of paracellular transport (Hsu et al., 2012). Integrin is a surface receptor which indirectly involved with regulation of cell shape and tight junction integrity. The role of integrin in tight junction integrity might be due to its correlation with the actin cytoskeleton (Hsu et al., 2012). Moreover, it was demonstrated that activation of integrin in MCK-10A cells decreased after MLCK inhibition (Connell and Helfman, 2006). It is likely that the triggering of MLC phosphorylation may be initiated from the integrin receptor (Figure 4).

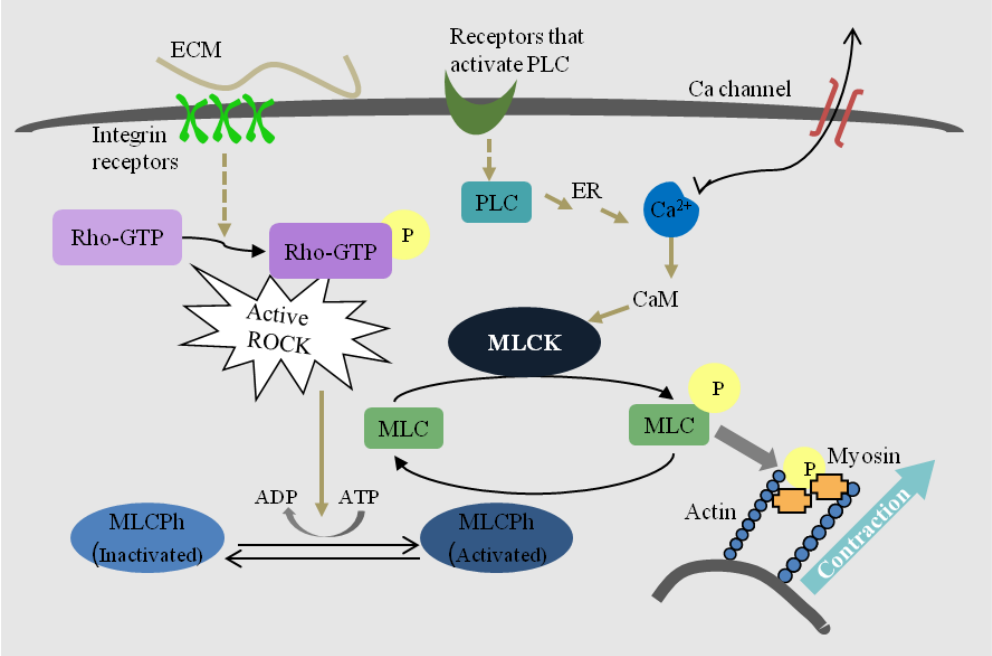

Figure 4. Interaction of integrin receptor leads to activation of the MLC phosphorylation signaling pathways (Labome, 2013: online).

Activation of integrin was also reported to associate with intracellular signaling protein including tyrosine kinase (Hsu et al., 2012). Integrin stimulation in Caco-2

cells resulted in the initiation of the signaling of tight junction opening such as phosphorylation of FAK and Src tyrosine kinases (Hsu et al., 2012). In addition, inhibition of PKC in Caco-2 cells prevented change of tight junction organization (Smith et al., 2005).

Permeation enhancers

In oral drug delivery, several excipients such as surfactants, cyclodextrins and cationic polymers can be used as permeation enhancers to overcome paracellular drug absorption in the intestinal epithelial barrier (Deli, 2009). For example, sodium dodecyl sulfate (SDS) and sodium cholate are able to increase the epithelial permeability in the concentration-dependent in the intestinal Caco-2 cells. (Anderberg, Nystrom, and Artursson, 1992; Yu et al., 2013). Beta-cyclodextrin derivatives enhanced the paracellular absorption of diosgenin across Caco-2 cells and increased the bioavailability of diosgenin and insulin in the rat intestine (Shao et al., 1994; Okawara et al., 2014).

Chitosan is a modified natural cationic polymer derived from chitin which is found in shells of shrimps, crabs and lobsters. Chitosan has been used extensively in food industry and dietary supplements such as food additive and weight-loss products. In pharmaceutical industry, chitosan is also used as an excipient because of its biocompatibility, biodegradability and low toxicity (Thanou et al., 2001; Baldrick, 2010). These properties make chitosan an ideal polymer carrier in the drug delivery system (Tiyaboonchai, 2003). In addition, chitosan is able to improve drug absorption through its ability to transiently open tight junction structure and its mucoadhesive effect. Because chitosan can enhance tight junction permeability, it can increase paracellular transport of molecule across intestinal epithelial cells (Artursson et al., 1994). Moreover, the cationic character of chitosan enables an interaction between

this polymer and the negatively charged membrane, leading to prolong the residence time of drug at the drug absorptive site (Rodrigues et al., 2012).

Chitosan is solely soluble in most organic acid solution, resulting in limitation of its biomedical application under the neutral and basic condition. Chemical modifications of chitosan have been done in order to improve chitosan solubility in neutral and basic solutions mimicking neutral and basic pH in the intestine and colon. The new synthetic derivatives should retain the positive charge property of chitosan which enables them to maintain the mucoadhesive property (Kotze et al., 1999; Riva et al., 2011; Sonia and Sharma, 2011).

Recently, the new derivatives of chitosan have been synthesized with various chemical modifications (Riva et al., 2011). HPTChC is a chitosan derivative prepared from the quaternization of chitosan by Quat-188, an aqueous solution of 3-chloro-2-hydroxypropyltrimethylammonium (Figure 5) (Sajomsang et al., 2009).

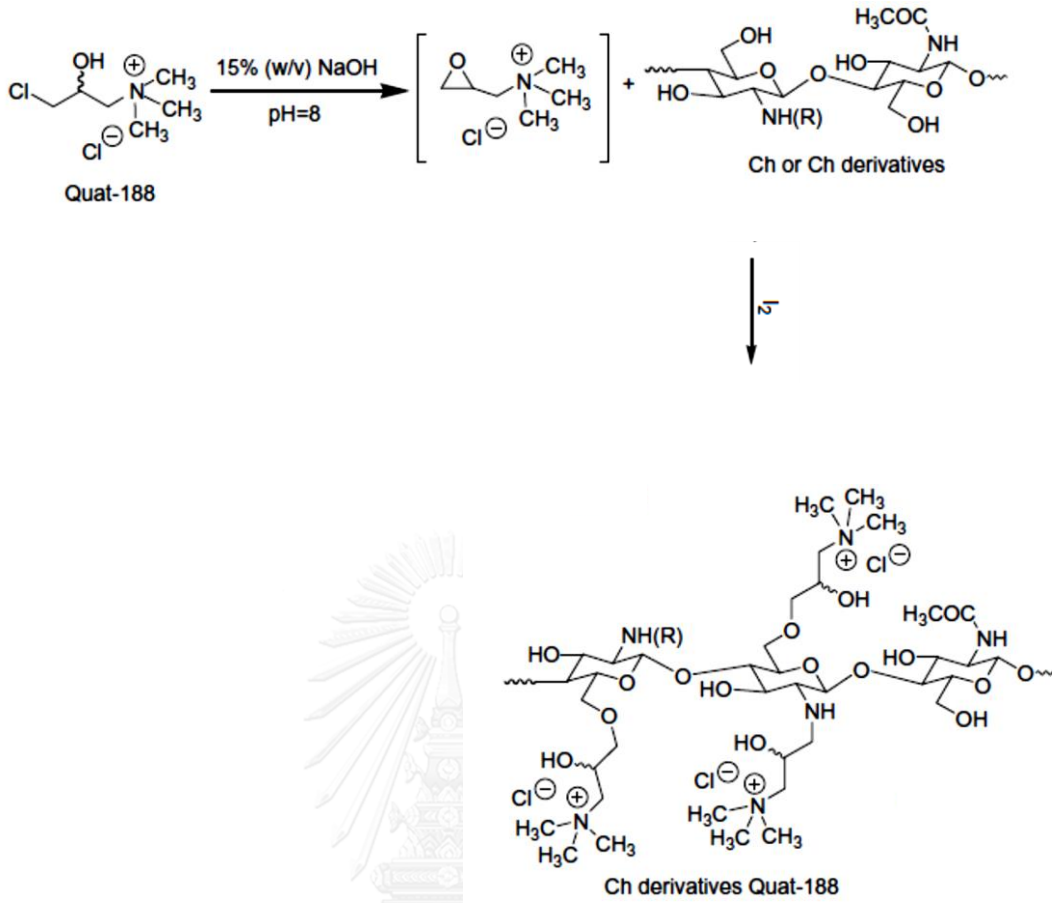

Figure 5. Synthesis of HPTChC (Sajomsang et al., 2009).

The chemically modified chitosan derivatives including HPTChC are synthesized from medium molecular weight of chitosan (200 kDa). These compounds have been demonstrated their capability to transiently disrupt the integrity of epithelial tight junction in Caco-2 cells within 2 h. Therefore these derivatives can enhance the paracellular permeability across intestinal epithelial barrier and increase the absorption of hydrophilic compounds such as mannitol, FITC-dextran and insulin (Thanou et al., 2000; Kowapradit et al., 2008; Sadeghi et al., 2008; Kowapradit et al., 2010). In addition, recovery of tight junction barrier was observed in the Caco-2 monolayer after removal of these 200-HPTChC for 24 h (Kowapradit et al., 2008; Sadeghi et al., 2008; Kowapradit et al., 2010).

CHAPTER III
MATERIALS AND METHODS

3.1 Materials

3.1.1 Synthesis of HPTChC

HPTChC was synthesized by chitosan with weight-average molecular weight (MW) of 200 and 600 kDa (Seafresh Chitosan (Lab) Co., Ltd., Chumphon, Thailand) in the various degrees of quaternization with N-(3-chloro-2-hydroxypropyl) trimethylammonium chloride (Quat-188; Sigma-Aldrich Co., St. Louis, MO, USA). Chemical characterizations of HPTChC were determined as described previously (Wongwanakul et al., 2016; Appendix A).

3.1.2 Preparation of FITC labeling with 600-HPTChC-1

FITC labeling with 600-HPTChC-1 was prepared according to Vongchan et al., 2011. Briefly, 600-HPTChC-1 dissolved in deionized water was added in the reaction mixtures of 1-ethyl-3-(3-dimethylaminopropyl)carbodiimide (EDC), FITC dissolved in DMSO (pH 3.0) and *N*-hydroxysuccinimide (NHS) and stirred at room temperature for 6 h. After completion of the FITC conjugation, dialysis of the mixtures was processed against distilled water and then lyophilized.

3.1.3 Chemical reagents

- TOX7 assay kit, 3-(4,5-dimethylthiazol-2-yl)-2,5-diphenyl tetrazolium bromide (MTT reagent), streptomycin sulfate, Triton X-100, non-essential amino acids, penicillin G sodium, bovine serum albumin (BSA), verapamil, calcein acetoxymethyl (calcein-AM), ethylenediamine tetraacetic acid (EDTA), Hanks' Balanced Salt solution (HBSS), 2-(N-Morpholino)ethanesulfonic acid hydrate (MES), N-(2-hydroxyethyl)piperazine-N'-(2-ethanesulfonic acid) (HEPES), fluorescein isothiocyanate-dextran 4000 (FITC-dextran 4000), mucin from porcine stomach type III, ML-7 (MLCK inhibitor), RO-318220 (protein kinase C

inhibitor), Genistein (tyrosine kinase inhibitor), 4',6-diamidino-2-phenylindole dihydrochloride (DAPI) and the monoclonal mouse anti-Na^+/K^+ ATPase (α Subunit) antibody were purchased from Sigma-Aldrich Co. (St. Louis, MO, USA).

- Dulbecco's modified eagle medium and L-glutamine were purchased from Gibco Life Technologies (Grand Island, NY, USA).
- Fetal bovine serum (FBS) was from Biochrome AG (Berlin, Germany).
- ZO-1 and occludin primary antibodies were from Invitrogen Corporation (Camarillo,
  CA, USA).
- Goat F(ab')2 anti-mouse IgG H&L (HRP) pre-absorbed, FITC conjugated monoclonal mouse anti-P-gp antibody (UIC2), goat anti-mouse IgG H&L Alexa Fluor® 488 and 568 secondary antibodies were obtained from Abcam (Cambridge, UK).
- Monoclonal mouse anti-BrdU antibody was from BD Biosciences (San Jose, CA, USA).
- Polyclonal goat anti-mouse IgG antibody conjugated with AlexaFluor® 488 was purchased from Molecular Probes (Eugene, OR, USA).
- Monoclonal mouse anti-P-gp antibody was from Santa Cruz Biotechnology (Dallas, TX, USA).
- Monoclonal mouse anti-P-gp antibody (C219) was from Alexis Biochemicals (Ann Arbor, MI, USA).
- RNase A was from AMRESCO (Solon, OH, USA).
- *p*-nitrophenol (pNP) was from Merck (Darmstadt, Germany).
- BCA protein assay kit was from Pierce (Rockford, IL, USA).
- P-gp-Glo™ assay kit was from Promega Corporation (Madison, WI, USA).
- ECL western blotting detection reagent was from GE Healthcare Life Sciences (Buckinghamshire, UK).
- Immuno-Blot Polyvinylidine difluoride (PVDF) membrane was from Pall Gelman Laboratory (Pensacola, FL, USA).

- KAPA SYBR Fast qPCR Kit was from KAPA BIOSYSTEMS (Boston, MA, USA).
- TGX™ FastCast™ Acrylamide Kit, 10% (SDS-polyacrylamide gel electrophoresis) and Bio-Rad Protein Assay Kit II were purchased from Bio-rad (Berkeley, CA, USA).
- Clear-sol I scintillation cocktail and 1% protease inhibitor cocktail were from nacalai Tesque (Kyoto, Japan).
- Other chemical reagents used throughout this study were all analytical grade.

3.1.4 Experimental instruments

1. Tissue culture flasks, multi well plate and transwell polycarbonate and polyester insert (0.4 μm pore size): Corning, Tewksbury, MA, USA
2. E-16 plates: ACEA Bioscience, San Diego, CA, USA
3. Untreated white polystyrene 96-well plates (Cat. No. 136101) and humidified carbon dioxide incubator (Series 8000 Water-Jacketed): Thermo Scientific, Waltham, MA, USA
4. Nucleospin RNA® Columns with collection tubes: Macherey-Nagel, Duren, Germany
5. *xCelligence* RTCA device: ACEA Biosciences, San Diego, CA, USA
6. Flow cytometer (FACSAria™II): BD Biosciences, San Jose, CA, USA
7. Millicell-ERS and probe: Millipore, Bedford, MA, USA
8. 2720 Thermal cycler and High-Capacity cDNA Reverse Transcription Kits: Applied Biosystems, Foster City, CA, USA
9. ECO Real-time PCR system: Illumina, San Diego, CA, USA
10. ImageQuant LAS 4000: GE Healthcare Life-Sciences Ltd., Branch, Taiwan
11. Humidified carbon dioxide incubator: Forma Scientific, Marietta, OH, USA
12. Inverted microscope: Axiovert 135, Zeiss, Konstanz, Germany
13. Confocal laser scanning microscope: Fluoview FV10i, Olympus, Tokyo, Japan

14. Confocal super-resolution microscope: TCS SP8 STED 3X, Leica, Buffalo Grove, IL, USA
15. Microplate reader: Wallac 1420 Perkin-Elmer Victor 3, Perkin Elmer lnc., Waltham, MA, USA
16. Multi-mode microplate reader: SpectraMax M5, Molecular Devices, Sunnyvale, CA, USA
17. Multi-mode microplate reader: FilterMax F5 Molecular devices, Sunnyvale, CA, USA
18. Liquid scintillation counter: LSC-6100, Aloka, Tokyo, Japan
19. Zetasizer Nano ZS: Malvern Instruments Ltd., Malvern, UK
20. BioSpec-nano Micro-volume UV-Vis Spectrophotometer: Shimadzu Biotech, Kyoto, Japan
21. Autoclave: Hirayama, Saitama, Japan
22. Hot air oven: MEMMERT, Buchenbach, Germany
23. Orbital shaker: OS-20, Biosan, Riga, Latvia
24. pH meter: CG 842, Schott, Hofheim, Germany
25. Ultracentrifuge: Himac CS 120EX, Hitachi Koki, Tokyo, Japan
26. Refrigerated centrifuge: Z 383K, Hermle Labortechink, Burladingen, Germany
27. Vortex mixer: mode K550-GE. Scientific Industries, New York, NY, USA
28. Water bath: WB22, Memmert, Hannover, Germany

3.1.5 Cell culture

Caco-2 cells, the human colon adenocarcinoma cell line, were obtained from the American Type Culture Collection (ATCC, Manassas, VA, USA). Cells were maintained in completed culture medium (CM: DMEM supplemented with 10% (v/v) heat-inactivated FBS, 100 U/mL penicillin, 100 µg/mL streptomycin, 1% (v/v) non-essential amino acids and 2 mM L-glutamine) at 37 °C in a humidified atmosphere of

5% (v/v) CO_2. The cells passage between 58 and 77 were cultured with fresh CM every other day and subcultured at approximately 70% confluence by using 0.25% trypsin solution containing 1 mM EDTA.

3.2 Methods

3.2.1 Acute cytotoxicity

Caco-2 cells were seeded in 96 well tissue culture plates at an initial seeding density of 78,125 cells/cm^2. After incubation for 24 h, the confluent Caco-2 cells were exposed to fresh CM containing various concentrations of 600-HPTChC with a different DQ for 4 h. The acute cytotoxicity of 600-HPTChC was subsequently assessed by the MTT and lactate dehydrogenase (LDH) assays.

For the MTT assay, the treated cells were washed once with phosphate buffered saline pH 7.4 (PBS) and then incubated with the MTT solution (0.5 mg/mL in serum free CM) for 4 h. The formazan crystals inside the cells were then dissolved in dimethylsulfoxide. The intensity of formazan products was measured by spectrophotometry at an absorbance of 570 nm using a microplate reader. The results are presented as the IC_{50} values, the concentration causing 50% cell death compared to 100% viability for the control.

For the LDH assay, the supernatant of treated cells was centrifuged at 9,000 *xg* to remove cell debris, and then assayed using the TOX7 assay kit according to the manufacturer's protocol. Briefly, the reaction was processed with the LDH assay mixture for 30 min at 37 ºC and stopped with 1 N HCl. The LDH activity was detected by colorimetric spectrophotometry at an absorbance of 490 nm using a microplate reader. The data are presented as the EC_{50} values, the concentration inducing a 50% LDH activity release compared to the total LDH activity of the control group. The IC_{50} and EC_{50} values were calculated by using the linear regression from the data under the linear range and curve fitted by the Sigma Plot 12.5 software.

3.2.2 Proliferation studies

3.2.2.1 MTT assay

Caco-2 cells cultured for 1 day at an initial seeding density of 15,625 cells/cm^2 were incubated with various concentrations of 600-HPTChC with different DQ for 0, 24, 48 and 72 h. The relative number of viable cells compared to the untreated control at each specific time was then determined by the MTT assay (section "Acute cytotoxicity"), and the IC_{50} value of the 3-day treatment with each 600-HPTChC was derived using the linear regression as described above.

3.2.2.2 Bromodeoxyuridine (BrdU) incorporation assay

For the BrdU incorporation assay, the Caco-2 cells treated with the respective 600-HPTChC (or CM only for control cells) for 0, 24, 48 or 72 h were labeled with 10 µM BrdU for 60 min at 37 °C, washed twice with PBS, trypsinized and suspended in cold PBS containing 3% (v/v) FBS. Thereafter, the cells were harvested by centrifugation at 2,300 *xg* at 4 °C for 5 min and fixed in ice-cold 70% (v/v) ethanol for 2 h at -20°C. The DNA was denatured as previously described (Yang et al., 2004). In brief, Caco-2 cells were incubated with 2 N HCl containing 0.5% (v/v) triton X-100 for 30 min at room temperature and then neutralized with 0.1 M sodium borate decahydrate (pH 8.5). Next, the cell suspension was labeled with a 1:100 dilution of the monoclonal mouse anti-BrdU antibody for 30 min at room temperature and subsequently incubated with a 1:400 dilution of the polyclonal goat anti-mouse IgG antibody conjugated with AlexaFluor® 488 for another 30 min at room temperature. The fluorescence intensity of BrdU incorporation was analyzed using a BD FACSAria™ II flow cytometer collecting at least 10,000 events.

3.2.2.3 Real-Time Cell Analysis (RTCA)

To monitor cell proliferation in real time, Caco-2 cells were seeded and cultured for 24 h in the E-16 plates at an initial cell density of 15,625 cells/cm^2. The cells were subsequently incubated with various concentrations of 600-HPTChC-1 in a final volume of 120 µL. The impedance signals were recorded every hour for 72 h

after treatment using the *xCelligence* RTCA device, and calculated as the cell index (CI) by the RTCA software Package 1.2 of the RTCA system (Moniri et al., 2014).

3.2.3 Cell cycle analysis

The progression of Caco-2 cells through the cell cycle was investigated as previously reported (Ding, Ko and Evers, 1998) with slight modification. Briefly, Caco-2 cells (15,625 cells/cm^2) were cultured for 24 h in a 12-well culture plate and then treated with various concentrations of 600-HPTChC-1 for 24, 48 and 72 h. The cells were harvested by trypsinization and diluted in cold PBS containing 3% (v/v) FBS. The cell suspension was then centrifuged at 2,300 *xg*, 4°C for 5 min and fixed in the ice cold 70% (v/v) ethanol for 2 h at -20 °C. After fixation, the cells were gradiently diluted with 35% (v/v) ethanol and finally cold PBS containing 3% (v/v) FBS, and then incubated in cold PBS containing 50 µg/mL propidium iodide (PI), 100 µg/mL RNase A and 3% (v/v) FBS for 90 min at room temperature in the dark. The fluorescent intensity of PI was analyzed by BD FACSAria™ II flow cytometer collecting at least 10,000 events.

3.2.4 Differentiation assay

For the differentiation assay, Caco-2 cells were cultured for 14 days after an initial seeding density of 20,000 cells/cm^2 to allow them to differentiate. After reaching the cell confluence at day 5, the Caco-2 cells were treated with 600-HPTChC-1 and cultured until day 14 in two different treatment schedules. The first was a discontinuous 4 h interval treatment, and the second a continuous treatment. The alkaline phosphatase (ALP) activity, a marker of intestinal epithelial differentiation, was measured at the specific time points as described previously (Ferruzza et al., 2012) with slight modification. Briefly, the cell monolayer was washed twice with cold PBS and scraped in lysis buffer. The obtained cell suspension was sonicated on ice and then 60 µL of the homogenate was added in a reaction tube to 180 µL of p-nitrophenol phosphate (pNPP) substrate. The

enzymatic reaction was performed at 37 ℃ for 20 min whereupon 200 µL of the reaction mixture was transferred to a 96 well-plate containing 50 µL of 0.5 M NaOH to stop the reaction. Finally, the amount of *p*-nitrophenol (pNP), the end-product of the ALP reaction, was measured at an absorbance of 405 nm. The ALP activity was calculated from a standard curve of pNP. The protein concentration in cell lysate was measured by the BCA protein assay kit. The enzyme activity was then normalized to the protein quantity and expressed as µM of pNP/min/mg protein.

3.2.5 Transepithelial electrical resistance (TEER) measurements

Paracellular permeability was determined by TEER measurement and transport study as described previously (Hubatsch et al., 2007). The cells were seeded in the density of 60,000 cells/cm^2 on transwell polycarbonate insert (0.4 µm pore size) for 21 days (Behrens and Kissel, 2003). The medium was changed every other day. Before the experiment, TEER value was measured by a Millicell-ERS in order to indicate the cell monolayer integrity. The cell monolayer with TEER value of greater than 300 $\Omega \cdot cm^2$ was used in these experiments (Goncalves et al., 2012). After culture for 21 days, the cells were washed twice with PBS and further incubated with 10 mM MES-HBSS, pH 6.5 in apical side and 25 mM HEPES-HBSS, pH 7.4 in basolateral side for 30 min in the incubator at 37°C. Subsequently, 600-HPTChC-1 or soluble chitosan 600 kDa in 1% acetic acid prepared in MES-HBSS was added to the apical side of the cells and incubated at 37°C on the orbital shaker for 4 h.

For the measurement of tight junction recovery, transport buffer was replaced with culture medium and the cells were incubated for another 24 h in CO_2 incubator at 37°C. TEER was measured in various time points during 4 h treatment and 24 h recovery.

The mechanism of tight junction opening was investigated by using the inhibitors of MLCK, PKC and tyrosine kinase (Ma et al., 1999; Smith et al., 2005; Hsu et

al., 2012). Caco-2 cells were pre-incubated with these inhibitors on both the apical and basolateral compartment for 30 min at 37°C. 600-HPTChC-1 or chitosan 600 kDa was then added with the inhibitors in the apical side for another 2 h and TEER value was obtained during the treatment.

3.2.6 Permeability study

In the study of drug permeability in paracellular pathway, Caco-2 cells were treated with 10 mM MES-HBSS containing 600-HPTChC-1 and FITC-dextran 4000 (120 µg/mL), fluorescence hydrophilic marker, in the apical side at 37°C for 4 h. At various time intervals, the buffer in the basolateral side was taken in order to measure the fluorescence intensity of FITC-dextran 4000 using a microplate reader at an excitation and an emission wavelength of 485 and 535 nm, respectively. The fluorescence intensity was calculated to quantify the amount of transported FITC-dextran 4000 (µg) in various time points.

In the study of drug absorption through transcellular pathway, bidirectional transport of P-gp substrate using [^{3}H]-digoxin, radiolabeled drug, was performed. [^{3}H]-digoxin (7.5 µCi/mL) with or without verapamil or 600-HPTChC-1 was added in either the apical or basolateral side of Caco-2 cells at 37°C. After incubation for 2 h, samples taken from the opposite compartments of compounds (50 µL (BL to AP) and 100 µL (AP to BL)) were diluted in 2 mL of clear-sol I scintillation cocktail. The amount of [^{3}H]-digoxin containing in this cocktail was measured by liquid scintillation counter and calculated eventually from pure [^{3}H]-digoxin. The apparent permeability coefficient (Papp) of [^{3}H]-digoxin was obtained from the following equation. An efflux ratio was calculated from the mean Papp BL to AP / Papp AP to BL.

$$Papp = (dQ/dt) \times (1/AC_0)$$

Papp = the apparent permeability coefficient (cm/min)

dQ/dt = the rate of appearance of [^{3}H]-digoxin on the basolateral side (µg/min)

A = the surface area of the monolayers (cm^2)

C_0 = the initial drug concentration in the donor compartment (μg/mL)

3.2.7 Immunofluorescence microscopy

Localization of tight junction proteins including ZO-1 and occludin in Caco-2 monolayers was determined by confocal laser scanning microscope following a protocol from Leica (http://www.leica-microsystems.com/science-lab/how-to-prepare-your-specimen-for-immunofluorescence-microscopy/). The cells density of 60,000 cells/cm^2 was seeded on transwell polyester membrane insert (0.4 μm pore size) and cultured for 21 days (Behrens and Kissel, 2003). After treatment with either 600-HPTChC-1 or its FITC conjugate, the cell monolayers were washed twice with PBS and fixed with acetone:methanol (1:1) for 5 min at 4 °C. The fixed cells were permeabilized with 0.1% Triton X-100 in PBS for 15 min before blocking in 1% bovine serum albumin in PBS (blocking buffer) for another 45 min. Cells were then incubated overnight in blocking buffer with either a 1:100 dilution of the monoclonal mouse anti-ZO-1 or anti-occludin antibody at 4°C or a 1:200 dilution of the monoclonal mouse anti-P-gp antibody at room temperature for 1 h and subsequently in secondary antibodies (goat Alexa Fluor 488 or Alexa Fluor 568 conjugated anti-mouse) for 60 min (ZO-1 and occludin) and 45 min (P-gp) at room temperature. Fluorescence staining cells were visualized and imaged by using Olympus laser scanning confocal microscope. For imaging the interaction of FITC labeling 600-HPTChC-1 with the cell monolayer, after probing the secondary antibody, cells were stained the nucleus by DAPI (1 μg/mL) in PBS for 10 min and imaged by using confocal super-resolution microscope.

3.2.8 Mucoadhesive property of 600-HPTChC-1 and chitosan 600 kDa using zeta potential measurement

The mucoadhesive properties of 600-HPTChC-1 and chitosan were determined by zeta potential at three different pH values (6.0, 6.5 and 7.4) to mimic pH conditions in the intestinal tract. Mucin samples (0.05% (w/v)) were dispersed

and stirred in various pH of MES-HBSS. Then, 600-HPTChC-1 or chitosan 600 kDa was added to the mucin solution in varying concentrations. Zeta potential of mucin solution in the presence or absence of 600-HPTChC-1 or chitosan 600 kDa was measured at a temperature of 25°C on a Zetasizer Nano ZS (Takeuchi et al., 2005).

3.2.9 Determination of P-gp activity

P-gp activity was determined by the accumulation of calcein in the presence or absence of P-gp inhibitor (Wongwanakul et al., 2013). The cells were seeded at 13,000 cells/cm^2 and grown for 21 days. On the day of experiment, the cells were treated with 600-HPTChC-1 for 30 minutes prior to addition of calcein-AM, P-gp substrate. The membrane permeable non-fluorescent calcein-AM was hydrolyzed to non-permeable fluorescent calcein by the intracellular esterase (Essodaigui et al., 1998). After 30 min-incubation, the cells were lysed and measured the fluorescent intensity of calcein with the microplate reader at an excitation wavelength and an emission wavelength of 485nm and 535 nm, respectively.

3.2.10 UIC2 shift assay

Effect of 600-HPTChC-1 on P-gp conformational transition change was evaluated by UIC2 shift assay (Collnot et al., 2010). UIC2 monoclonal antibody labeling with FITC was used to detect the P-gp epitope during the conformational change of P-gp upon consecutive step of catalytic cycle in Caco-2 cells (Goda et al., 2002). Caco-2 cells grown in transwell insert for 21 days were harvested by trypsinization and washed with 3% (v/v) FBS in PBS. The suspended cells were pre-incubated with or without verapamil 100 µM (P-gp inhibitor) or 600-HPTChC-1 for 30 min at 37°C. Then, 10 µL of FITC labeled mouse monoclonal anti-P-gp antibody (UIC2) (1.0 µg) was added in the suspended cells for another 30 min at 37°C. After incubation, UIC2 antibody was removed by centrifugation at 2,300 *xg* and washed twice with PBS. The fluorescence intensity was detected and analyzed by BD

FACSAria™ II flow cytometer collecting at least 10,000 events. The graphs was overlaid by FCS express 6 plus research edition.

3.2.11 P-gp ATPase assay

Effect of 600-HPTChC-1 on P-gp ATPase activity was monitored by using the P-gp-Glo™ assay with recombinant human P-gp membranes according to the manufacturer's instruction. 600-HPTChC-1 or verapamil at 500 μM (P-gp ATPase stimulator) or sodium vanadate at 250 μM (selective P-gp ATPase inhibitor) in the provided buffer solution was incubated with 25 μg of P-gp membranes in untreated white polystyrene 96-well plates at 37°C for 5 min. P-gp ATPase reaction was started by adding 5 mM Mg-ATP and all solution was gently mixed by trapping the plate before incubation for 40 min at 37°C in water bath. Then, the reaction was stopped by remove the plate and luminescence signal was initiated by adding ATP detection reagent. After 20 min, remaining ATP was detected by luciferase-generated luminescence signal which was measured by FilterMax F5 multi-mode microplate reader in luminescence detection mode. The luminescence signal (RLU) represented the remaining ATP. Differences in sample luminescence between sodium vanadate-treated reaction and untreated sample or 600-HPTChC-1-treated samples (ΔRLU_{basal} and $\Delta RLU_{600\text{-}HPTChC\text{-}1,}$ respectively) were used to analyze the effect of 600-HPTChC-1 on basal P-gp ATPase activity.

3.2.12 Quantitative real-time polymerase chain reaction (qPCR)

Effect of 600-HPTChC-1 on *MDR1* was determined by qRT-PCR. Total RNA of Caco-2 cells treated with 600-HPTChC-1 for 1 day were isolated using Nucleospin RNA® Columns with collection tubes, according to the manufacturer's instructions and kept at -80 ^{o}C. The amounts of RNA samples were quantified using a BioSpec-nano Micro-volume UV-Vis Spectrophotometer at the wavelengths 260 and 280 nm. Reverse transcription of 2 μg of total RNA to cDNA was performed by High-Capacity cDNA Reverse Transcription Kits. To amplification of cDNA derived from mRNA, the

qPCR reactions were determined by the specific primers (Table 1) using KAPA SYBR Fast qPCR kit. *MDR1* and *GAPDH* expression was detected by ECO Real-time PCR system in the conditions as follows: an initial denaturing at 95 $^{\circ}$C for 20 sec, 40 cycles of denaturing at 95 $^{\circ}$C for 3 sec, annealing at 53 $^{\circ}$C (*MDR1*) or 60 $^{\circ}$C (*GAPDH*) for 20 sec and extension at 72 $^{\circ}$C for 10 sec. Finally, *MDR1* expression was normalized to *GAPDH* and calculated using by the $2^{-\Delta\Delta CT}$ method.

Table 1. Primers used for qRT-PCR analyses

Gene	Oligonucleotides	Sequences (5'-3')	Product size (bp)
MDR1	Forward	AAGCCAATGCCTATGACT	277
	Reverse	ATGACGTCAGCATTACGAA	
GAPDH	Forward	AGCCACATCGCTCAGACAC	66
	Reverse	GCCCAATACGACCAAATCC	

3.2.13 Protein expression of P-gp

Protein expression of P-gp was quantified with western blot analysis. 600-HPTChC-1 treated cells for 1 day were washed with PBS twice and lysed with ice-cold 1% protease inhibitor cocktail in HBSS. Next, membrane fraction was prepared by collecting the supernatant after centrifuged at 828 *xg* twice and then ultracentrifugation at 33,000 *xg* for 1 h at 4°C. The remaining cell pellet was collected and quantified the protein concentration by using Bio-Rad protein assay kit II. 20 µg of total protein samples were separated using TGX™ FastCast™ Acrylamide Kit, 10% SDS-polyacrylamide gel electrophoresis at 20 mA for 30 min, 100 mA for another 40 min and transferred to PVDF membrane at 100 V and 300 mA for 60 min at 4°C. Then, the unspecific protein on PVDF membrane was blocked with 5% skim milk in TBS-Tween (10 mM Tris-base, 350 mM NaCl and 0.05% Tween 20) for 1 h at room temperature with shaking. After blocking, the membranes were probed with primary antibodies for P-gp (1:1000) and Na^+/K^+ ATPase (1:5000) (internal standard) at

4°C overnight. Subsequently, the membranes were washed six times with TBS-Tween and further incubated with HRP-conjugated secondary antibody (1:5000) for 1 h at room temperature. After incubation, the membranes were washed and started the chemiluminescent reaction by using ECL western blotting detection reagents. The chemiluminescent intensity was detected with a GE ImageQuant LAS 4000 and quantified with image J program.

3.2.14 Data analysis

All data are reported as the mean ± SEM or the mean ± SD and are derived from at least three independent experiments. Statistical analysis was performed by one-way analysis of variance (ANOVA) followed by post-hoc Dunnett's analysis in the group comparison and independent samples t-test in pair comparison (SPSS version 21.0), accepting significance at the $p < 0.05$ level.

CHAPTER IV

RESULTS

4.1 Cytotoxic effects of 600-HPTChC on Caco-2 cells

4.1.1 Acute toxicity

The acute cytotoxicity of 600-HPTChC with different DQ against Caco-2 cells after 4 h exposure was dose- and DQ-dependent (Figure 6). The lowest DQ (the 600-HPTChC-1 preparation) had the lowest cytotoxicity. The IC_{50} and EC_{50} values of 600-HPTChC-1 obtained from MTT and LDH assays were > 0.8 and > 0.02% (w/v), respectively (Table 2).

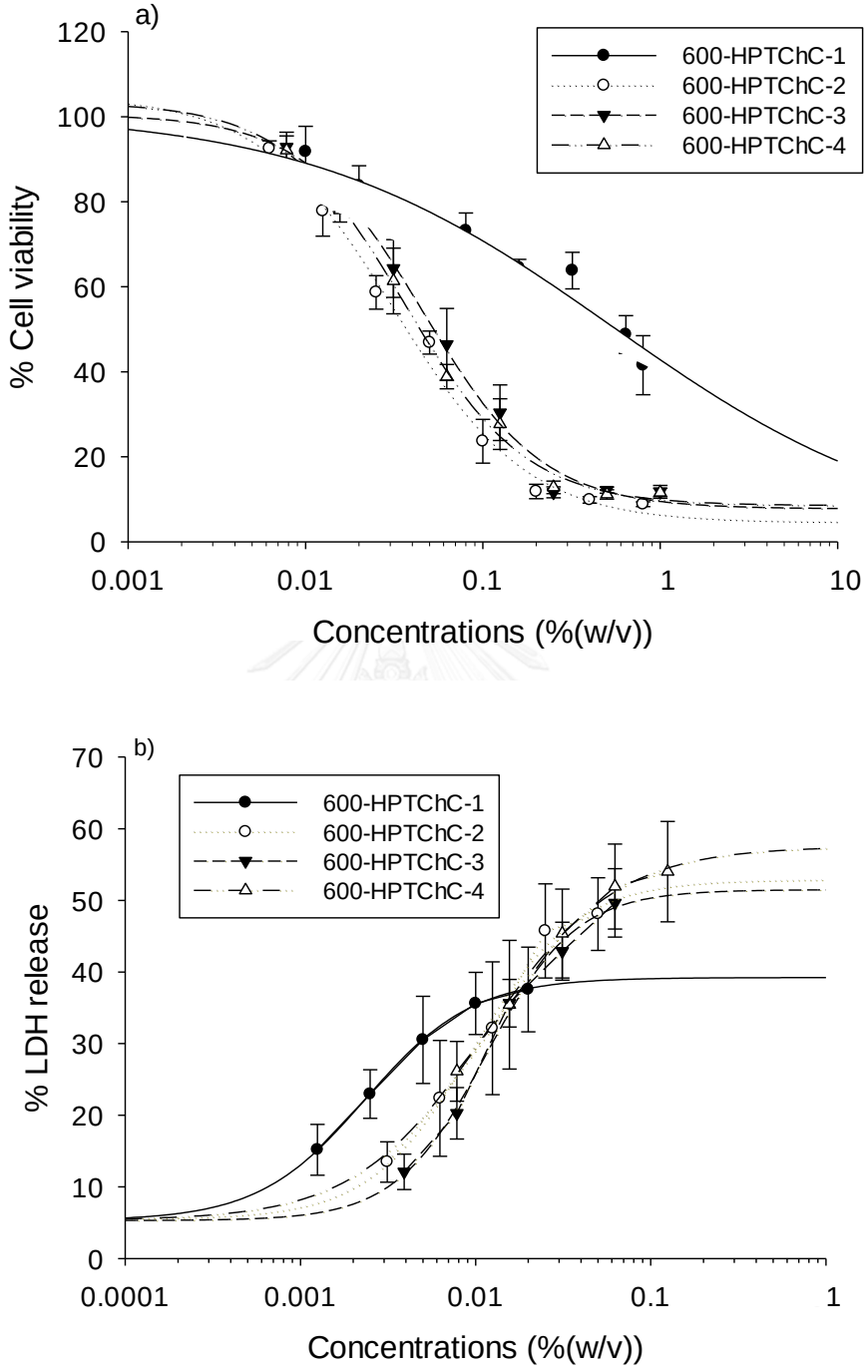

Figure 6. Acute cytotoxicity of 600-HPTChC with different DQ against Caco-2 cells after 4-h exposure as determined by the (a) MTT and (b) LDH release assays. The data are expressed as the percentage of (a) cell viability and (b) LDH release compared to that of the control (100%) and are shown as the mean ± SEM (n=3–4).

4.1.2 Anti-proliferative effect of 600-HPTChC

After 3-day treatment, 600-HPTChC with different DQ was able to inhibit and slightly effect on Caco-2 cells proliferation in concentration- and time-dependent manner, respectively (Figure 7). The 600-HPTChC with the lowest DQ (600-HPTChC-1) had the lowest anti-proliferative effect with the highest IC_{50} value (Table 2). In this regard, 600-HPTChC-1, the lowest degree of cytotoxicity and anti-proliferative effect, was selected for all further experiments.

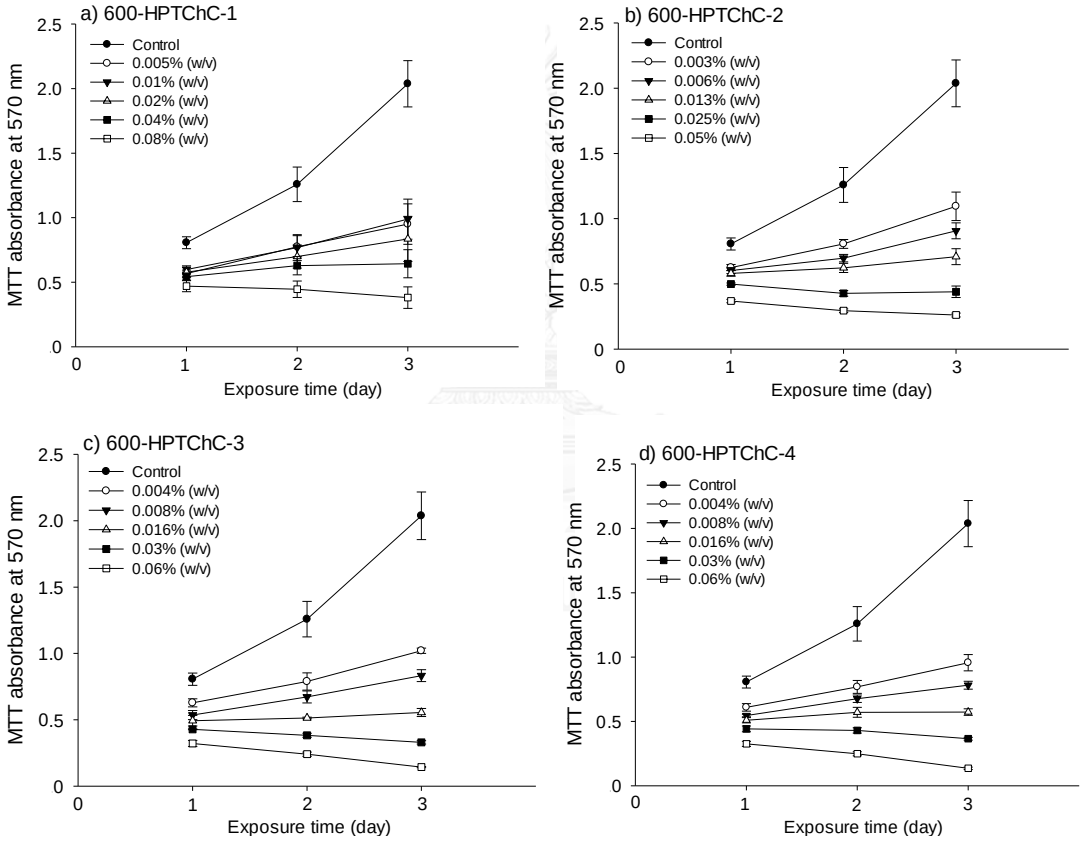

Figure 7. Anti-proliferative effect of 600-HPTChC with DQ of (a) 65% (600-HPTChC-1), (b) 86% (600-HPTChC-2), (c) 108% (600-HPTChC-3) and (d) 124% (600-HPTChC-4) against Caco-2 cells after treatment for up to 3 days. The cell viability, as the number of viable cells relative to the control (100%), was measured each day after treatment by the MTT assay. The data are expressed as the mean ± SEM (n=3) of MTT absorbance at 570 nm.

Table 2. The IC_{50} and EC_{50} values of 600-HPTChC with different DQ against Caco-2 cells after exposure for 4 h and 3 days.

600-HPTChC	MTT assay (IC_{50} at 4 h) (% (w/v))	LDH assay (EC_{50} at 4 h) (% (w/v))	MTT assay (IC_{50} at 3 days) (% (w/v))
600-HPTChC-1	>0.8	>0.02	0.013 ± 0.0015
600-HPTChC-2	0.071 ± 0.0075	0.045 ± 0.0052	0.008 ± 0.0038
600-HPTChC -3	0.096 ± 0.0118	0.056 ± 0.0053	0.006 ± 0.0026
600-HPTChC-4	0.088 ± 0.0098	0.086 ± 0.0178	0.005 ± 0.0015

The acute cytotoxicity of 600-HPTChC in the MTT and LDH assay are expressed as the IC_{50} and EC_{50} values, respectively, after a 4-h exposure to the respective 600-HPTChC, whereas the anti-proliferative effect of 600-HPTChC in the MTT assay are expressed as the IC_{50} value after exposure for 3 days. All data are shown as the mean ± SEM (n=3–4).

The inhibitory effect of 600-HPTChC-1 on cell proliferation was further monitored in real time by RTCA, a novel technique for the real time monitoring of cell migration, cytotoxicity and adherence/proliferation of cells (Moniri et al., 2014). The anti-proliferative effect of 600-HPTChC-1 against Caco-2 cells clearly occurred in a time-dependent manner. As seen in Figure 8, 600-HPTChC-1, even at the low concentration of 0.005% (w/v), suppressed cell indexes significantly.

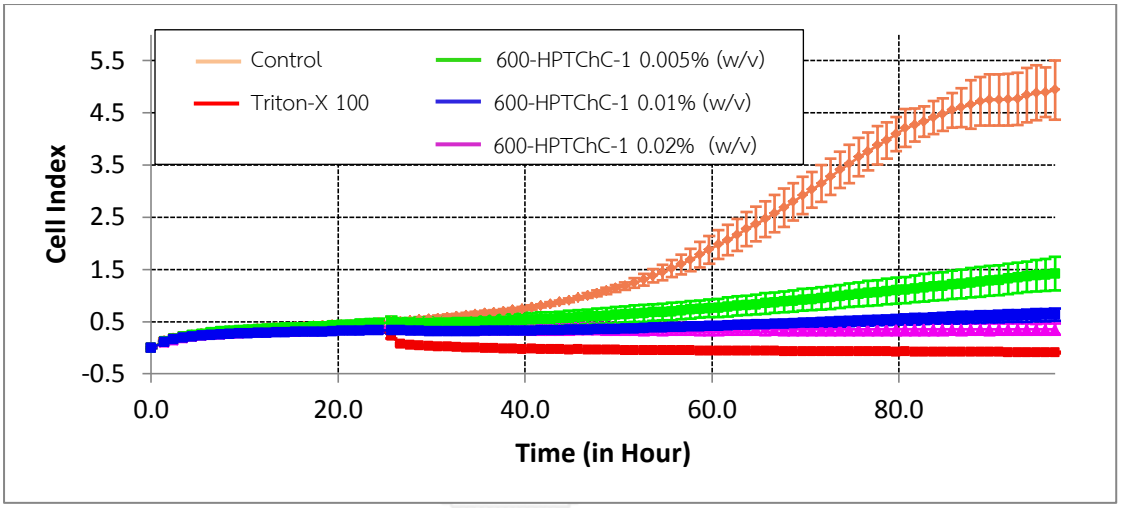

Figure 8. Effect of 600-HPTChC-1 on the real-time proliferation of Caco-2 cells. The cells were cultured for 1 day, followed by treatment with 600-HPTChC-1 for 3 days. The cell spread was expressed as the cell index as calculated by the RTCA software. The data are shown as the mean ± SD (n=3).

In addition, the evaluation of DNA synthesis was executed using the BrdU assay to confirm the anti-proliferative effect of 600-HPTChC. The results of the BrdU assay (Figure 9) were consistent with those of the MTT and RTCA assays. As seen in Figure 9, 600-HPTChC-1 was likely to suppress the intensity of BrdU in dose-dependent manner. These results indicated that the level of DNA synthesis may decrease after continuous exposure to 600-HPTChC-1.

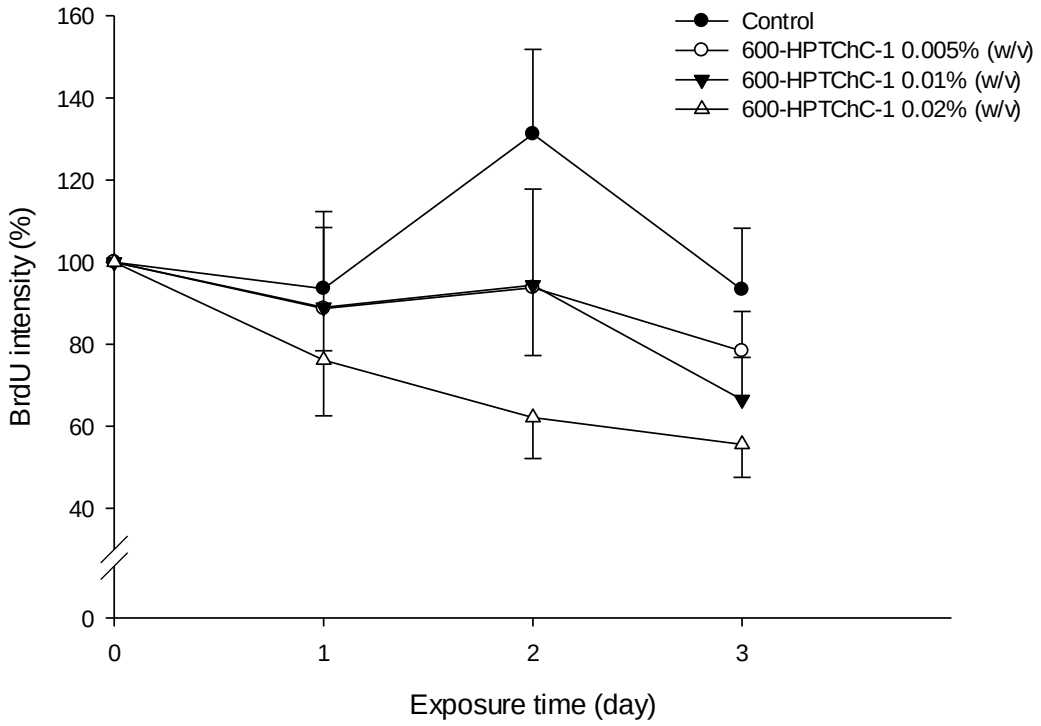

Figure 9. Effect of 600-HPTChC-1 on DNA synthesis of Caco-2 cells. Cells were exposed to 600-HPTChC-1 for 3 days, followed by the BrdU incorporation assay. The percentage of BrdU intensity was calculated and expressed as the mean ± SEM (n=4). Statistical analysis in the group comparison between each concentration of 600-HPTChC-1 and control (no treatment) in the same day was performed by one-way ANOVA following post-hoc Dunnett's test.

4.1.3 Cell cycle analysis

A shown in figure 6, 600-HPTChC-1 significantly decreased proportion of G_0/G_1 cells in dose- and time-dependent manner. Apparently, 600-HPTChC-1 increased proportion of cells in the S and G_2/M phases in dose-dependent manner (Figure 10). The effect of 600-HPTChC-1 on the G_2/M phase was mostly marked at day 3. These findings suggested that 600-HPTChC-1 induced cell cycle arrest in the S and G_2/M phases.

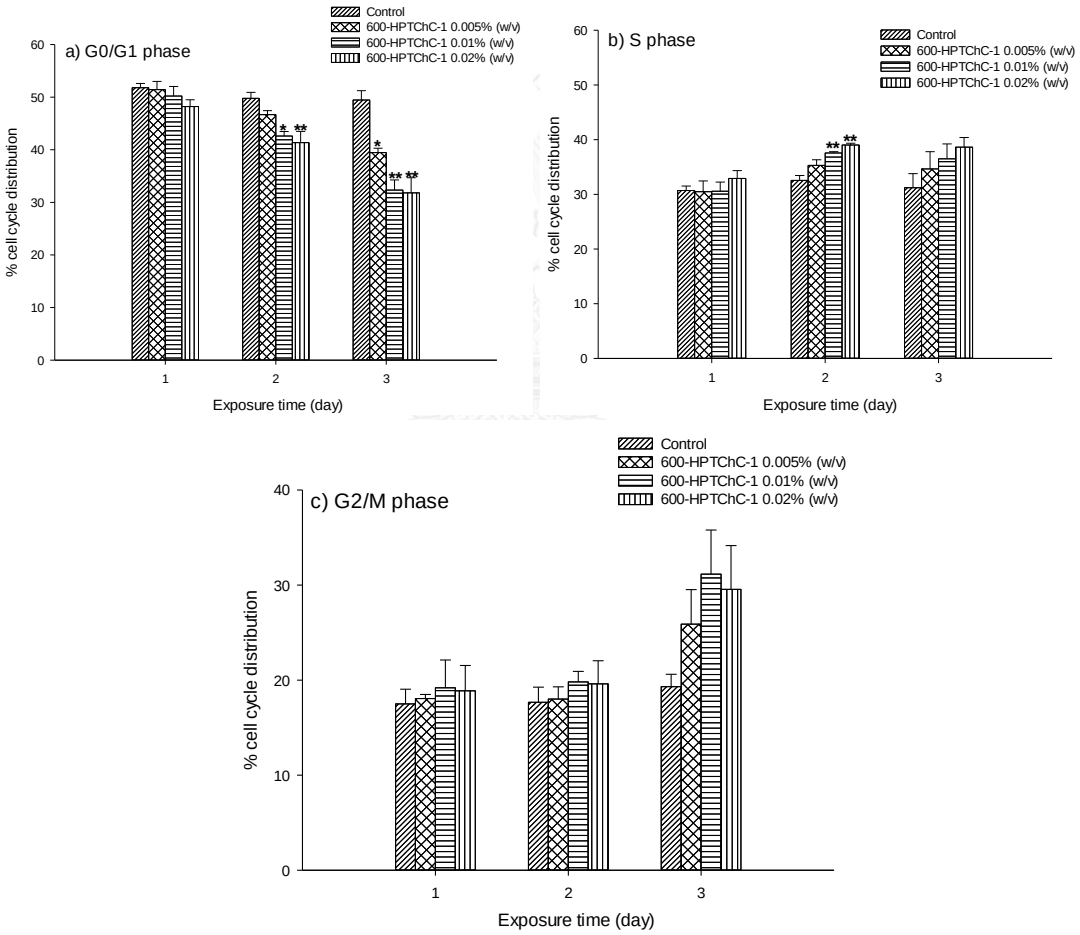

Figure 10. Effect of 600-HPTChC-1 on the cell cycle of Caco-2 cells. Cells were treated with 600-HPTChC-1 for up to 3 days, followed by PI staining and flow cytometry. The data are expressed as percentage of cells in each phase of the cell cycle (n=3). *$p < 0.05$ and **$p < 0.01$ (ANOVA/ Dunnett's test) indicated significant

difference in the group comparison between each concentration of 600-HPTChC-1 and control (no treatment) in the same day.

4.1.4 Effects of 600-HPTChC on intestinal differentiation

The effect of 600-HPTChC on intestinal differentiation into absorptive enterocytes was determined. Caco-2 cells were cultured until forming a confluent monolayer with the use of ALP activity as a marker of intestinal epithelial differentiation (Ferruzza et al., 2012). As shown in Figure 11, 600-HPTChC-1 suppressed the ALP activity in concentration- and time-dependent manner. In addition, 600-HPTChC-1 at a concentration of 0.02% (w/v) significantly reduced ALP activity starting from day 10 to day 14. However, under the intermittent exposure with 4/20 h-on/off period a day for 9 days, 600-HPTChC-1 at a concentration of 0.005% (w/v) had no effect on the ALP activity (Figure 12). These results suggested that the effect of 600-HPTChC-1 on intestinal differentiation depended on exposure period. The mimic condition of internal exposure could attenuate the effect on intestinal differentiation.

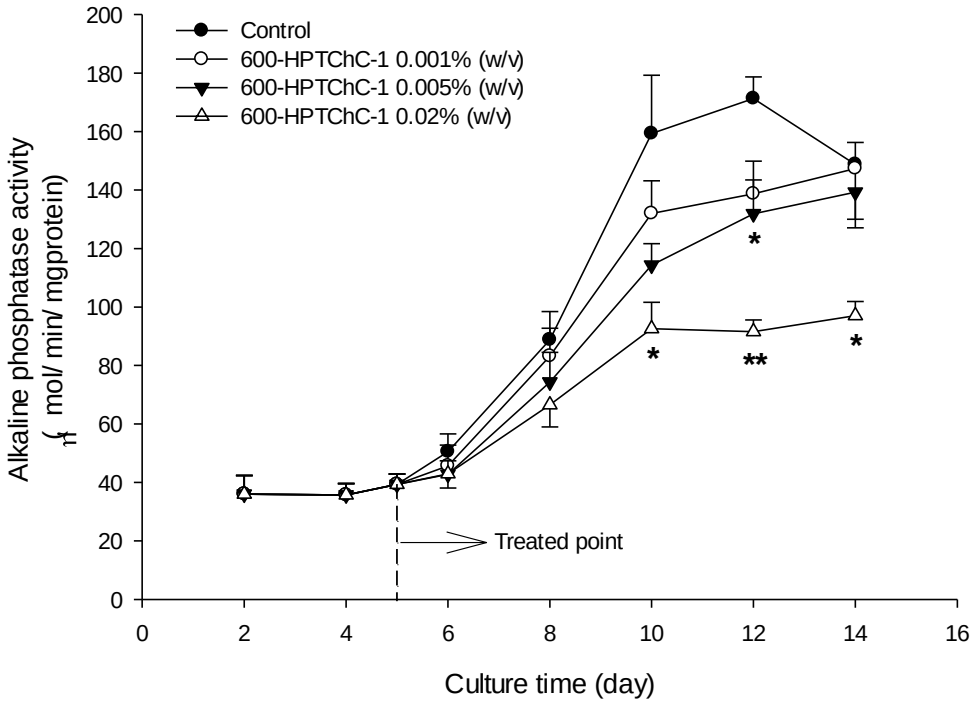

Figure 11. The effect of long-term continuous exposure to 600-HPTChC-1 on ALP activity of Caco-2 cells. Cells were treated with 600-HPTChC-1 starting from day 5 up to day 14. The data are shown as the mean ± SEM (n=3). *$p < 0.05$ and **$p < 0.01$ (ANOVA/ Dunnett's test) indicated significant difference in the group comparison between each concentration of 600-HPTChC-1 and control (no treatment) in the same time point.

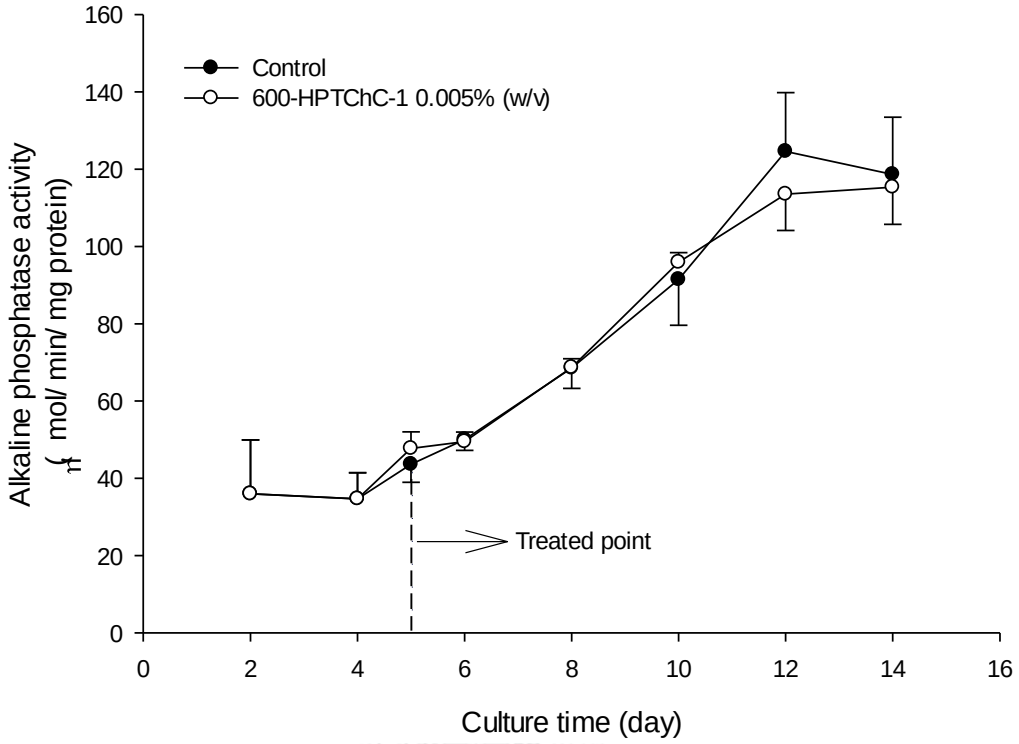

Figure 12. The effect of a short-term continuous exposure to 600-HPTChC-1 on ALP activity of Caco-2 cells. Cells were exposed to 600-HPTChC-1 (0.005% (w/v)) for 4 h/day starting from day 5 up to day 14. The data are shown as the mean ± SEM (n=3). Statistical analysis in the pair comparison between 600-HPTChC-1 and control (no treatment) in the same time point was performed by independent t-test.

4.2 The effect of 600-HPTChC on the tight junction integrity and its mechanism on tight junction disassembly

4.2.1 Effects on tight junction permeability

The exposure dose and time demonstrating well biocompatibility to monolayer Caco-2 cells were chosen to use in the study of paracellular transport. In general, tight junction integrity of Caco-2 cells without treatment was unchangeable, resulting in the expressed TEER value as the percentage of 100% (Hsu et al., 2012; Hsu et al., 2013). The results showed that treatment Caco-2 cells with either 200-HPTChC-1 or 600-HPTChC-1 at the concentration of 0.005% (w/v) for 4 h decreased the TEER values and increased the transport of FITC-dextran 4000 (Figure 13). In addition, 600-HPTChC-1 suppressed the TEER values in the higher degree than 200-HPTChC-1 (Figure 13a). Moreover, the effect of 600-HPTChC-1 on the transport of FITC-dextran 4000 across the cell monolayers was greater than that of 200-HPTChC-1 (Figure 13b). These results suggested that HPTChC-1 synthesized from high molecular weight chitosan (600 kDa) had greater enhancing effect on the tight junction permeability than HPTChC-1 synthesized from low molecular weight chitosan (200 kDa).

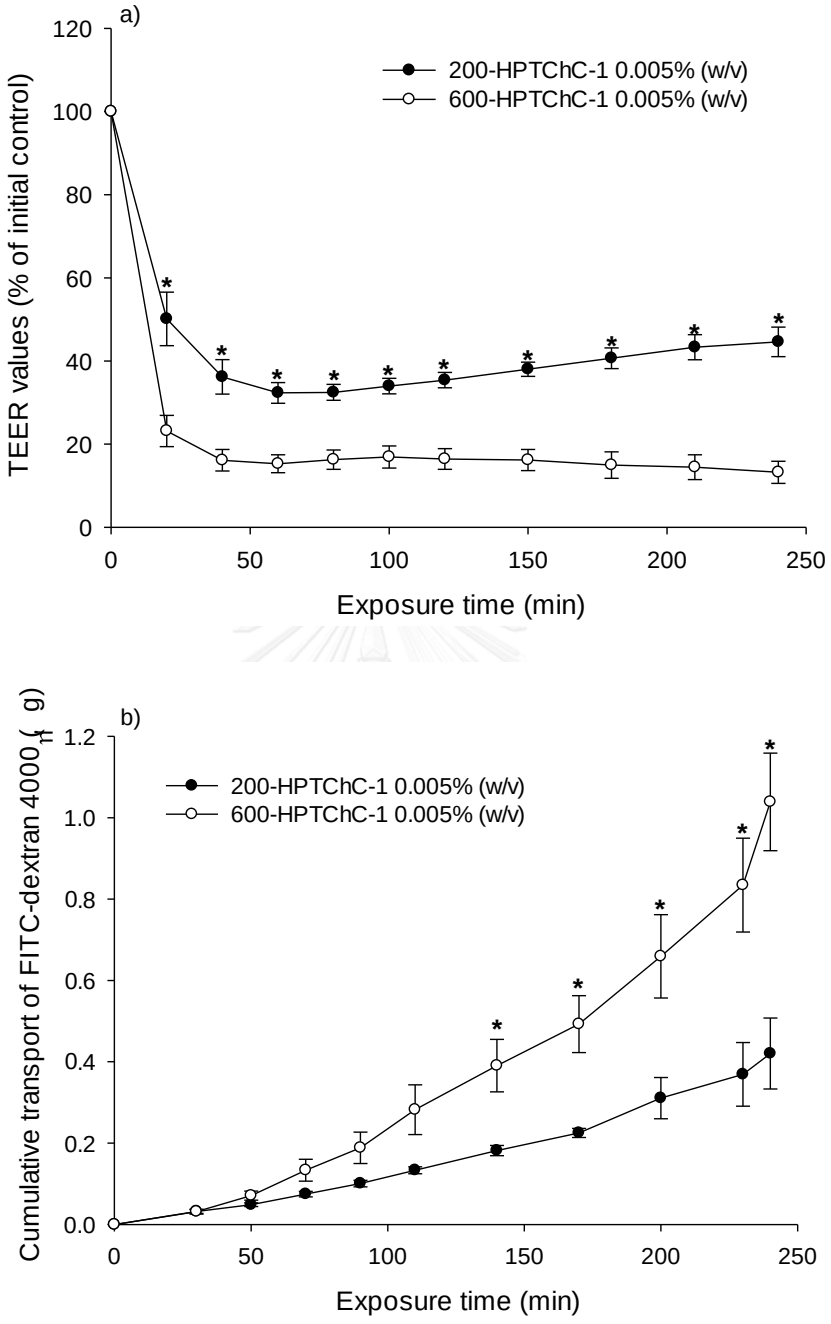

Figure 13. Effects of different molecular weights of HPTChC-1 on tight junction integrity of Caco-2 cell monolayers cultured for 21 days. Tight junction integrity was measured through (a) TEER (% of initial control) and (b) transport of FITC-dextran 4000 (μg) (n=4) (mean ± SEM). *$p < 0.05$ (independent t-test) indicated significant difference between 200- and 600-HPTChC-1 in the same time point.

4.2.2 Effect of concentration on tight junction opening

As shown in Figure 14, 600-HPTChC-1 at concentrations of 0.005%, 0.01% and 0.02% (w/v) had comparable effect on the TEER values and permeable amount of FITC-dextran 4000 transport. Thus, it was likely that the effect of 600-HPTChC-1 under the concentration ranging from 0.005%-0.02% (w/v) on tight junction opening was not concentration-dependent.

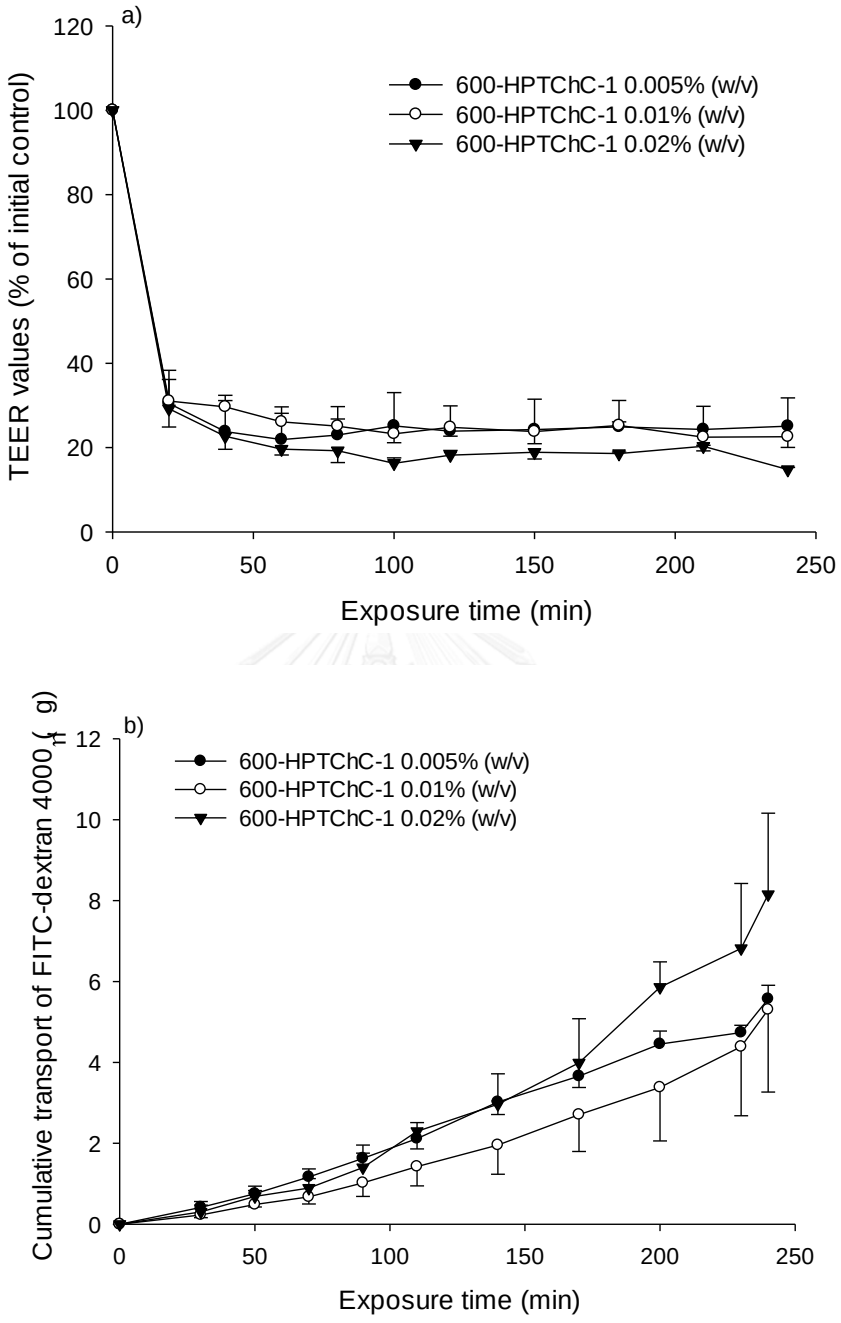

Figure 14. Effect of concentration of 600-HPTChC-1 (0.005%-0.02% (w/v)) on tight junction integrity of Caco-2 cell monolayers cultured for 21 days. Tight junction integrity of Caco-2 cells was measured through (a) TEER (% of initial control) and (b) transport of FITC-dextran 4000 (μg) (n=3). Statistical analysis in the group comparison

in the same time point was performed by one-way ANOVA following post-hoc Dunnett's test.

4.2.3 Effect of quaternary ammonium substituent in chitosan on tight junction permeability and the reversion

The effect of modification of chitosan 600 kDa with quaternary ammonium substituent on tight junction integrity was determined. As shown in Figure 15, either 600-HPTChC-1 or chitosan 600 kDa was able to reduce TEER value and induce the transport of FITC-dextran 4000 across Caco-2 monolayers. However, 600-HPTChC-1 increased tight junction opening more rapidly than chitosan 600 kDa, as evidenced by rapid reduction of the TEER values (Figure 15a). 600-HPTChC-1 was able to reduce the TEER values within the first 40 min of exposure but chitosan 600 kDa did not. In contrast, the effect of 600-HPTChC-1 and chitosan 600 kDa on transport of FITC-dextran 4000 was not different (Figure 15b). Taken together, the results suggested that the quaternary ammonium substituent in chitosan 600 kDa improved the tight junction opening property of chitosan.

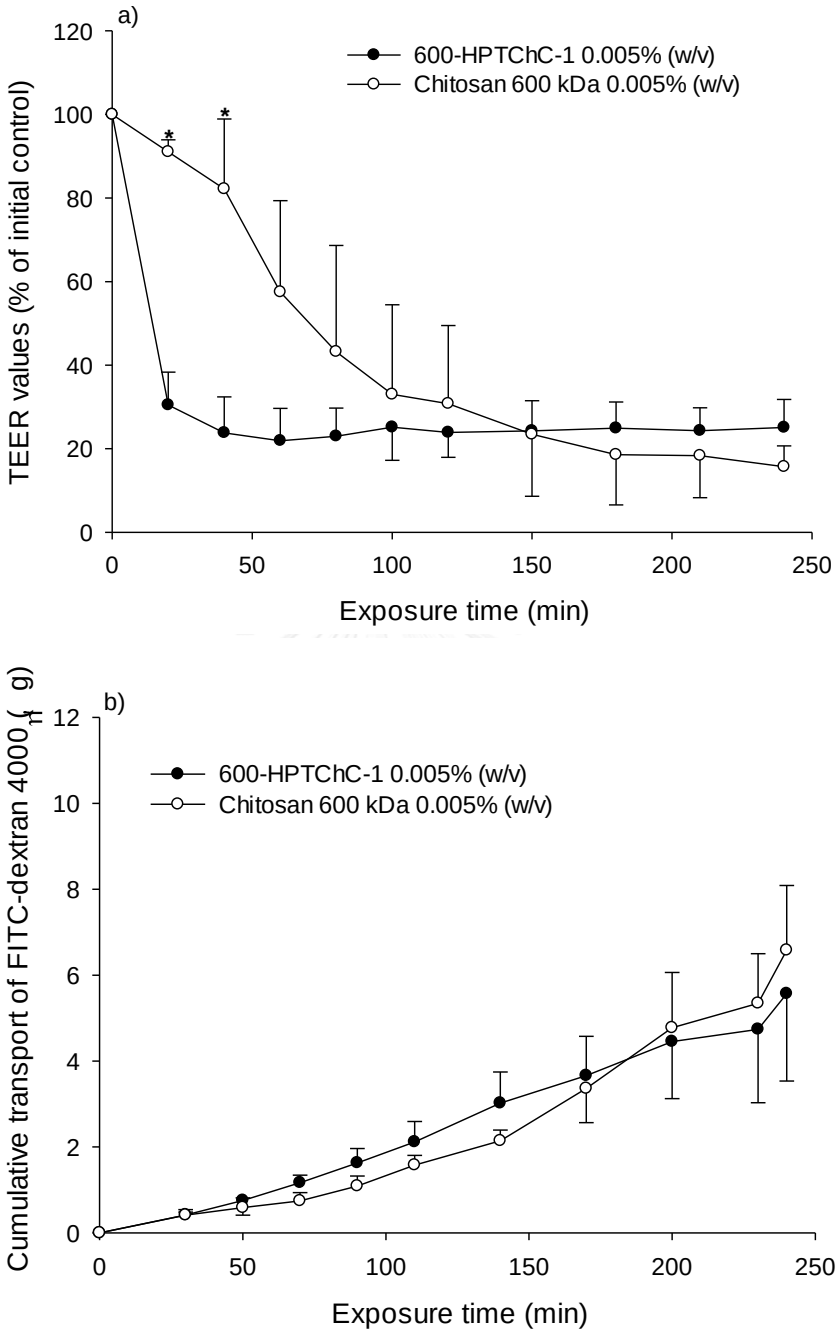

Figure 15. Effect of 600-HPTChC-1 and chitosan 600 kDa (0.005% (w/v)) on tight junction integrity of Caco-2 cells monolayers cultured for 21 days. Tight junction integrity was measured through (a) TEER (% of initial control) and (b) transport of FITC-dextran 4000 (μg) (n=3). *$p < 0.05$ (independent t-test) indicated significant difference between 600-HPTChC-1 and chitosan 600 kDa in the same time point.

Furthermore, the reversible effect of 600-HPTChC-1 and chitosan 600 kDa on tight junction opening was determined after 1-h incubation. During the experiment of tight junction recovery, differentiated Caco-2 cells without exposure normally maintained stable integrity of tight junction (100%) (Yeh et al., 2011), indicating no condition effect in this experiment. Recovery of TEER value was observed after removal either 600-HPTChC-1 or chitosan 600 kDa from the medium (Figure 16). Apparently, the integrity of monolayers treated with 600-HPTChC-1 seemed to recover faster than those treated with chitosan 600 kDa. The TEER values of the monolayers treated with 600-HPTChC-1 appeared to recover at the higher rate than those treated with chitosan and reached the level of completed recovery (100%) within 6 h.

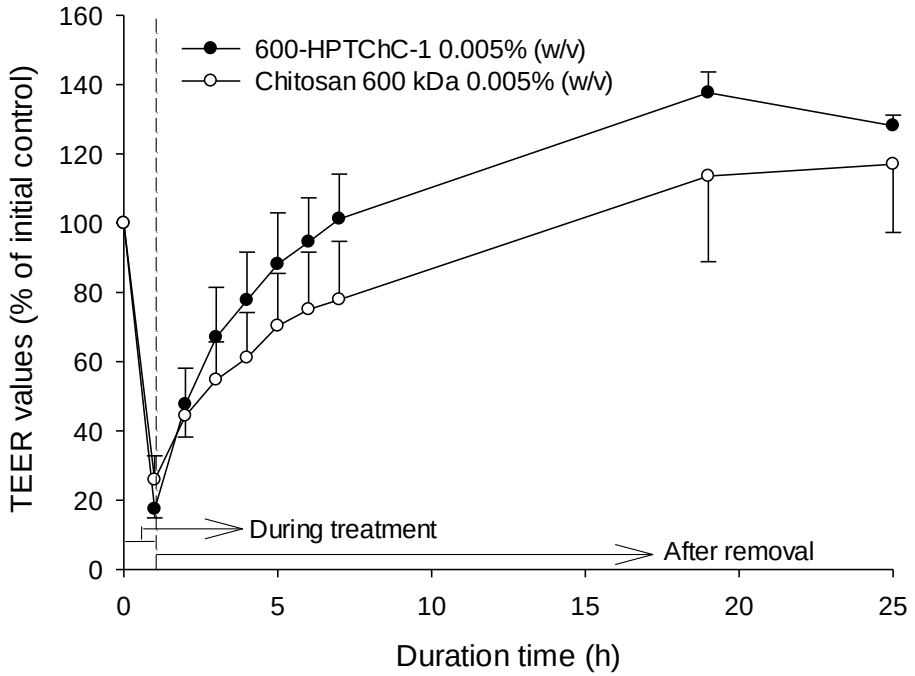

Figure 16. Reversibility of tight junction opening in Caco-2 monolayers after treated with either 600-HPTChC-1 or chitosan 600 kDa for 1 h. Tight junction integrity was measured and presented as the percentage change of TEER values from the initial control (100%) (n=3). Statistical analysis in the pair comparison between 600-HPTChC-1 and chitosan 600 kDa in the same time point was performed by independent t-test.

4.2.4 Effects of 600-HPTChC-1 on tight junction proteins (ZO-1 and occludin)

Immunofluorescence images of 21 day-cultured Caco-2 cells using confocal laser scanning microscopy demonstrated ZO-1 and occludin localization in the intact tight junction structure. Exposure of 600-HPTChC-1 at 0.005% (w/v) for 3 h resulted in a partial breakdown of tight junction complexes in particular ZO-1 and occludin (Figure 17a). Incomplete structure of tight junction proteins partially reversed after removal of 600-HPTChC-1 for 24 h (Figure 17b). These results suggested that partial reversible of 600-HPTChC-1 caused tight junction opening via disruption of the organization of tight junction proteins (ZO-1 and occludin).

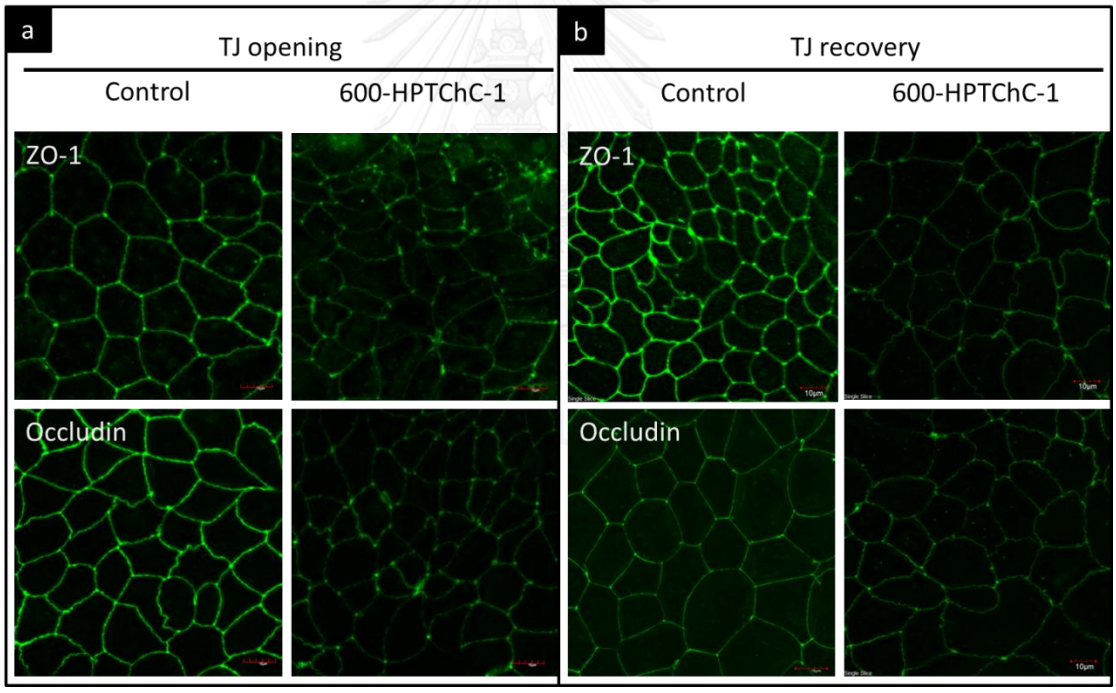

Figure 17. Tight junction opening and recovery after (a) exposure and (b) removal of 600-HPTChC-1 in Caco-2 cells. ZO-1 and occludin localization in 21 day-cultured Caco-2 cells were imaged by confocal laser scanning microscopy (scale bar, 10 μm) after (a) treatment with 600-HPTChC-1 (0.005% (w/v)) for 3 h and after (b) removal for 24 h.

4.2.5 Involvement of signaling pathways in 600-HPTChC-1 mediated tight junction opening

To investigate whether the signaling pathway involved in 600-HPTChC-1-mediated tight junction opening, the cell monolayers were treated with 600-HPTChC-1 at 0.005% (w/v) either in the presence or absence of the specific inhibitors of MLCK, PKC or tyrosine kinase. The results demonstrated that the inhibitors of MLCK, PKC and tyrosine kinase did not inhibit 600-HPTChC-1-mediated TEER reduction (Figures 18a, 18c and 18e). Moreover, inhibition of PKC and tyrosine kinase had no effect on chitosan-mediated tight junction opening (Figures 18d and 18f). However, inhibition of MLCK by ML-7 could partially prevent chitosan-mediated TEER reduction (Figure 18b). These results suggested that the mechanisms of 600-HPTChC-1 induced tight junction opening did not relate to MLCK, PKC and tyrosine kinase pathways. In contrast, chitosan could activate MLCK pathway, leading to tight junction disassembly.

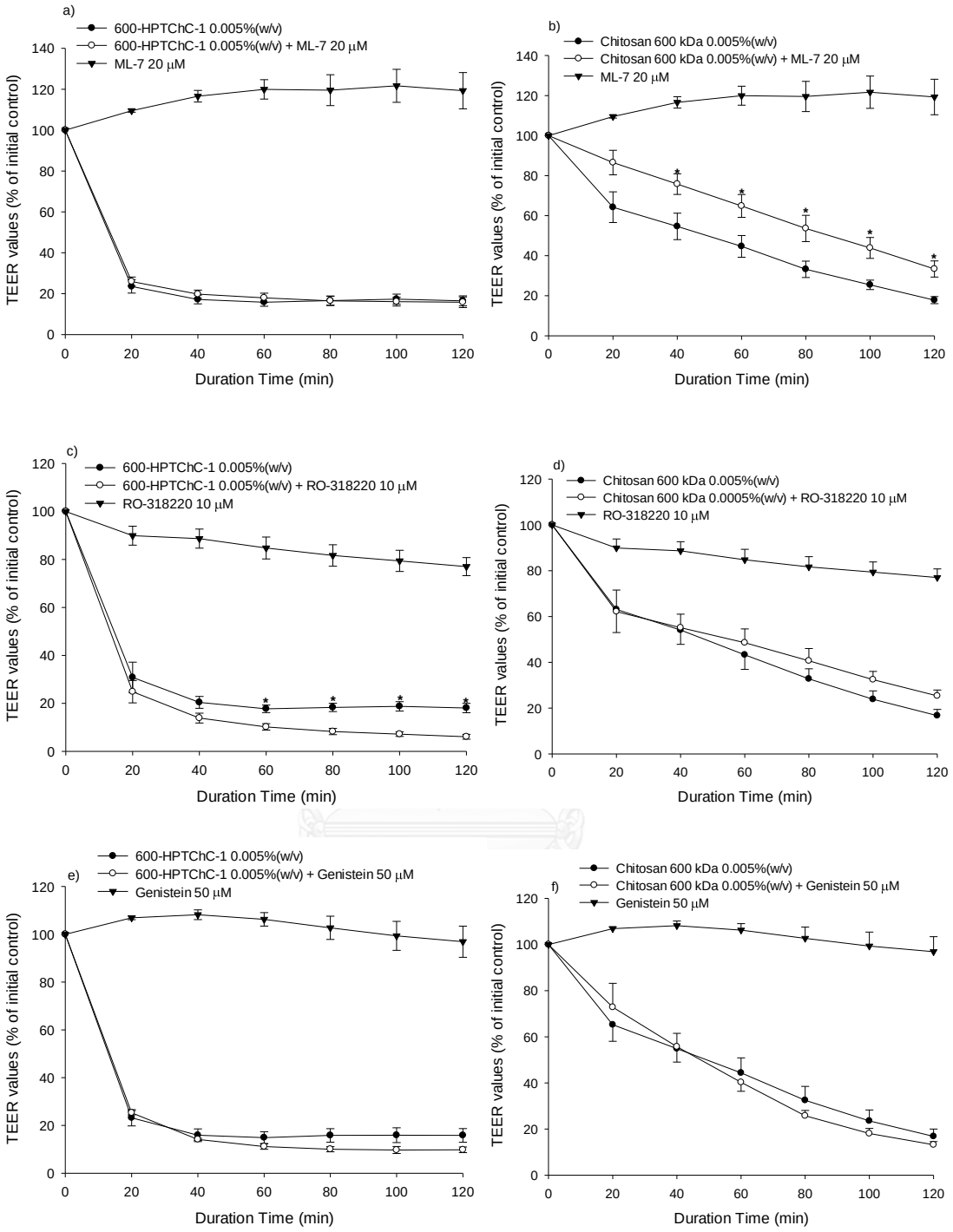

Figure 18. Effect of ML-7 (MLCK inhibitor; a-b), RO-318220 (PKC inhibitor; c-d) and genistein (tyrosine kinase inhibitor; e-f) on either 600-HPTChC-1 or chitosan-mediated tight junction opening). Data are expressed as mean ± SEM from four independent

experiments. *$p < 0.05$ (independent t-test) indicated significant difference between 600-HPTChC-1 groups with and without inhibitors.

4.2.6 Localization of 600-HPTChC-1 and ZO-1 on Caco-2 monolayer

The 3D immunofluorescent images visualized by confocal laser scanning microscopy were performed to illustrate the localization of FITC-600-HPTChC-1 and ZO-1 on Caco-2 monolayer after 4 h treatment (Figure 19). The results showed that green fluorescence of FITC-600-HPTChC-1 was mainly observed at the areas of cell surface and intercellular space nearby tight junction protein. However, there was no green fluorescent signal distributed at intracellular compartment, indicating that 600-HPTChC-1 could not permeate into the cells (Figures 19b and 19c). These findings clearly indicated that 600-HPTChC-1 mainly adhered to cell membrane and intercellular space, which might relate to the disruption of tight junction complex.

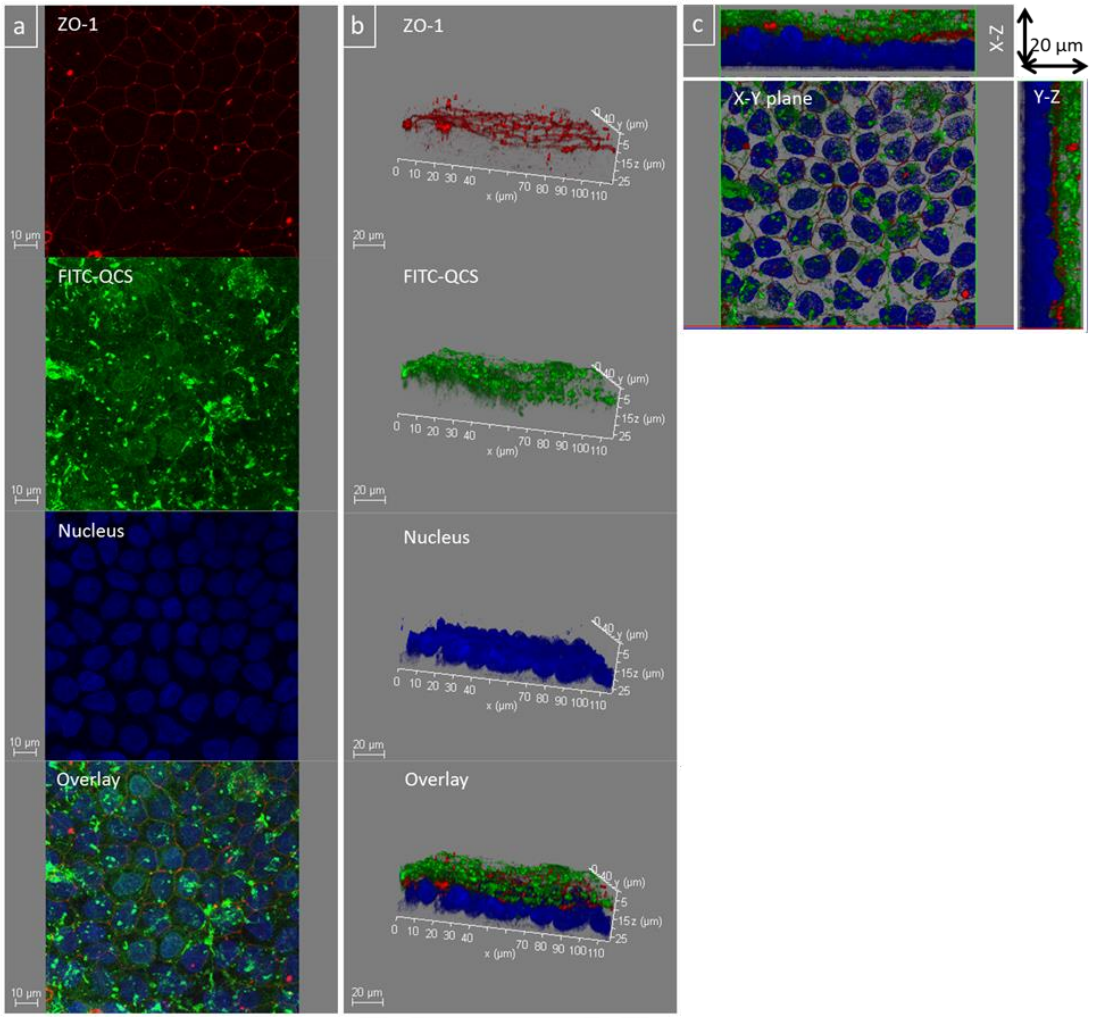

Figure 19. Localization of FITC-600-HPTChC-1 and ZO-1 protein on Caco-2 cell monolayers. Immunofluorescence images of FITC-labeled 600-HPTChC-1 (green), ZO-1 (red) and nucleus (dark blue) were visualized by confocal laser scanning microscopy in (a) 2D (scale bar, 10 µm), (b) 3D (scale bar, 20 µm) and (c) cross section (scale bar, 20 µm) (X-Y plane: the horizontal plane; X-Z and Y-Z planes: the vertical planes) after treatment with FITC-600-HPTChC-1 in 21 day-cultured Caco-2 cells for 4 h.

4.2.7 Effect of the quaternary ammonium substituent of chitosan on mucoadhesive property

The pH effect on a mucoadhesive property of modified chitosan was determined by measuring the zeta potential in mucin solution at various pH (pH 6, 6.5 and 7.4). As shown in Figures 20a and 20b, either 600-HPTChC-1 or chitosan increased the zeta potential in concentration- and pH- dependent manners. The binding of high concentration of 600-HPTChC-1 to mucin surface was much greater than the low concentration. However, at the equivalent concentration, the effect of chitosan on the zeta potential trended to less than that of 600-HPTChC-1 at pH 7.4 (Figure 20c). These findings suggested that chitosan was likely to form the complex with mucin at the lesser amount than modified chitosan did at neutral pH 7.4. Therefore, introducing the quaternary ammonium substituent into chitosan may improve the mucoadhesive property to plasma membrane especially in pH 7.4.

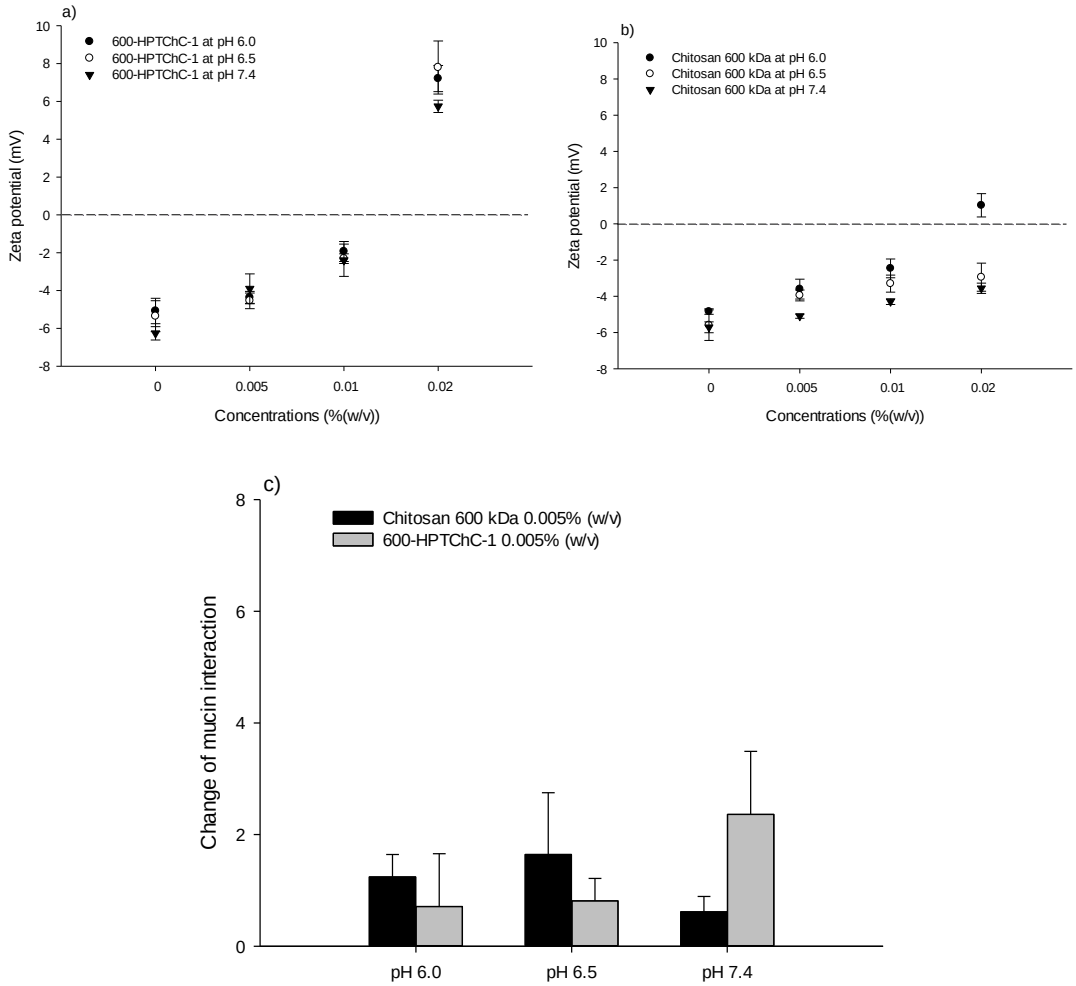

Figure 20. Zeta potential of SS-mucin particles after mixing with either chitosan 600 kDa or 600-HPTChC-1 at different pH conditions. The effect of pH and concentrations of (a) 600-HPTChC-1 and (b) chitosan 600 kDa on the zeta potential of mucin were investigated. (c) Change of the zeta potential of mucin interaction with either chitosan 600 kDa or 600-HPTChC-1 at the concentration 0.005% (w/v). The data are presented by mean ± SEM of three independent experiments. In figure 20C, statistical analysis in the pair comparison between 600-HPTChC-1 and chitosan 600 kDa in each pH treatment and the group comparison between pH 6.5 or 7.4 and pH 6.0 was performed by one-way ANOVA following post-hoc Dunnett's test.

4.3 Effect of 600-HPTChC on transcellular transport via drug efflux transporter (P-gp)

4.3.1 Effect of 600-HPTChC-1 on digoxin absorption

The effect of 600-HPTChC-1 on drug permeability was evaluated by using of [^{3}H]-digoxin as a representative P-gp substrate. As shown in Figure 21, 600-HPTChC-1 enhanced Papp of [^{3}H]-digoxin in the AP-BL direction comparing to the control group. In the BL-AP direction, 600-HPTChC-1 decreased efflux transport of [^{3}H]-digoxin. Under the calculation from Papp, 600-HPTChC-1 reduced the efflux ratio of [^{3}H]-digoxin in Caco-2 cells (ER=5.20-5.78), similar to the result of verapamil (P-gp inhibitor) (ER=1.52). These results demonstrated that 600-HPTChC-1 increased [^{3}H]-digoxin transport across the intestinal epithelial model.

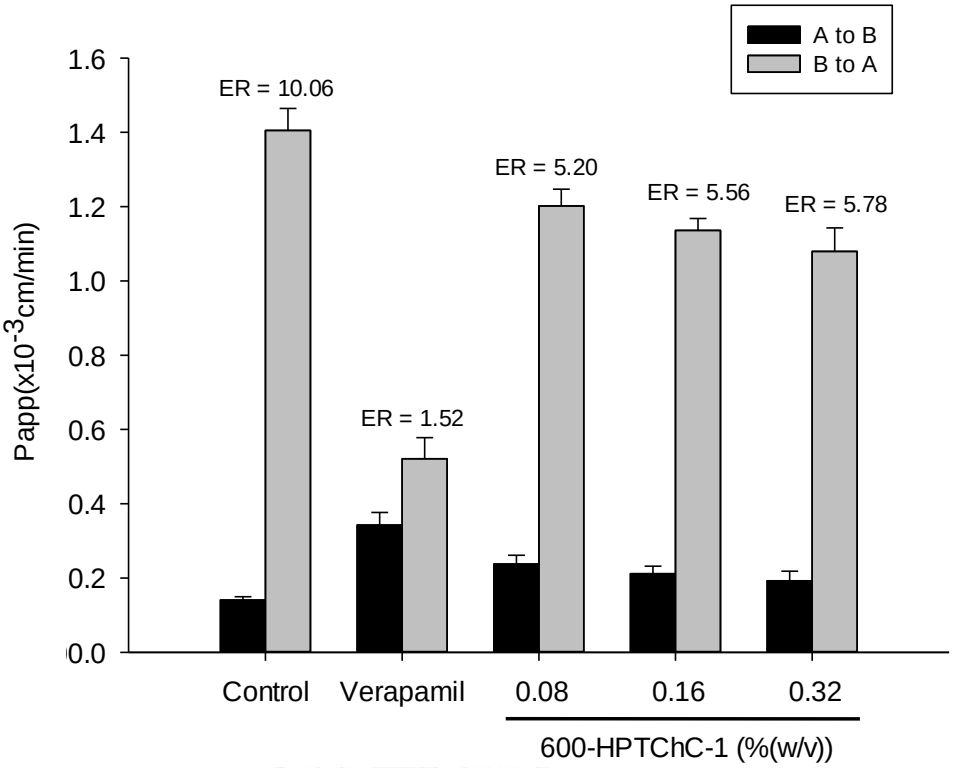

Figure 21. Effect of 600-HPTChC-1 on bi-directional transport of [^{3}H]-digoxin across Caco-2 cells. Data are expressed as the apparent permeability coefficient (Papp) and efflux ratio (ER) (mean ± SEM) (n=4).

4.3.2 Inhibition of 600-HPTChC-1 on P-gp function

The specific effect of 600-HPTChC-1 on P-gp function was further examined in Caco-2 cells using calcein accumulation assay. Verapamil (P-gp inhibitor) was used as positive control. As shown in Figure 22, verapamil increased intracellular calcein accumulation by 3-fold, suggesting an appreciable level of P-gp activity in the cells under this experiment condition. In this study, 600-HPTChC-1 was able to increase intracellular calcein accumulation in dose-dependent manner. At the highest concentration (0.8% (w/v)), an increase of calcein accumulation was obviously observed in Caco-2 cells (Figure 22). Hence, it was likely that 600-HPTChC-1 could suppress P-gp function.

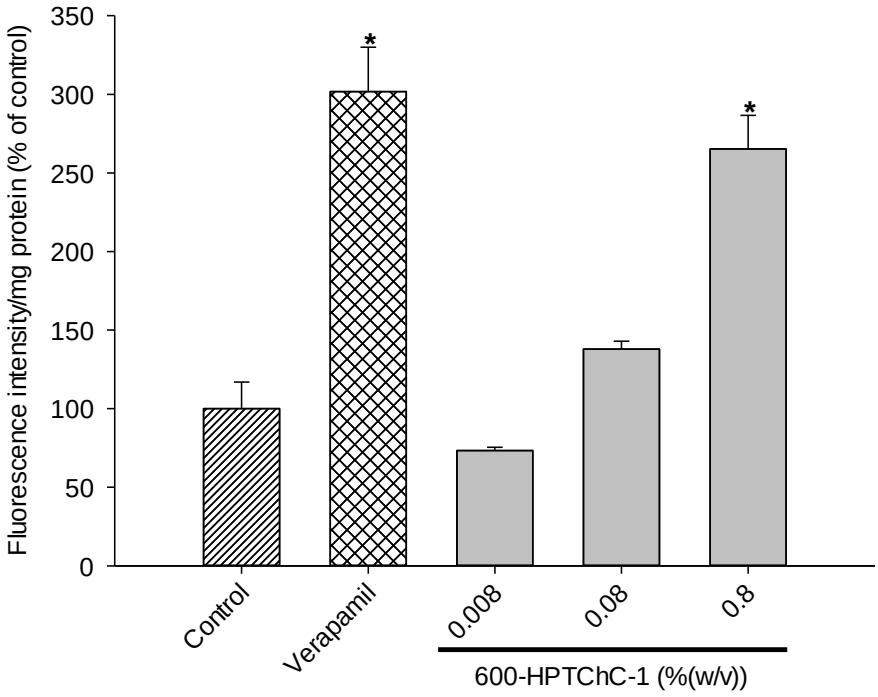

Figure 22. Effect of 600-HPTChC-1 on P-gp function in Caco-2 cells by calcein accumulation assay. Data are expressed as the mean ± SEM (n=3). *$p < 0.05$ (ANOVA/ Dunnett's test) indicated significant difference in the group comparison between each treatment and the control.

4.3.3 Interaction of 600-HPTChC-1 with P-gp and effect on conformation change

The interaction between 600-HPTChC-1 (FITC) and P-gp expressed on the apical side was demonstrated by immunofluorescence imaging under a confocal laser scanning microscope. As seen in Figure 23, the green color of FITC-600-HPTChC-1 overlapped with P-gp protein, suggesting direct interaction of FITC-600-HPTChC-1 with P-gp protein. In addition, detection of P-gp epitope using UIC2 demonstrated the conformational change of P-gp in 600-HPTChC-1 treated group, as shown by rightward shift of fluorescence signal of FITC after addition of FITC-conjugated UIC2 to 600-HPTChC-1 treated cells (Figure 24). These findings suggested that the 600-HPTChC-1 treated cells caused the higher amount of UIC2-P-gp complexes, comparing with untreated group. Remarkably, the shift of 600-HPTChC-1 was stronger than verapamil which is the positive control.

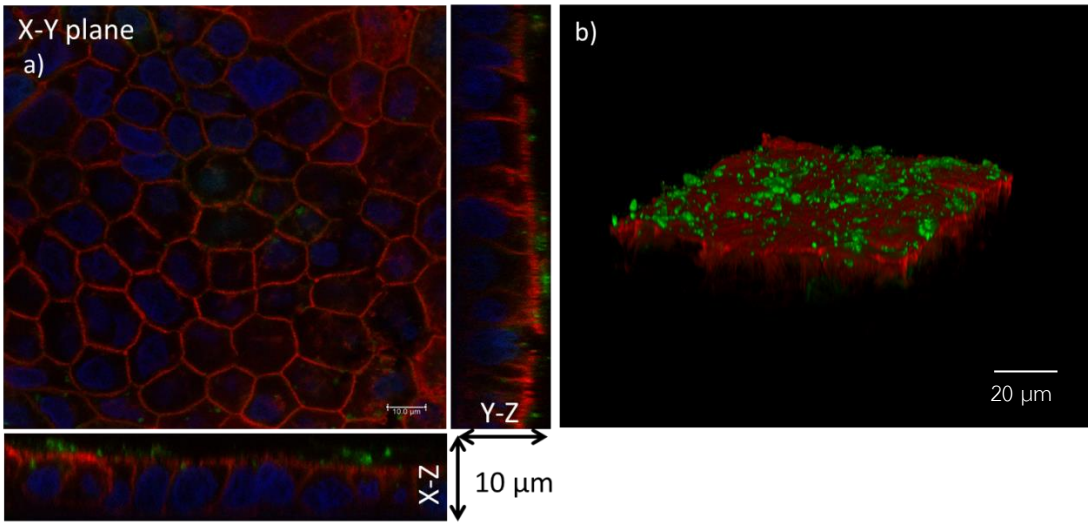

Figure 23. Immunofluorescent images of the Caco-2 cells visualized by confocal laser scanning microscopy. Immunofluorescence images of FITC-labeled 600-HPTChC-1 (green), Alexa Flour 568 labeled P-gp (red) and nucleus (dark blue) were collected by confocal laser scanning microscopy in (a) 2D and cross sectional image (scale bar, 10 µm) (X-Y plane: the horizontal plane; X-Z and Y-Z planes: the vertical planes) and (b) 3D images after treatment with FITC-600-HPTChC-1 in 21 day-cultured Caco-2 cells for 4 h (scale bar, 20 µm).

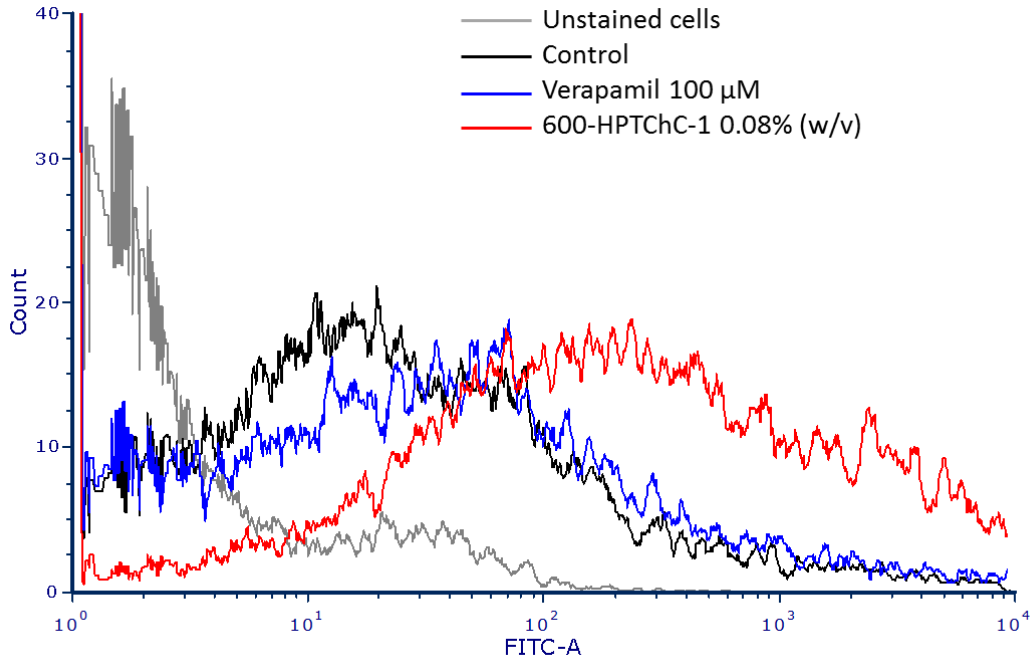

Figure 24. Binding of FITC-monoclonal antibody UIC2 to P-gp epitope in Caco-2 cells. The cells were incubated with FITC-UIC2 antibody in the absence (control) or presence of either verapamil 100 µM or 600-HPTChC-1 (0.08 % (w/v)) and analyzed by flow cytometer. The cells without FITC-UIC2 labeling were unstained cells. The representative images from 3 independents experiments were shown.

4.3.4 Effect of 600-HPTChC-1 on P-gp ATPase activity

The measurement of the P-gp ATPase activity was used sodium vanadate (P-gp ATPase inhibition) to express the P-gp independent ATPase activity (background) (Appendix G). Difference between the luminescent signal from sodium vanadate treated group and the others was determined as the consumption of ATP. To confirm the condition use in P-gp ATPase study, verapamil was used as P-gp ATPase stimulation. The results demonstrated that change in luminescence of ATPase in verapamil was higher than the untreated group, indicating increase of the ATP consumption from basal P-gp ATPase activity (Figure 25). Similar to verapamil, 600-HPTChC-1 at the concentrations higher than 0.08% (w/v) also seems to increase cellular ATPase activity by induction of the change level of intracellular luminescence, reflecting an ATPase mediated – conversion of ATP to ADP. These results suggested that 600-HPTChC-1 may act as P-gp ATPase stimulator.

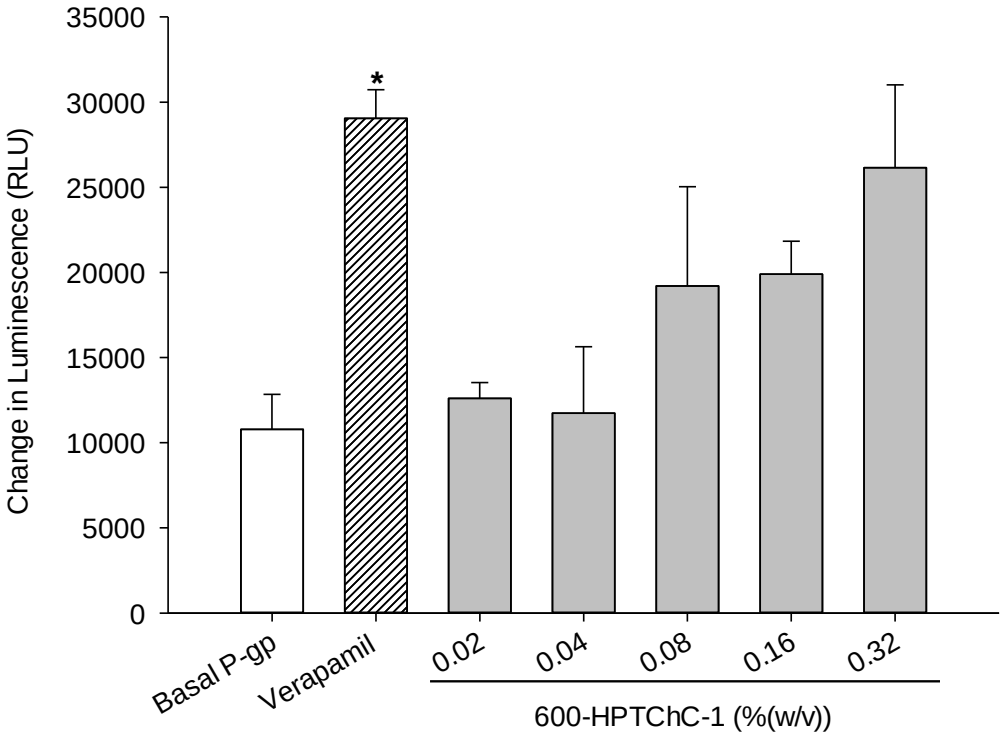

Figure 25. Effect of 600-HPTChC-1 on P-gp ATPase activity in recombinant human P-gp membranes. Verapamil was used as P-gp stimulator (the positive control). The results were measured as the change in luminescence (RLU) in triplicate and expressed as the mean ± SEM (n=3). *$p < 0.05$ (ANOVA/ Dunnett's test) indicated significant difference in the group comparison between each treatment and Basal P-gp.

4.3.5 Effect of 600-HPTChC-1 on P-gp expression

The effect of 600-HPTChC-1 on P-gp expression was further investigated. After 1-day treatment, 600-HPTChC-1 even at the high concentration of 0.32% (w/v) had no effect on amount of *MDR1* mRNA (Figure 26) and P-gp protein expression (Figure 27). These results revealed that the suppressive effect of 600-HPTChC-1 on P-gp function did not involve at transcriptional and translational level.

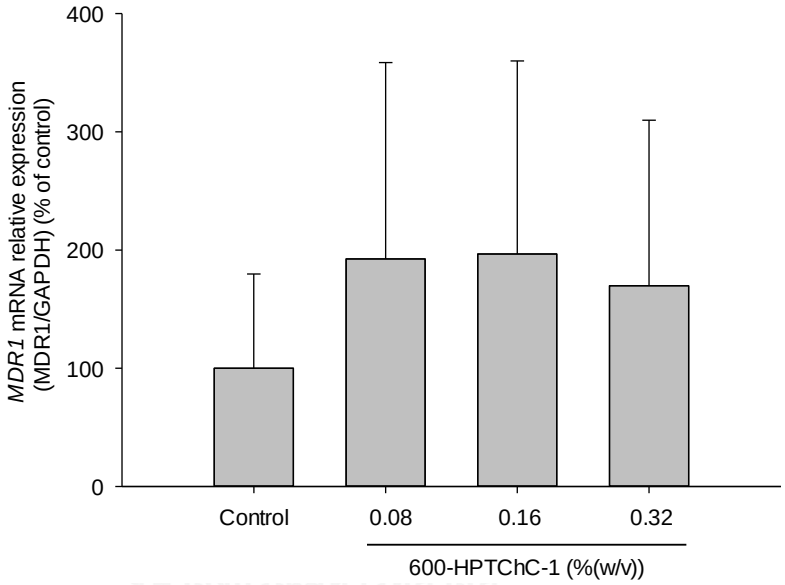

Figure 26. Effect of 600-HPTChC-1 on *MDR1* expression after 1 day-treatment in Caco-2 cells measured by qRT-PCR. The expression of *MDR1* mRNA was normalized by the expression of house-keeping *GAPDH*. Each bar represents the mean ± SEM (n=3). Statistical analysis in the group comparison between each treatment and the control was performed by one-way ANOVA following post-hoc Dunnett's test.

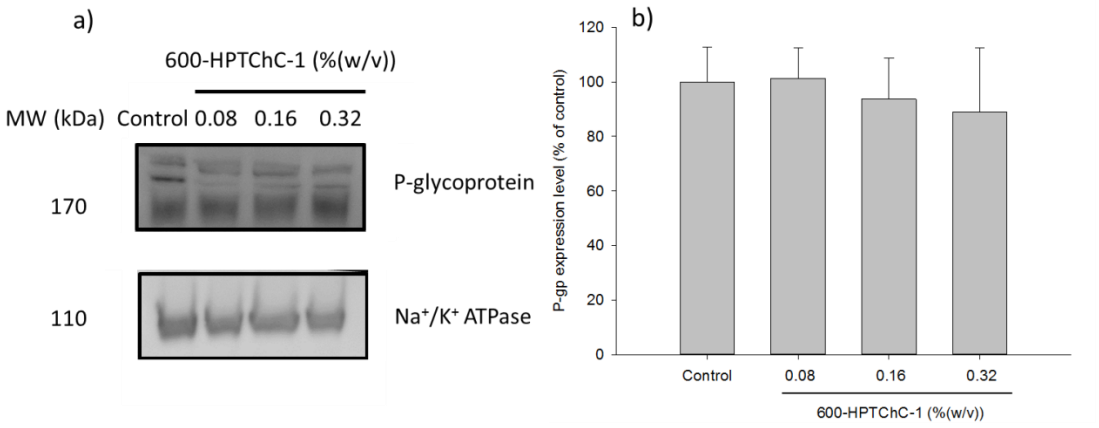

Figure 27. Effect of 600-HPTChC-1 on P-gp expression after 1-day treatment in Caco-2 cells. (a) Western blot analysis and (b) densitometric analysis of P-gp expression level (mean ± SEM) obtained from three experiments. Na^+/K^+ ATPase was used as the internal standard. Statistical analysis in the group comparison between each treatment and the control was performed by one-way ANOVA following post-hoc Dunnett's test.

CHAPTER V

DISCUSSION AND CONCLUSIONS

To overcome the limitation of the low solubility of chitosan in physiological fluids, HPTChC was synthesized by quaternization of chitosan with Quat-188. With its good mucoadhesive properties and improvement of solubility, HPTChC was studied *in vitro* as a potential gene delivery carrier (Theerawanitchpan et al., 2012). In this study to further evaluate the possibility of applying 600-HPTChC as a drug delivery carrier in humans by oral administration, the biocompatibility of 600-HPTChC and its enhanced mechanisms on paracellular and transcellular transport across the human intestinal barrier was evaluated *in vitro* using the Caco-2 cell line as a model of intestine system.

Biocompatibility of 600-HPTChC

The potential biological effects of 600-HPTChC on the acute cytotoxicity, proliferation, and long term effect on intestinal differentiation, plus the important factors that influence the biocompatibility of 600-HPTChC, were evaluated and discussed. Although chitosan has a high biocompatibility to cells, the biological effects of 600-HPTChC on the intestinal barrier are not clear. Thus, following the recommended testing methods for biocompatibility assessment (ISO10993-10995, 2009), the biological effects of 600-HPTChC was examined for the metabolic impairment of mitochondria (MTT assay) by measuring the mitochondria enzyme activity and the membrane integrity through the leakage of intracellular LDH. Exposure to 600-HPTChC resulted in both acute cytotoxicity and inhibition of proliferation of Caco-2 cells, but was clearly dependent upon the DQ of 600-HPTChC (Figures 6, 7 and 8). The lower the DQ of 600-HPTChC the higher was the observed biocompatibility, in terms of the cytotoxicity (the higher 600-HPTChC-1 IC_{50} and EC_{50} values in the MTT and LDH assays, respectively, after 4 h) and the inhibition of

proliferation (higher 600-HPTChC-1 IC_{50} value in the MTT assay after 3 days) of Caco-2 cells (Table 2). The lower biocompatibility of 600-HPTChC preparations with a higher DQ would mainly be caused by the increasing level of the substitution moiety, since Quat-188 itself was cytotoxic to Caco-2 cells after 4 h while chitosan was not (Appendix C).

In addition to the factor of DQ, the number of positive charge would be able to determine from the molecular mass and possibly cause the differential effect to the cells. It has been reported that high MW generates the long length of chitosan chain and high density of positive charge on a single molecule causing more interaction with cell membrane and then more disturbance of cell membrane (Chae, et al., 2005; Wiegand, Winter and Hipler, 2010). However, Huang, Khor and Lim, (2004) showed a greater influence of the degree of modification of chitosan on the uptake and cytotoxicity of chitosan nanoparticles than MW. In the present study, the results of the molecular mass after modification among 600-HPTChC did not significantly different as shown in Appendix A. In addition, we did not observed the correlation between the molecular mass on cellular toxicity. Therefore, in our study, the molecular mass is unlikely the main factor playing the role on differential cytotoxicity among 600-HPTChC.

Since the high molecular weight chitosan derivatives could not pass though the cell membrane (Tan et al., 2013), the mechanism of cytotoxicity of 600-HPTChC with a high DQ is likely to be mediated by disrupting and damaging the cell membrane integrity. The DQ of 600-HPTChC determines the number of positive charges available on the molecule for interaction with the negatively charged sites on the epithelial membrane and thereby influences its drug-absorption enhancing properties (Hamman, Schultz and Kotze, 2003). However, these can cause membrane disruption and leakage of intracellular enzyme across the cell membrane (Frohlich, 2012). Moreover, the presence of Quat-188 in 600-HPTChC made a more

branched structure compared with the back bone chitosan. The high density of cationic residues and branch structure likely increased the ability of 600-HPTChC to interact with access the cell membrane (Fischer et al., 2003) and so result in cell membrane damage.

The inhibitory effect of 600-HPTChC on Caco-2 cell proliferation probably results from cell cycle disturbance in these cells, where exposure to 600-HPTChC-1 for 3 days markedly decreased the proportion of cells in the G_0/G_1 phase and caused cell cycle arrest in the S and G_2/M phases in a concentration-dependent manner. That the alteration of the proportion of Caco-2 cells in each phase of the cell cycle by 600-HPTChC-1 occurred slowly (detectable from day 3) is because the population doubling time for these cells is 62 h. The potential cell cycle arrest induced by 600-HPTChC-1 was consistent with its anti-proliferative effect and reduced DNA synthesis (Figures 7 and 9). In addition, the anti-proliferative activity of other compounds, such as resveratrol and other polyphenols, has been reported previously to also increase the proportion of cells at S phase (Joe et al., 2002; Cilla et al., 2010), where a blockade of the S phase correlates with the inhibition of DNA replication (Xu et al., 2001). Moreover, the cell cycle arrest at the G_2/M phase during cell proliferation, in order to respond to the toxic effects, such as oxidative stress, consequently induces the cells to undergo premature senescence (Rajesh et al., 2013). Overall, the data supports that the inhibitory effects of 600-HPTChC on Caco-2 cell proliferation could reflect the perturbed DNA synthesis from cell cycle arrest.

With respect to the physiology of intestinal cells, the differentiation of epithelial cells is required to generate a functional enterocyte on the top of villi after cell proliferation to regenerate the cell layer (Snoeck et al., 2005). The disturbance of the cell cycle and cell proliferation by 600-HPTChC might consequently delay their differentiation and so delay the formation of the intestinal barrier with a normal absorptive function. Therefore, the biocompatibility of 600-HPTChC on intestinal

differentiation was evaluated in vitro using both long-term and short-term treatment with a 600-HPTChC-1 dose that caused a low effect on Caco-2 cell proliferation. For evaluating Caco-2 differentiation the apical brush border ALP enzyme, which is expressed at higher levels during cell differentiation (Snoeck et al., 2005; Ferruzza et al., 2012), was used as a differentiation marker. This enzyme plays an important role in nutrient metabolism and neutralized inflammation in the intestine (Lalles, 2010). In the long-term continuous treatment over 9 days, the highest biocompatibility 600-HPTChC (600-HPTChC-1) at a dose of 0.005% (w/v) decreased the level of ALP compared to the untreated control, indicating a likely delayed cell differentiation (Figure 11). If so, the long-term continuous treatment with 600-HPTChC-1 might delay differentiation of polarized intestinal epithelial cells to functional enterocytes.

The exit from the cell cycle after growth arrest is an important event leading to cell differentiation in transformed cell lines, such as oligodendrocytes and chondrocytes (Miller et al., 2007). Interestingly, the Caco-2 cell cycle pattern was different between unpolarized Caco-2 cells exposed to 600-HPTChC-1 or not. Exposure to 600-HPTChC-1 reduced the proportion of cells in the G_1 phase, and blocked the cell cycle at the S and G_2/M phases in unpolarized cells, while the untreated Caco-2 cells arrested at the G_1 phase before entering the differentiation process (Figure 10). The involvement of the normal cell cycle arrest at G_1 phase and differentiation of Caco-2 cells was reported to occur via suppression of the cyclin-dependent kinases, CDK2 and CDK4 (Ding et al., 1998), as was the importance of cell cycle protein suppression and p21 induction in differentiating Caco-2 cells (Evers et al., 1996). Therefore, it remains plausible that 600-HPTChC-1 might delay the differentiation process in unpolarized Caco-2 cells by alteration of the cell cycle pattern and the expression of cell cycle proteins.

In addition to the disturbance of the cell cycle, the loss of contact inhibition in Caco-2 cells, as a result of the anti-proliferative effects of 600-HPTChC reducing

the degree of confluency of the cultures compared to the control cells at each time point, might be another factor reducing the cell differentiation level in the long-term continuous treatment of Caco-2 cells with 600-HPTChC-1. At a high cell density (high % confluency), the increasing contact inhibition of confluent cells suppresses their cell growth through cadherin adhesion molecules (Gerard and Goldbeter, 2014). E-cadherin-mediated cell-cell contact is an important event in the assembly of adherent junctions and differentiation (Young et al., 2003), and contact inhibition signals the proliferating epithelial cells to differentiate (Puliafito et al., 2012). Thus, the anti-proliferation effect of 600-HPTChC-1 may have reduced the cell density and so contact inhibition level in the 600-HPTChC-1 treated cells and consequently delayed the differentiation process.

In contrast to the long-term continuous treatment of 600-HPTChC-1, the short-term discontinuous exposure, that more likely simulated the intestinal exposure time, could attenuate the inhibitory effect of 600-HPTChC-1 on cell differentiation. In the present study, we observed that short-term discontinuous treatment (4 h/day for 9 day) of 600-HPTChC-1 at 0.005% (w/v) did not alter the level or rate of Caco-2 differentiation, as determined by the ALP activity level (Figure 12). Moreover, exposure to 600-HPTChC-1 at 0.005% (w/v) was non-toxic to Caco-2 cells after a non-repeated exposure for 4 h, with a cell viability of more than 90%. On the other hand, an altered cell cycle was evident after a 3 day-treatment of 600-HPTChC-1 at 0.005% (w/v), which likely relates to the delayed differentiation of Caco-2 cells. This result is consistent with other reports showing the suppression of cell differentiation in Caco-2/15 cells in the long-term continuous treatment with a stress-activated protein kinase inhibitor (Houde et al., 2001), and that peroxide-induced oxidative stress could suppress cell differentiation in other types of cells, such as osteoblastic cells (Bai et al., 2004). Therefore, it is possible that the long-term continuous treatment of 600-HPTChC-1 could induce cellular stress and

consequently suppress the cell differentiation process, but the short-term discontinuous exposure did not and so the differentiation process continued. Taken together, these results suggest that in addition to the DQ and concentration, the exposure time is another crucial factor that plays an important role in the biological responses, including the intestinal differentiation delay, to 600-HPTChC-1 exposure.

However, formulation of 600-HPTChC should be further developed to achieve the approach of the potential drug release *via* oral route. To reach the target site in the intestine, the drug carrier should be appropriately formulated to overcome the obstacles in the GI tract for acid-intolerance chitosan and chitosan derivatives. Formulation in the controlled drug delivery or acid resistance would avoid the drug release and degradation in the stomach (Fukui et al., 2000; Jayakumar, Reis and Mano, 2006), and therefore increase the appropriate amount of drug on the target site. Once 600-HPTChC finally reaches the intestine, 600-HPTChC possibly attach to the intestinal barrier with their mucoadhesive properties and enhance drug delivery *via* their properties as tight junction opener.

It is necessary to highlight that the biocompatible concentrations of 600-HPTChC-1 in the undifferentiated and differentiated cells were different. According to the cell viability more than 80%, the non-toxic concentrations of undifferentiated and differentiated Caco-2 cells were less than 0.005% (Figure 6a) and 0.04% (w/v) (Appendix F), respectively. The morphology and biology systems of undifferentiated cells need biological development to resist the cytotoxic of high concentrations compared to the differentiated cells (Sasaki, Baba and Matsuo, 2001; Thompson et al., 2012). Selection of the optimum concentrations for treatment in different morphology of cells by considering the cytotoxicity and effectiveness could clearly demonstrate the properties of 600-HPTChC-1 on intestinal barrier without interferences.

The *in vitro* biocompatibility assessment of 600-HPTChC is important in its development as a drug carrier in humans by oral administration. The important influencing factors for biocompatibility of 600-HPTChC were the DQ, concentration and exposure time. The results presented here demonstrated that 600-HPTChC with a low DQ and at a low concentration had a low effect on the proliferation and differentiation in Caco-2 cells. Moreover, under physiological conditions that mimic the likely short-term exposure time of the intestine, 600-HPTChC-1 had a good compatibility with no effect on Caco-2 differentiation after a 4 h/day exposure over a 9 day period. Therefore, consideration of the optimum DQ and appropriated dose of 600-HPTChC with low biological response to the intestinal barrier is necessary in its application as a drug carrier in humans.

Effect of 600-HPTChC on tight junction in paracellular transport

The use of drug carriers has been investigated to overcome the problem of low bioavailability of drugs in crossing the intestine (Laksitorini et al., 2014). Among pathway of drug transport, paracellular transport is one of the crucial drug delivery pathways focused to improve drug bioavailability, especially delivery of large hydrophilic molecules (proteins and peptides) (Laksitorini et al., 2014). Paracellular pathway is able to transport drugs or large molecules via opening tight junction (Renukuntla et al., 2013). In this study, 600-HPTChC-1 used as a drug carrier was therefore examined its potential effect on enhancing the drug absorption in paracellular transport across the intestinal barrier.

To improve the drug absorption via paracellular permeability, HPTChC has been developed by increasing the molecular weight of chitosan in the synthesis of HPTChC. Results of the present study demonstrated that 600-HPTChC-1 significantly enhanced the tight junction opening at greater degree than 200-HPTChC-1, as evidenced by the levels of TEER decrease and FITC-dextran 4000 transport increase

(Figure 13). This result was consistent with previous report showing that high molecular weight chitosans apparently increased paracellular permeability better than the low molecular weight chitosans (Opanasopit et al., 2007). These findings supported that HPTChC-1 synthesized from chitosan with different molecular weights would have different absorptive enhancing property, in particular tight junction opening effect. It might be anticipated that the higher molecular weight chitosan was, the greater degree of interaction between chitosan and dipalmitoylphosphatidylcholine (DPPC) lipid bilayer could be expected (Fang et al., 2001). Long chain of high molecular weight chitosan (600 kDa) probably interacted with the negatively charged surface of plasma membrane at the higher degree than medium molecular weight chitosan (200 kDa), leading to better enhancing paracellular permeability. Hence, 600-HPTChC-1 was chosen to the further study due to the higher ability on enhancing permeability than 200-HPTChC-1 did.

Chemical modification of chitosan as 600-HPTChC-1 not only increased solubility, but also improved the enhancing permeation effect comparing to chitosan 600 kDa. The maximal enhancing property of modified chitosan on paracellular transport was observed at 0.005% (w/v) from the concentration ranging between 0.005% (w/v) and 0.02% (w/v) (Figure 14). Comparing to chitosan, 600-HPTChC-1 at 0.005% (w/v) was much more decreased the TEER value after immediate exposure (Figure 15a). It was likely that introducing Quat-188 which is a cationic charge on an amino group of chitosan increased its interaction with plasma membrane and tight junction proteins. Previous studies have shown that the cationic polymers such as poly-L-lysine (PLL), polyethylenimine (PEI) and diethylaminoethyl-dextran (DEAE-DEX) enhanced the membrane permeability by interacting with the cell membrane to form nanoscale holes in supported lipid bilayers (Hong et al., 2006). The enhancement of paracellular transport also depended on the polymer structure (Hong et al., 2006; Sadeghi et al., 2008). The branched polymers (PLL) or ring-

containing structure (DEAE-DEX) was much more increased the membrane permeability than the linear polymer such as poly(ethylene glycol) (PEG) and poly(vinyl alcohol) (PVA) due to the capable of cell membrane internalization (Hong et al., 2006). Therefore, it is possible that the branched structure of 600-HPTChC-1 was be better than chitosan 600 kDa in interacting with plasma membrane, leading to rapidly increase in the tight junction permeability.

Since TEER values could not reflect the transport of large molecules, the assessment of macromolecular flux was determined by the diffusion of FITC-dextran 4000 (Shen et al., 2011). In contrast to the TEER results, 600-HPTChC-1 and chitosan 600 kDa had no different effect on FITC-dextran 4000 transport across Caco-2 monolayers (Figure 15b). To describe this differential effect, it is important to mention that measurements of tight junction integrity by TEER and FITC-dextran 4000 diffusion determine the different parameters. TEER reflects the ion permeability of paracellular pathway, while flux of FITC-dextran 4000 demonstrates the wider size of paracellular passage on the diffusion of macromolecule (Srinivasan et al., 2015). Therefore, it is possible that little change in tight junction integrity might allow the ion to move, whereas larger size of FITC-dextran 4000 could not, indicating more sensitive measurement of TEER on paracellular barrier. These findings suggested that the 600-HPTChC-1 rapidly enhanced the transport of small molecule than chitosan; however, there was no difference on transport of macromolecule between 600-HPTChC-1 and chitosan 600 kDa.

In addition to the effect of tight junction opening, a good drug absorptive enhancer should recover its effect without permanent cell damage. Interestingly, the reversible tight junction opening of 600-HPTChC-1 was demonstrated and seemed to shorter than that of chitosan 600 kDa (Figure 16). However, recovery of TEER to reach 100% was observed gradually for 6 h because of the removal impediment of 600-HPTChC-1 that displays the mucoadhesive property. Moreover,

the restoration of tight junction could be explained by the translocation of tight junction proteins (Weber, 2012). Previous study demonstrated that an increase in paracellular permeability resulted in the transient redistribution of ZO-1 and occludin from membrane to cytoskeletal fraction (Smith et al., 2004; Shen, Weber and Turner, 2008). Similarly, 600-HPTChC-1 produced loss of tight junction integrity by delocalization of ZO-1 and occludin. After removal 600-HPTChC-1 for 24 h, the localization of tight junction proteins could be partially recovered (Figure 17). These evidences supported that the reversible of tight junction opening by 600-HPTChC-1 probably resulted from the dynamic behavior of tight junction proteins.

In the molecular mechanism of tight junction opening, regulation of tight junction permeability is mediated by various signaling pathways such as MLCK, PKC and tyrosine kinase (Smith et al., 2005, Hsu et al., 2012, Qasim et al., 2014). However, inhibitors of these signaling cascades did not prevent the effect of 600-HPTChC-1 on tight junction opening (Figures 18a, 18c and 18e). 600-HPTChC-1 mediated tight junction opening did not involve intracellular signaling of MLCK, PKC and tyrosine kinase. In contrast, MLCK signaling partially affected the disassembly of tight junction in chitosan treatment (Figure 18b), whereas signaling of PKC and tyrosine kinase had no effect (Figure 18d and 18e). Based on the results, 600-HPTChC-1 and chitosan might opened tight junction via different mechanism; however, the other molecular mechanisms and also physical pathway related to tight junction opening of 600-HPTChC-1 are further needed to be clarified.

Unlike the intracellular signaling mechanism, the effect of 600-HPTChC-1 on tight junction opening might be explained by mechanical process through physical interaction. Previous studies demonstrated that interaction of peptides on the extracellular domain of occludin induced the modulation on the tight junction permeability (Wong and Gumbiner, 1997; Lacaz-Vieira et al., 1999; Tavelin et al., 2003; Everett et al., 2006). In this study, 600-HPTChC-1 could not permeate into the

cells, and localized in the intercellular space which enacted its direct interaction with tight junction proteins (Figure 19). Moreover, 600-HPTChC-1 contained good mucoadhesive property which could enhance its interaction with proteins at neutral and basic pH (Figure 20c). However, the detail of mechanical mechanism of 600-HPTChC-1 on tight junction opening remained limited and should be further studied using fluorescent live cell imaging and other techniques.

To sum up, molecular weight of chitosan and chemical modification by introducing of Quat-188 to chitosan have influenced on the paracellular permeability. HPTChC-1 synthesized from high molecular weight chitosan (600-HPTChC-1) is more efficient in decreasing of the tight junction integrity than that of low molecular weight chitosan (200-HPTChC-1) and chitosan 600 kD, and enhancing of the paracellular transport of hydrophilic macromolecule (FITC-dextran 4000) across Caco-2 cells than that of low molecular weight chitosan (200-HPTChC-1). Moreover, 600-HPTChC-1 is able to rapidly reverse the tight junction opening effect. Although mechanism(s) underlying the tight junction opening by 600-HPTChC-1 are still needed to further clarify, these results indicated the usefulness of 600-HPTChC-1 as the drug enhancer via paracellular pathway.

Effect of 600-HPTChC on P-gp in transcellular transport

In addition to paracellular pathway, drug bioavailability could be enhanced by alteration of transcellular transport especially by disruption of P-gp function in intestinal barrier. To investigate whether 600-HPTChC-1 can increase drug absorption via transcellular transport, the effect of 600-HPTChC-1 on bi-directional transport of P-gp substrate using [^{3}H]-digoxin across Caco-2 cells was conducted. In this study, verapamil was chosen as the positive control because of its well-known inhibitor effect on P-gp transport (Garrigos, Mir and Orlowski, 1997). 600-HPTChC-1 slightly enhanced the [^{3}H]-digoxin transport from AP to BL and inhibited the transport of the

opposite direction (BL to AP), similar to the effect of verapamil (Figure 21). Therefore, it was likely that 600-HPTChC-1 affected the function of P-gp by reducing the efflux ratio of [^{3}H]-digoxin to the apical side. Although these results were inconsistent with previous reports showing the selective inhibitory effect of α-tocopheryl polyethylene glycol 800 succinate on the efflux of Rho-123 (P-gp substrate) in the BL to AP direction (Rege, Kao and Polli, 2002), 600-HPTChC-1 behaved same property as polyethylene glycol causing both induction of AP to BL and inhibition of BL to AP transport of paclitaxel and doxorubicin (Hugger, Audus and Borchardt, 2002). These results revealed that polymers could differentially behave in inhibition of drug transport via P-gp. However, it is necessary to note that the increase of [^{3}H]-digoxin transport by 600-HPTChC-1 might partially cause by combination effect of both paracellular and transcellular transport, since 600-HPTChC-1 could also act as tight junction opener.

To further investigate the specificity of 600-HPTChC-1 on P-gp inhibition, calcein accumulation assay was performed to detect the efflux ability of P-gp by measuring intracellular converted P-gp substrate (calcein). 600-HPTChC-1 increased the intracellular calcein accumulation in Caco-2 cells in dose-dependent manner, which showed the same effect as verapamil did (Figure 22). This finding was consistent with the previous study on the P-gp inhibitory effect of other synthetic polymers, expected to use in applications of cancer treatment and drug delivery (Martin, 2008). These results demonstrated the existence of the specific inhibitory effect of 600-HPTChC-1 on P-gp function.

The inhibitory effect of 600-HPTChC-1 on P-gp function is likely to be involved with direct interaction of 600-HPTChC-1 and conformation change of P-gp epitope. The immunofluorescent images illustrated the interaction between 600-HPTChC-1 and P-gp in the apical side of Caco-2 monolayer without cell membrane permeation (Figure 23). This result was consistent with previous tight junction study

showing no permeation of 600-HPTChC-1 (Figure 19) or other chitosan derivatives (Tan et al., 2013; Kim, 2014) into the cells. In addition, conformation change of P-gp epitope was confirmed by flow cytometry using FITC-UIC2 antibody. Interaction between 600-HPTChC-1 and P-gp (Figure 24) induced the P-gp conformational change in Caco-2 cells with increasing of the inside P-gp epitope presenting to the cell membrane. However, mechanisms behind the interaction between 600-HPTChC-1 and P-gp resulting in the conformation change of P-gp were needed to be further investigated.

It has been reported that after drug binding to the P-gp ATPase, transmembrane domain of P-gp was able to change the conformational transition (Loo et al., 2012). In general, the catalytic cycle of P-gp function undergoes during drug efflux transport through ATP hydrolysis (Goda et al., 2002). Interestingly, inhibition of P-gp function can occur either by reduction or stimulation of P-gp ATPase in ATP hydrolysis (Sharom et al., 1995; Watanabe et al., 1997). 600-HPTChC-1 stimulated the P-gp ATPase by increase the conversion of ATP to ADP in a recombinant human P-gp membrane fraction (Figure 25). These stimulation effects of 600-HPTChC-1 on P-gp ATPase were similar to the effect of verapamil. In addition, previous reports demonstrated that Inhibition of P-gp via stimulated P-gp ATPase activity of verapamil could mediate through non-competitive binding mechanism with other P-gp substrates for transporting out of P-gp expressed cells (Orlowski et al., 1996). Following the stimulation of P-gp ATPase on drug binding site such as verapamil and rhodamine, the transmembrane domain of P-gp was able to change the conformational transition for drug transport (Loo, Bartlett and Clarke, 2003a; Loo et al., 2003b; Loo et al., 2006). Taken together, it is possible that direct interaction of 600-HPTChC-1 to P-gp resulted in stimulation of ATPase activity and subsequently changed the P-gp conformational transition state.

Given that, 600-HPTChC-1 cannot complete the P-gp membrane binding site like soluble drugs such as verapamil due to the large size. In addition, it has been report that the P-gp inhibition effect of other polymeric materials such as P85, Tween 80, Cremophor EL and TPGS 1000 showed the alteration of membrane fluidity resulting in ATP hydrolysis (Chen et al., 2015). Therefore, it is probably that the steric hindrance of 600-HPTChC-1 might be the important factor that disturbs the plasma membrane and cause eliciting the catalytic cycle of P-gp function.

Furthermore, the effects of 600-HPTChC-1 on the expressions of *MDR1* gene and P-gp protein were also investigated to fulfill P-gp inhibition mechanism both on function and expression level. Some excipients such as Peceol and Gelucire 44/14 have been shown as P-gp inhibitors by decreasing *MDR1* gene and P-gp protein expression (Sachs-Barrable et al., 2007). Thus, mechanistic study on P-gp inhibition could not limit to P-gp activity, but could also focus on the gene and protein expressions. After treatment for 1 day, 600-HPTChC-1 had no effect on the expression of *MDR1* gene and P-gp protein, indicating no involvement of *MDR1* and P-gp protein expression related to the inhibitory effect of 600-HPTChC-1 (Figure 26 and 27). These finding supported that 600-HPTChC-1 has no undesirable effect on molecular level of P-gp inside the cells.

In conclusion, the results of this part indicated that 600-HPTChC-1 could enhance drug bioavailability through P-gp inhibitory mechanism via direct interaction with P-gp, stimulation of P-gp ATPase, and resulted in conformation change of P-gp. These evidences also support the merit of 600-HPTChC-1 in enhancement of transcellular permeability without undesirable effect on molecular level of P-gp inside the cells.

Conclusions

Overall, results of the present study showed the cytotoxicity effect and effects on proliferation and differentiation of 600-HPTChC in non-polarized Caco-2 cells. In addition, the potential effects of 600-HPTChC as an absorptive enhancer via paracellular and transcellular pathways across polarized Caco-2 cells as the intestinal model were demonstrated. All results were concluded as the following:

1. The low degree of substitution and the low concentration of 600-HPTChC caused well biocompatibility to intestinal model rather than high degree of substitution and concentration.

2. The cytotoxic effect of high concentration of 600-HPTChC caused alteration of the mitochondria metabolism and the cell membrane damage.

3. At the non-toxic concentrations, 600-HPTChC-1 was found to inhibit proliferation by cell cycle arrest in the S and G_2/M phases, subsequently delay cell differentiation.

4. The biocompatible concentrations of 600-HPTChC-1 without effects on cytotoxic, proliferative and differentiating inhibition in non-polarized Caco-2 cells were lower than 0.005% (w/v) after long-term continuous (9 days) or short-term discontinuous treatment (4 h/day for 9 day).

5. The differentiated Caco-2 cells were more resistant to the high concentrations of 600-HPTChC-1 than undifferentiated or proliferating Caco-2 cells, leading to the different concentrations use (less than 0.005% and 0.04% (w/v) in undifferentiated and differentiated cells) in exposure.

6. 600-HPTChC-1 had the dual synergistic effects to enhance drug bioavailability on both transcellular and paracellular transport by decreasing the drug efflux via impairing the P-gp function and by increasing drug absorption via reversible opening the tight junction protein.

7. The highly efficient concentration of 600-HPTChC-1 on reversible tight junction opening with non-toxic effect in polarized Caco-2 cells was 0.005% (w/v) in the 4-h treatment.

8. The molecular mechanism of tight junction opening by 600-HPTChC-1 did not mediate through MLCK, PKC and tyrosine kinase signaling, but probably the mechanical process related to the physical property of 600-HPTChC-1.

9. Increasing drug absorption of 600-HPTChC-1 via P-gp inhibition could be explained by its effect on the change of P-gp conformational function after the stimulation of P-gp ATPase, leading to the less drug efflux.

10. The effective concentrations of 600-HPTChC-1 on P-gp inhibition with less than IC_{50} of 1-day treatment in differentiated Caco-2 cells was observed at 0.08% (w/v).

Taken together, our results suggested that 600-HPTChC-1 would be the efficient absorptive enhancer in development of the oral drug delivery system; however, further studies of drug encapsulation and *in vivo* are needed to confirm the usefulness of 600-HPTChC-1 as a drug carrier.

REFERENCES

REFERENCES

1. Anderberg, E.K., Nystrom, C., and Artursson, P. Epithelial transport of drugs in cell culture. VII: Effects of pharmaceutical surfactant excipients and bile acids on transepithelial permeability in monolayers of human intestinal epithelial (Caco-2) cells. Journal of Pharmaceutical Sciences. 1992;81(9):879-87.

2. Artursson, P., Lindmark, T., Davis, S.S., and Illum, L. Effect of chitosan on the permeability of monolayers of intestinal epithelial cells (Caco-2). Pharmaceutical Research. 1994;11(9):1358-61.

3. Bai, X.C., Lu, D., Bai, J., Zheng, H., Ke, Z.Y., Li, X.M., et al. Oxidative stress inhibits osteoblastic differentiation of bone cells by ERK and NF-kappaB. Biochemical and Biophysical Research Communications. 2004;314(1):197-207.

4. Balda, M.S., and Matter, K. Tight junctions at a glance. Journal of Cell Science. 2008;121(22):3677-82.

5. Baldrick, P. The safety of chitosan as a pharmaceutical excipient. Regulatory Toxicology and Pharmacology. 2010;56(3):290-9.

6. Baumert, C., and Hilgeroth, A. Recent advances in the development of P-gp inhibitors. Anti-cancer Agents in Medicinal Chemistry. 2009;9(4):415-36.

7. Behrens, I., and Kissel, T. Do cell culture conditions influence the carrier-mediated transport of peptides in Caco-2 cell monolayers? European Journal of Pharmaceutical Sciences. 2003;19(5):433-42.

8. Benais-Pont, G., Matter, K., and Balda, M.S. Intracellular signaling in classical and new tight junction functions. In M. Cereijido and J. Anderson (eds.), Tight Junctions, pp.367-394. Florida: CRC Press, 2001.

9. Betanzos, A., Javier-Reyna, R., Garcia-Rivera, G., Banuelos, C., Gonzalez-Mariscal, L., Schnoor, M., et al. The EhCPADH112 complex of Entamoeba histolytica interacts with tight junction proteins occludin and claudin-1 to produce epithelial damage. PloS One. 2013;8(6):e65100.

10. Brand, W., Schutte, M.E., Williamson, G., van Zanden, J.J., Cnubben, N.H.P., Groten, J.P., et al. Flavonoid-mediated inhibition of intestinal ABC transporters may affect the oral bioavailability of drugs, food-borne toxic compounds and bioactive ingredients. Biomedicine and Pharmacotherapy. 2006;60(9):508-19.

11. Chae, S.Y., Jang, M.K., and Nah, J.W. Influence of molecular weight on oral absorption of water soluble chitosans. Journal of Controlled Release. 2005;102(2):383-94.

12. Chen, X., Zhang, Y., Yuan, L., Zhang, H., Dai, W., He, B., et al. The P-glycoprotein inhibitory effect and related mechanisms of thiolated chitosan and its S-protected derivative. RSC Advances. 2015;5(126):104228-38.

13. Cilla, A., Lagarda, M.J., Barbera, R., and Romero, F. Polyphenolic profile and antiproliferative activity of bioaccessible fractions of zinc-fortified fruit beverages in human colon cancer cell lines. Nutricion Hospitalaria. 2010;25(4):561-71.

14. Collnot, E.M., Baldes, C., Schaefer, U.F., Edgar, K.J., Wempe, M.F., and Lehr, C.M. Vitamin E TPGS P-glycoprotein inhibition mechanism: influence on conformational flexibility, intracellular ATP levels, and role of time and site of access. Molecular Pharmaceutics. 2010;7(3):642-51.

15. Connell, L.E., and Helfman, D.M. Myosin light chain kinase plays a role in the regulation of epithelial cell survival. Journal of Cell Science. 2006;119(11):2269-81.

16. Deli, M.A. Potential use of tight junction modulators to reversibly open membranous barriers and improve drug delivery. Biochimica et Biophysica Acta (BBA) - Biomembranes. 2009;1788(4):892-910.

17. Dhaliwal, A. Activators and inhibitors in cell biology research. Materials and Methods [Online]. 2013. Available from: http://www.labome.com/method/Activators-and-Inhibitors-in-Cell-Biology-Research.html [2015, April 29]

18. Ding, Q.M., Ko, T.C., and Evers, B.M. Caco-2 intestinal cell differentiation is associated with G1 arrest and suppression of CDK2 and CDK4. The American Journal of Physiology. 1998;275(5 Pt 1):C1193-200.

19. Dodane, V., Amin Khan, M., and Merwin, J.R. Effect of chitosan on epithelial permeability and structure. International Journal of Pharmaceutics. 1999;182(1):21-32.

20. Dunnhaupt, S., Kammona, O., Waldner, C., Kiparissides, C., and Bernkop-Schnurch, A. Nano-carrier systems: Strategies to overcome the mucus gel barrier. European Journal of Pharmaceutics and Biopharmaceutics. 2015;96:447-53.

21. Essodaigui, M., Broxterman, H.J., and Garnier-Suillerot, A. Kinetic analysis of calcein and calcein-acetoxymethylester efflux mediated by the multidrug resistance protein and P-glycoprotein. Biochemistry. 1998;37(8):2243-50.

22. Everett, R.S., Vanhook, M.K., Barozzi, N., Toth, I., and Johnson, L.G. Specific modulation of airway epithelial tight junctions by apical application of an occludin peptide. Molecular Pharmacology. 2006;69(2):492-500.

23. Evers, B.M., Ko, T.C., Li, J., and Thompson, E.A. Cell cycle protein suppression and p21 induction in differentiating Caco-2 cells. The American Journal of Physiology. 1996;271(4 Pt 1):G722-7.

24. Fang, N., Chan, V., Mao, H.Q., and Leong, K.W. Interactions of phospholipid bilayer with chitosan: effect of molecular weight and pH. Biomacromolecules. 2001;2(4):1161-8.

25. Ferruzza, S., Rossi, C., Scarino, M.L., and Sambuy, Y. A protocol for differentiation of human intestinal Caco-2 cells in asymmetric serum-containing medium. Toxicology In Vitro. 2012;26(8):1252-5.

26. Fischer, D., Li, Y., Ahlemeyer, B., Krieglstein, J., and Kissel, T. In vitro cytotoxicity testing of polycations: influence of polymer structure on cell viability and hemolysis. Biomaterials. 2003;24(7):1121-31.

27. Forster, C. Tight junctions and the modulation of barrier function in disease. Histochemistry and Cell Biology. 2008;130(1):55-70.

28. Frohlich, E. The role of surface charge in cellular uptake and cytotoxicity of medical nanoparticles. International Journal of Nanomedicine. 2012;7:5577-91.

29. Fukui, E., Miyamura, N., Uemura, K., and Kobayashi, M. Preparation of enteric coated timed-release press-coated tablets and evaluation of their function by in vitro and in vivo tests for colon targeting. International Journal of Pharmaceutics. 2000;204(1–2):7-15.

30. Garrigos, M., Mir, L.M., and Orlowski, S. Competitive and non-competitive inhibition of the multidrug-resistance-associated P-glycoprotein ATPase--further experimental evidence for a multisite model. European Journal of Biochemistry. 1997;244(2):664-73.

31. Gerard, C., and Goldbeter, A. The balance between cell cycle arrest and cell proliferation: control by the extracellular matrix and by contact inhibition. Interface Focus. 2014;4(3):20130075.

32. Goda, K., Nagy, H., Mechetner, E., Cianfriglia, M., and Szabo G, J.R. Effects of ATP depletion and phosphate analogues on P-glycoprotein conformation in live cells. European Journal of Biochemistry. 2002;269(11):2672-7.

33. Gonçalves, J.E., Ballerini, F.M., Chiann, C., Gai, M.N., De Souza, J., and Storpirtis, S. Effect of pH, mucin and bovine serum on rifampicin permeability through Caco-2 cells. Biopharmaceutics and Drug Disposition. 2012;33(6):316-23.

34. Groschwitz, K.R., and Hogan, S.P. Intestinal barrier function: molecular regulation and disease pathogenesis. The Journal of Allergy and Clinical Immunology. 2009;124(1):3-20.

35. Hamman, J.H., Schultz, C.M., and Kotze, A.F. N-trimethyl chitosan chloride: optimum degree of quaternization for drug absorption enhancement across epithelial cells. Drug Development and Industrial Pharmacy. 2003;29(2):161-72.

36. Hayashi, M., Sakai, T., Hasegawa, Y., Nishikawahara, T., Tomioka, H., Iida, A., et al. Physiological mechanism for enhancement of paracellular drug transport. Journal of Controlled Release. 1999;62(1-2):141-8.

37. Hochman, J., and Artursson, P. Mechanisms of absorption enhancement and tight junction regulation. Journal of Controlled Release. 1994;29(3):253-67.

38. Hoff, F. How to prepare your specimen for immunofluorescence microscopy. [Online]. 2015 Available from : http://www.leica-microsystems.com/science-lab/how-to-prepare-your-specimen-for-immunofluorescence-microscopy/. [2015, April 13].

39. Hong, S., Leroueil, P.R., Janus, E.K., Peters, J.L., Kober, M.M., Islam, M.T., et al. Interaction of polycationic polymers with supported lipid bilayers and cells: nanoscale hole formation and enhanced membrane permeability. Bioconjugate Chemistry. 2006;17(3):728-34.

40. Houde, M., Laprise, P., Jean, D., Blais, M., Asselin, C., and Rivard, N. Intestinal epithelial cell differentiation involves activation of p38 mitogen-activated protein kinase that regulates the homeobox transcription factor CDX2. The Journal of Biological Chemistry. 2001;276(24):21885-94.

41. Hsu, L.W., Lee, P.L., Chen, C.T., Mi, F.L., Juang, J.H., Hwang, S.M., et al. Elucidating the signaling mechanism of an epithelial tight-junction opening induced by chitosan. Biomaterials. 2012;33(26):6254-63.

42. Huang, M., Khor, E., and Lim, L.Y. Uptake and Cytotoxicity of Chitosan Molecules and Nanoparticles: Effects of Molecular Weight and Degree of Deacetylation. Pharmaceutical Research. 2004;21(2):344-53.

43. Hubatsch, I., Ragnarsson, E.G.E., and Artursson, P. Determination of drug permeability and prediction of drug absorption in Caco-2 monolayers. Nature Protocols. 2007;2(9):2111-9.

44. Hugger, E.D., Audus, K.L., and Borchardt, R.T. Effects of Poly(ethylene glycol) on Efflux Transporter Activity in Caco-2 Cell Monolayers. Journal of Pharmaceutical Sciences. 2002;91(9):1980-90.

45. ISO. Biological Evaluation of Medical Devices Part5: Tests for in vitro cytotoxicity, 10993-5:2009. Geneva, Switzerland: International Organization for Standardization; 2009.

46. Jayakumar, R., Reis, R.L., and Mano, J.F. Phosphorous containing chitosan beads for controlledoral drug delivery. Journal of Bioactive and Compatible Polymers. 2006; 21(4):327-340.

47. Joe, A.K., Liu, H., Suzui, M., Vural, M.E., Xiao, D., and Weinstein, I.B. Resveratrol induces growth inhibition, S-phase arrest, apoptosis, and changes in biomarker expression in several human cancer cell lines. Clinical Cancer Research. 2002;8(3):893-903.

48. Kharasch, E.D., Hoffer, C., Whittington, D., and Sheffels, P. Role of P-glycoprotein in the intestinal absorption and clinical effects of morphine. Clinical Pharmacology and Therapeutics. 2003;74(6):543-54.

49. Kim, J.E., Yoon, I.S., Cho, H.J., Kim, D.H., Choi, Y.H., and Kim, D.D. Emulsion-based colloidal nanosystems for oral delivery of doxorubicin: Improved intestinal paracellular absorption and alleviated cardiotoxicity. International Journal of Pharmaceutics. 2014;464(1-2):117-26.

50. Kotze, A.F., Luessen, H.L., de Boer, A.G., Verhoef, J.C., and Junginger, H.E. Chitosan for enhanced intestinal permeability: prospects for derivatives soluble in neutral and basic environments. European Journal of Pharmaceutical Sciences. 1999;7(2):145-51.

51. Kowapradit, J., Opanasopit, P., Ngawhiranpat, T., Apirakaramwong, A., Rojanarata, T., Ruktanonchai, U., et al. Methylated N-(4-N,N-Dimethylaminobenzyl)

Chitosan, a novel chitosan derivative, enhances paracellular permeability across intestinal epithelial cells (Caco-2). AAPS PharmSciTech. 2008;9(4):1143-52.

52. Kowapradit, J., Opanasopit, P., Ngawhirunpat, T., Apirakaramwong, A., Rojanarata, T., Ruktanonchai, U., et al. In vitro permeability enhancement in intestinal epithelial cells (Caco-2) monolayer of water soluble quaternary ammonium chitosan derivatives. AAPS PharmSciTech. 2010;11(2):497-508.

53. Lacaz-Vieira, F., Jaeger, M.M., Farshori, P., and Kachar, B. Small synthetic peptides homologous to segments of the first external loop of occludin impair tight junction resealing. The Journal of Membrane Biology. 1999;168(3):289-97.

54. Laksitorini, M., Prasasty, V.D., Kiptoo, P.K., and Siahaan, T.J. Pathways and progress in improving drug delivery through the intestinal mucosa and blood-brain barriers. Therapeutic Delivery. 2014;5(10):1143-63.

55. Lalles, J.P. Intestinal alkaline phosphatase: multiple biological roles in maintenance of intestinal homeostasis and modulation by diet. Nutrition Reviews. 2010;68(6):323-32.

56. Lin, J.H., and Yamazaki, M. Role of P-glycoprotein in pharmacokinetics: clinical implications. Clinical Pharmacokinetics. 2003;42(1):59-98.

57. Linton, K.J. Structure and function of ABC transporters. Physiology. 2007;22:122-30.

58. Loo, T.W., Bartlett, M.C., and Clarke, D.M. Simultaneous binding of two different drugs in the binding pocket of the human multidrug resistance P-glycoprotein. The Journal of Biological Chemistry. 2003;278(41):39706-10.

59. Loo, T.W., Bartlett, M.C., and Clarke, D.M. Permanent activation of the human P-glycoprotein by covalent modification of a residue in the drug-binding site. The Journal of Biological Chemistry. 2003;278(23):20449-52.

60. Loo, T.W., Bartlett, M.C., and Clarke, D.M. Transmembrane segment 7 of human P-glycoprotein forms part of the drug-binding pocket. The Biochemical Journal. 2006;399(2):351-9.

61. Loo, T.W., Bartlett, M.C., Detty, M.R., and Clarke, D.M. The ATPase activity of the P-glycoprotein drug pump is highly activated when the N-terminal and central regions of the nucleotide-binding domains are linked closely together. The Journal of Biological Chemistry. 2012;287(32):26806-16.

62. Ma, T.Y., Nguyen, D., Bui, V., Nguyen, H., and Hoa, N. Ethanol modulation of intestinal epithelial tight junction barrier. The American Journal of Physiology. 1999;276(4 Pt 1):G965-74.

63. Miller, J.P., Yeh, N., Vidal, A., and Koff, A. Interweaving the cell cycle machinery with cell differentiation. Cell Cycle. 2007;6(23):2932-8.

64. Okawara, M., Tokudome, Y., Todo, H., Sugibayashi, K., and Hashimoto, F. Effect of beta-cyclodextrin derivatives on the diosgenin absorption in Caco-2 cell monolayer and rats. Biological and Pharmaceutical Bulletin. 2014;37(1):54-9.

65. Opanasopit, P., Aumklad, P., Kowapradit, J., Ngawhiranpat, T., Apirakaramwong, A., Rojanarata, T., et al. Effect of salt forms and molecular weight of chitosans on *in vitro* permeability enhancement in intestinal epithelial cells (Caco-2). Pharmaceutical Development and Technology. 2008;12(5):447-55.

66. Orlowski, S., Mir, L.M., Jean Belehradek, J.R., and Garrigos, M. Effects of steroids and verapamil on P-glycoprotein ATPase activity: progesterone, desoxycorticosterone, corticosterone and verapamil are mutually non-exclusive modulators. The Biochemical Journal. 1996;317(Pt 2):515-22.

67. Puliafito, A., Hufnagel, L., Neveu, P., Streichan, S., Sigal, A., Fygenson, D.K., et al. Collective and single cell behavior in epithelial contact inhibition. Proceedings of the National Academy of Sciences of the United States of America. 2012;109(3):739-44.

68. Qasim, M., Rahman, H., Ahmed, R., Oellerich, M., and Asif, A.R. Mycophenolic acid mediated disruption of the intestinal epithelial tight junctions. Experimental Cell Research. 2014;322(2):277-89.

69. Rajesh, K., Papadakis, A.I., Kazimierczak, U., Peidis, P., Wang, S., Ferbeyre, G., et al. eIF2alpha phosphorylation bypasses premature senescence caused by oxidative stress and pro-oxidant antitumor therapies. Aging. 2013;5(12):884-901.

70. Rege, B.D., Kao, J.P., and Polli, J.E. Effects of nonionic surfactants on membrane transporters in Caco-2 cell monolayers. European Journal of Pharmaceutical Sciences. 2002;16(4-5):237-46.

71. Renukuntla, J., Vadlapudi, A.D., Patel, A., Boddu, S.H.S., and Mitra, A.K. Approaches for Enhancing Oral Bioavailability of Peptides and Proteins. International Journal of Pharmaceutics. 2013;447(0):75-93.

72. Riva, R., Ragelle, H., des Rieux, A., Duhem, N., Jérôme, C., and Préat, V. Chitosan and Chitosan Derivatives in Drug Delivery and Tissue Engineering. In R. Jayakumar, M. Prabaharan, R.A.A. Muzzarelli (eds.), Chitosan for Biomaterials II. Advances in Polymer Science. pp. 19-44. Online : Springer Berlin Heidelberg, 2011.

73. Rodrigues, S., Dionisio, M., Lopez, C.R., and Grenha, A. Biocompatibility of chitosan carriers with application in drug delivery. Journal of Functional Biomaterials. 2012;3(3):615-41.

74. Roshan M.M., Young, A., Reinheimer, K., Rayat, J., Dai, L.J., and Warnock, G.L. Dynamic assessment of cell viability, proliferation and migration using real time cell analyzer system (RTCA). Cytotechnology. 2015;67(2):379-86.

75. Sachs-Barrable, K., Thamboo, A., Lee, S.D., and Wasan, K.M. Lipid excipients Peceol and Gelucire 44/14 decrease P-glycoprotein mediated efflux of rhodamine 123 partially due to modifying P-glycoprotein protein expression within Caco-2 cells. Journal of Pharmacy and Pharmaceutical sciences. 2007;10(3):319-31.

76. Sadeghi, A., Dorkoosh, F., Avadi, M., Weinhold, M., Bayat, A,, Delie, F., et al. Permeation enhancer effect of chitosan and chitosan derivatives: Comparison of formulations as soluble polymers and nanoparticulate systems on insulin absorption in Caco-2 cells. European Journal of Pharmaceutics and Biopharmaceutics. 2008;70(1):270-8.

77. Sajomsang, W., Gonil, P., and Tantayanon, S. Antibacterial activity of quaternary ammonium chitosan containing mono or disaccharide moieties: preparation and characterization. International Journal of Biological Macromolecules. 2009;44(5):419-27.

78. Sasaki, N., Baba, N., and Matsuo, M. Cytotoxicity of reactive oxygen species and related agents toward undifferentiated and differentiated rat phenochromocytoma PC12 cells. Biological and Pharmaceutical Bulletin. 2001;24(5):515-9.

79. Schipper, N.G., Varum, K.M., and Artursson, P. Chitosans as absorption enhancers for poorly absorbable drugs. 1: Influence of molecular weight and degree of acetylation on drug transport across human intestinal epithelial (Caco-2) cells. Pharmaceutical research. 1996;13(11):1686-92.

80. Shao, Z., Li, Y., Chermak, T., and Mitra, A.K. Cyclodextrins as mucosal absorption promoters of insulin. II. Effects of beta-cyclodextrin derivatives on alpha-chymotryptic degradation and enteral absorption of insulin in rats. Pharmaceutical Research. 1994;11(8):1174-9.

81. Sharom, F.J., Yu, X., Chu, J.W., and Doige, C.A. Characterization of the ATPase activity of P-glycoprotein from multidrug-resistant Chinese hamster ovary cells. Biochemical Journal. 1995;308(Pt 2):381-90.

82. Shen, L., Black, E.D., Witkowski, E.D., Lencer, W.I., Guerriero, V., Schneeberger, E.E., et al. Myosin light chain phosphorylation regulates barrier function by remodeling tight junction structure. Journal of Cell Science. 2006;119(Pt 10):2095-106.

83. Shen, L., Weber, C.R., and Turner, J.R. The tight junction protein complex undergoes rapid and continuous molecular remodeling at steady state. The Journal of Cell Biology. 2008;181(4):683-95.

84. Shen, L., Weber, C.R., Raleigh, D.R., Yu, D., and Turner, J.R. Tight Junction Pore and Leak Pathways: A Dynamic Duo. Annual Review of Physiology. 2011;73(1):283-309.

85. Shukla, S., Robey, R.W., Bates, S.E., and Ambudkar, S.V. Sunitinib (Sutent, SU11248), a small-molecule receptor tyrosine kinase inhibitor, blocks function of the ATP-binding cassette (ABC) transporters P-glycoprotein (ABCB1) and ABCG2. Drug Metabolism and Disposition: the Biological Fate of Chemicals. 2009;37(2):359-65.

86. Smith, J., Wood, E., and Dornish, M. Effect of chitosan on epithelial cell tight junctions. Pharmaceutical Research. 2004;21(1):43-9.

87. Smith, J.M., Dornish, M., and Wood, E.J. Involvement of protein kinase C in chitosan glutamate-mediated tight junction disruption. Biomaterials. 2005;26(16):3269-76.

88. Snoeck, V., Goddeeris, B., and Cox, E. The role of enterocytes in the intestinal barrier function and antigen uptake. Microbes and Infection. 2005;7(7-8):997-1004.

89. Sonia, T.A., and Sharma, C. Chitosan and Its Derivatives for Drug Delivery Perspective. In R. Jayakumar, M. Prabaharan, R.A.A. Muzzarelli (eds.), Chitosan for Biomaterials I. Advances in Polymer Science. pp. 23-53. Online : Springer Berlin Heidelberg, 2011.

90. Srinivasan, B., Kolli, A.R., Esch, M.B., Abaci, H.E., Shuler, M.L., and Hickman, J.J. TEER measurement techniques for in vitro barrier model systems. Journal of Laboratory Automation. 2015;20(2):107-26.

91. Takano, M., Yumoto, R., and Murakami, T. Expression and function of efflux drug transporters in the intestine. Pharmacology and Therapeutics. 2006;109(1-2):137-61.

92. Takeuchi, H., Thongborisute, J., Matsui, Y., Sugihara, H., Yamamoto, H., and Kawashima, Y. Novel mucoadhesion tests for polymers and polymer-coated particles to design optimal mucoadhesive drug delivery systems. Advanced Drug Delivery Reviews. 2005;57(11):1583-94.

93. Tan, H., Ma, R., Lin, C., Liu, Z., and Tang, T. Quaternized chitosan as an antimicrobial agent: antimicrobial activity, mechanism of action and biomedical applications in orthopedics. International Journal of Molecular Sciences. 2013;14(1):1854-69.

94. Tavelin, S., Hashimoto, K., Malkinson, J., Lazorova, L., Toth, I., and Artursson, P. A new principle for tight junction modulation based on occludin peptides. Molecular Pharmacology. 2003;64(6):1530-40.

95. Thanou, M., Verhoef, J.C., and Junginger, H.E. Chitosan and its derivatives as intestinal absorption enhancers. Advanced Drug Delivery Reviews. 2001;50 Suppl 1:S91-101.

96. Thanou, M.M., Kotze, A.F., Scharringhausen, T., Luessen, H.L., de Boer, A.G., Verhoef, J.C., et al. Effect of degree of quaternization of N-trimethyl chitosan chloride for enhanced transport of hydrophilic compounds across intestinal caco-2 cell monolayers. Journal of Controlled Release. 2000;64(1-3):15-25.

97. Theerawanitchpan, G., Saengkrit, N., Sajomsang, W., Gonil, P., Ruktanonchai, U., Saesoo, S., et al. Chitosan and its quaternized derivative as effective long dsRNA carriers targeting shrimp virus in Spodoptera frugiperda 9 cells. Journal of Biotechnology. 2012;160(3-4):97-104.

98. Thompson, C.M., Fedorov, Y., Brown, D.D., Suh, M., Proctor, D.M., Kuriakose, L., et al. Assessment of Cr(VI)-induced cytotoxicity and genotoxicity using high content analysis. PloS One. 2012;7(8):e42720.

99. Tiyaboonchai, W. Chitosan nanoparticles: a promising system for drug delivery. Naresuan University Journal. 2003;11:51-66.

100. Turner, J.R., Rill, B.K., Carlson, S.L., Carnes, D., Kerner, R., Mrsny, R.J., et al. Physiological regulation of epithelial tight junctions is associated with myosin light-chain phosphorylation. The American Journal of Physiology. 1997;273(4 Pt 1):C1378-85.

101. Ulluwishewa, D., Anderson, R.C., McNabb, W.C., Moughan, P.J., Wells, J.M., and Roy, N.C. Regulation of tight junction permeability by intestinal bacteria and dietary components. The Journal of Nutrition. 2011;141(5):769-76.

102. Vilar, G., Tulla-Puche, J., and Albericio, F. Polymers and drug delivery systems. Current Drug Delivery. 2012;9(4):367-94.

103. Vongchan, P., Wutti-In, Y., Sajomsang, W., Gonil, P., Kothan, S., and Linhardt, R.J. N,N,N-Trimethyl chitosan nanoparticles for the delivery of monoclonal antibodies against hepatocellular carcinoma cells. Carbohydrate Polymers. 2011;85(1):215-20.

104. Watanabe, T., Kokubu, N., Charnick, S.B., Naito, M., Tsuruo, T., and Cohen, D. Interaction of cyclosporin derivatives with the ATPase activity of human P-glycoprotein. British Journal of Pharmacology. 1997;122(2):241-8.

105. Weber, C.R. Dynamic properties of the tight junction barrier. Annals of the New York Academy of Sciences. 2012;1257(1):77-84.

106. Werle, M. Natural and Synthetic Polymers as Inhibitors of Drug Efflux Pumps. Pharmaceutical Research. 2008;25(3):500-11.

107. Wiegand, C., Winter, D., and Hipler, U.C. Molecular-weight-dependent toxic effects of chitosans on the human keratinocyte cell line HaCaT. Skin Pharmacology and Physiology. 2010;23(3):164-70.

108. Wong, V., and Gumbiner, B.M. A synthetic peptide corresponding to the extracellular domain of occludin perturbs the tight junction permeability barrier. The Journal of Cell Biology. 1997;136(2):399-409.

109. Wongwanakul, R., Jianmongkol, S., Gonil, P., Sajomsang, W., Maniratanachote, R., and Aueviriyavit, S. Biocompatibility study of quaternized chitosan on the

proliferation and differentiation of Caco-2 cells as an in vitro model of the intestinal barrier. Journal of Bioactive and Compatible Polymers. 2016:1-16. doi: 10.1177/0883911516658780.

110. Wongwanakul, R., Vardhanabhuti, N., Siripong, P., and Jianmongkol, S. Effects of rhinacanthin-C on function and expression of drug efflux transporters in Caco-2 cells. Fitoterapia. 2013;89:80-5.

111. Xu, X., Hamhouyia, F., Thomas, S.D., Burke, T.J., Girvan, A.C., McGregor, W.G., et al. Inhibition of DNA replication and induction of S phase cell cycle arrest by G-rich oligonucleotides. The Journal of Biological Chemistry. 2001;276(46):43221-30.

112. Yeh, T.H., Hsu, L.W., Tseng, M.T., Lee, P.L., Sonjae, K., Ho, Y.C., et al. Mechanism and consequence of chitosan-mediated reversible epithelial tight junction opening. Biomaterials. 2011;32(26):6164-73.

113. Young, P., Boussadia, O., Halfter, H., Grose, R., Berger, P., Leone, D.P., et al. E-cadherin controls adherens junctions in the epidermis and the renewal of hair follicles. The EMBO journal. 2003;22(21):5723-33.

114. Yu, Q., Wang, Z., Li, P., and Yang, Q. The effect of various absorption enhancers on tight junction in the human intestinal Caco-2 cell line. Drug Development and Industrial Pharmacy. 2013;39(4):587-92.

APPENDICES

APPENDIX A

Characterization of 600-HPTChC

Table 3. The DQ and MW of the different 600-HPTChC preparations derived from chitosan 600 kDa.

Sample	Quat-188[c] (mL)	DQ (%)	F_W[b]
Chitosan 600 kDa	-	-	163.52
600-HPTChC-1[a]	100	65 ± 9	184.97
600-HPTChC-2[a]	125	86 ± 3	230.4
600-HPTChC-3[a]	150	108 ± 2	268.16
600-HPTChC-4[a]	200	124 ± 7	194.48

[a]Started from chitosan with a MW = 600 kDa

[b]F_W is the formula weight of the HPTChC repeating unit

[c]Quat-188 is N-(3-chloro-2-hydroxypropyl) trimethylammonium chloride, used as a quaternizing agent

APPENDIX B

Solubility of chitosan 600 kDa and 600-HPTChC

Table 4. Solubility of chitosan 600 kDa and the derivatives of 600-HPTChC in pH 6.5 and 7.4.

Compounds	Quat-188[b] (mL)	DQ (%)	Maximum soluble concentration (%w/v) at pH 7.4	Solubility at pH (1 %w/v)	
				6.5	7.4
Chitosan 600kDa	-	-	-	Clear	Insoluble
600-HPTChC-1[a]	100	65 ± 9	1.4	Clear	Clear
600-HPTChC-2[a]	125	86 ± 3	4	Clear	Clear
600-HPTChC-3[a]	150	108 ± 2	5	Clear	Clear
600-HPTChC-4[a]	200	124 ± 7	5	Clear	Clear

[a]Started from chitosan with a MW = 600 kDa

[b]Quat-188 is N-(3-chloro-2-hydroxypropyl) trimethylammonium chloride, used as a quaternizing agent.

APPENDIX C

The viability of Caco-2 cells in chitosan 600 kDa and Quat-188

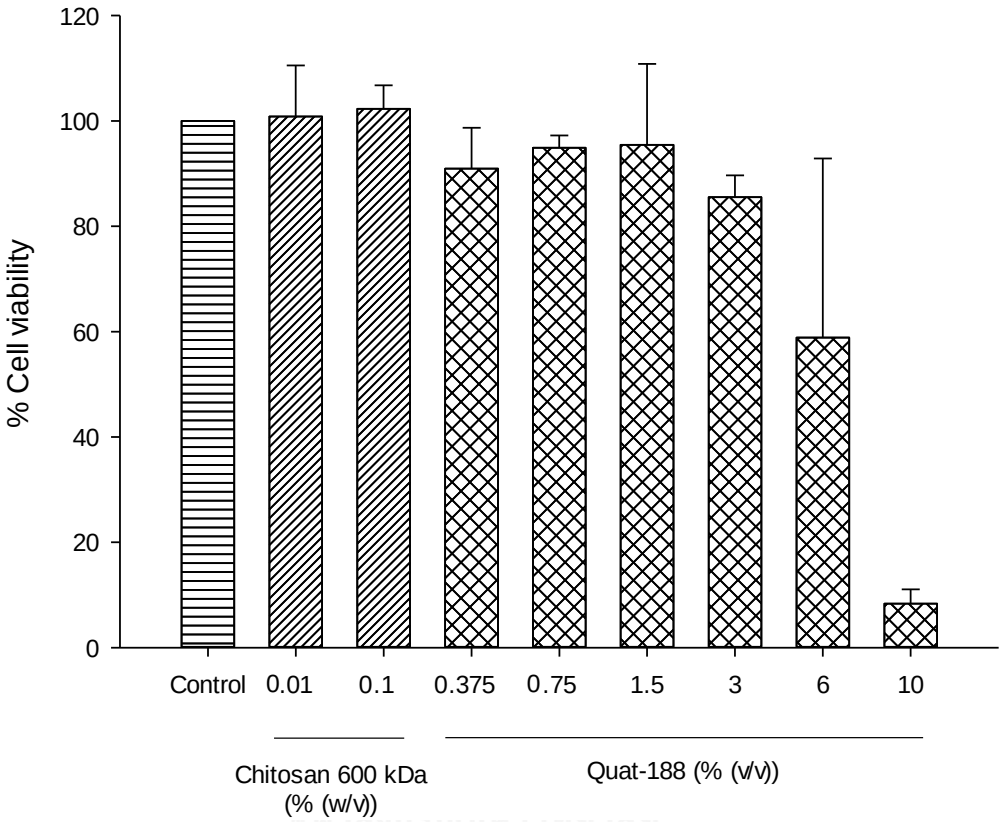

Figure 28. Acute cytotoxicity of chitosan 600 kDa and Quat-188 against Caco-2 cells. Caco-2 cells were exposed to various concentrations of the chitosan 600 kDa or Quat-188 for 4 h and then subject to the MTT assay. The data are expressed as the mean ± SEM (n = 3-6) percentage of viable cells relative to that of the control (100%).

APPENDIX D

The morphology of Caco-2 cells after 600-HPTChC-1 exposure

Culture day	No treatment	Treatment with QCS-1 0.02% (w/v)
Day 6	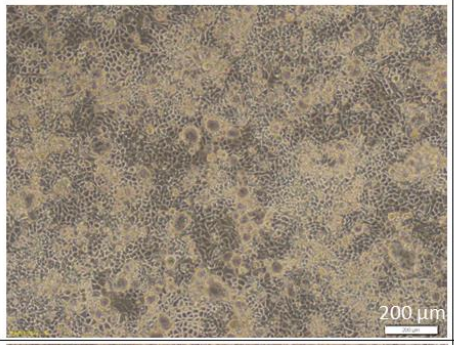	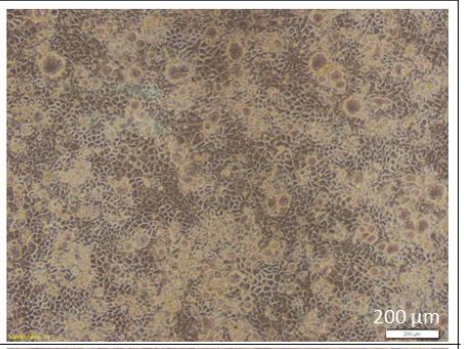
Day 10	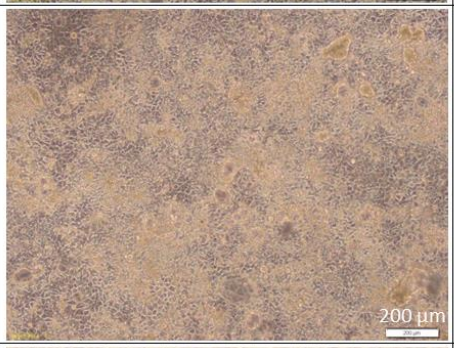	
Day 14	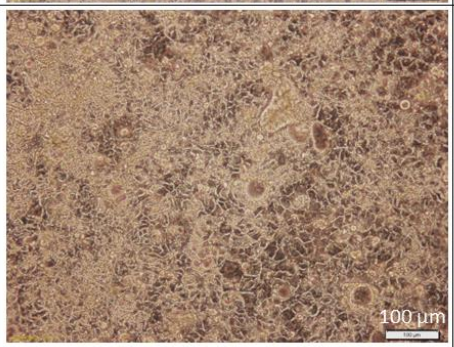	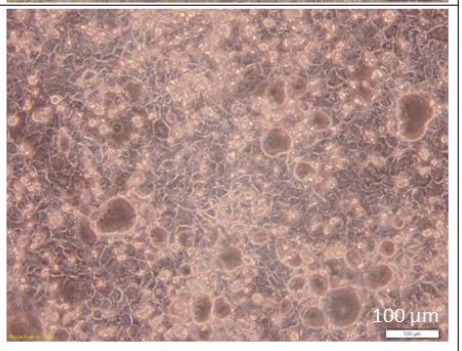

Figure 29. Morphology of Caco-2 cells with or without long-term continuous exposure (over 9 days) of 600-HPTChC-1 0.02% (w/v) from day 6 to day 14.

Culture day	No treatment	Treatment with QCS-1 0.005% (w/v)
Day 6	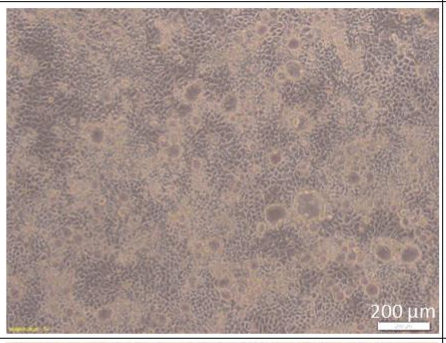	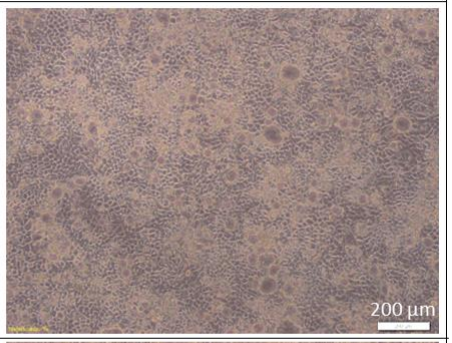
Day 10	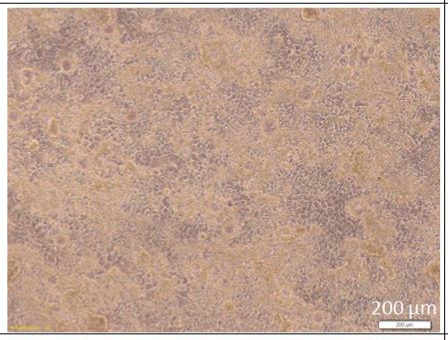	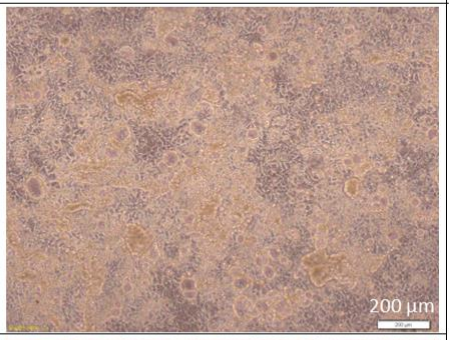
Day 14	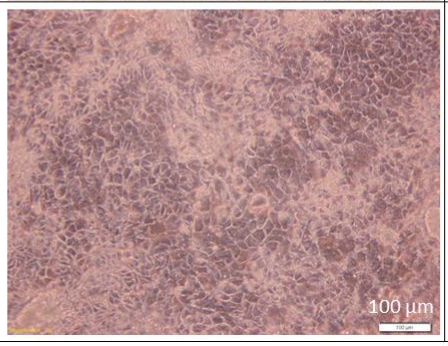	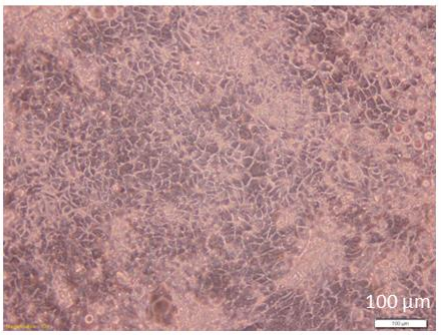

Figure 30. Morphology of Caco-2 cells with or without short-term discontinuous exposure (4 hr/day) of 600-HPTChC-1 at 0.005% (w/v) from day 6 to day 14.

Duration of treatment	No treatment	Treatment with QCS-1 0.005% (w/v)
Short-term discontinuous exposure (4 h/day, over 9 days)	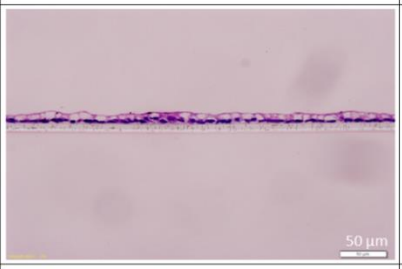	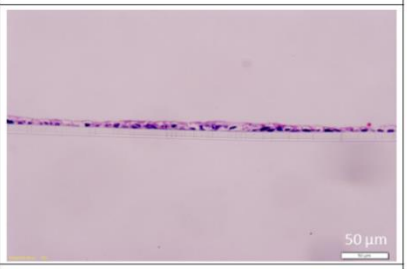
Long-term continuous exposure (over 9 days)	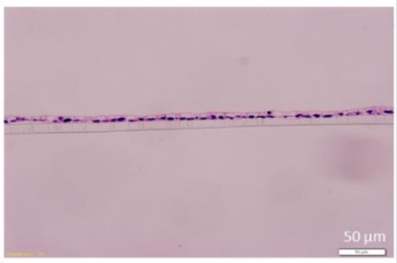	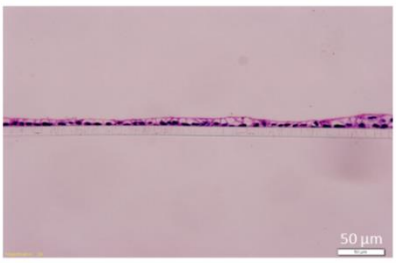

Figure 31. Cross-sectional morphology of 14-day Caco-2 cell culture after treatment with or without 600-HPTChC-1 at 0.005% (w/v).

APPENDIX E

The viability of Caco-2 cells in 200-HPTChC-1 and 600-HPTChC-1

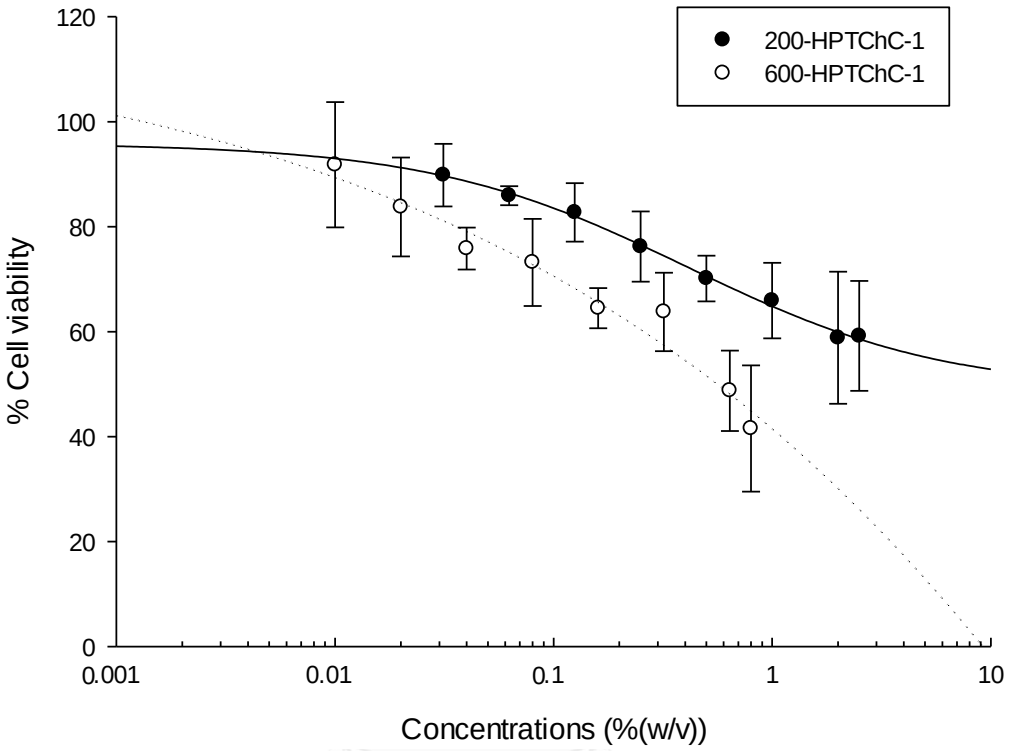

Figure 32. Acute cytotoxicity of 200-HPTChC-1 and 600-HPTChC-1 against differentiated Caco-2 cells. Differentiated Caco-2 cells were exposed to various concentrations of 200-HPTChC-1 or 600-HPTChC-1 for 4 h and then subject to the MTT assay. The data are expressed as the percentage of viable cells relative to that of the control (100%) (Mean ± SEM, n = 4).

APPENDIX F

The viability of Caco-2 cells in 1-day treatment of 600-HPTChC-1

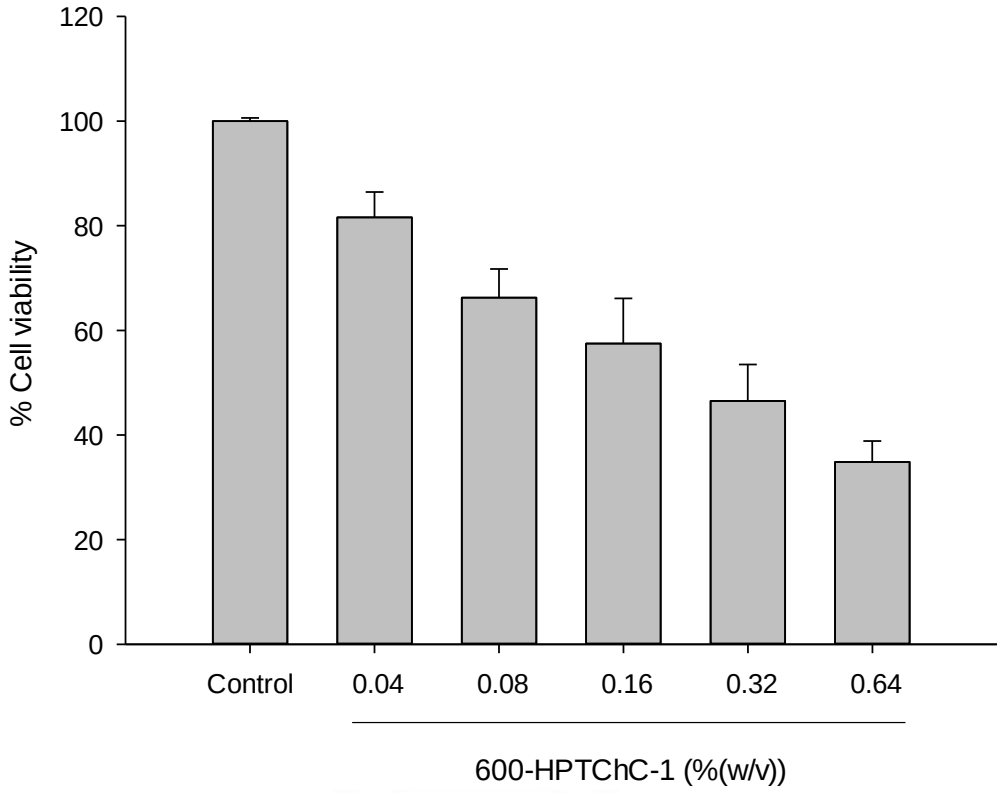

Figure 33. Cytotoxicity of 600-HPTChC-1 against differentiated Caco-2 cells. Differentiated Caco-2 cells were exposed to various concentrations of 600-HPTChC-1 for 1 day and then subject to the MTT assay. The data are expressed as the mean ± SEM (n = 3) percentage of viable cells relative to that of the control (100%).

APPENDIX G

Data of P-gp ATPase activity

Table 5. ATP level expressed as relative light units (RLU) by the basal P-gp ATPase activity in the treatment with sodium vanadate, verapamil or 600-HPTChC-1 (0.02% - 0.32% (w/v)).

	Na_3VO_4 (μM)	Control	Verapamil (μM)	600-HPTChC (%(w/v))				
Conc.		N /A		0.02	0.04	0.08	0.16	0.32
N1	79740	72820	51722	66346	69499	52270	56644	50537
N2	142937	129027	110608	129272	123819	120733	122744	126291
N3	162652	151135	135858	151908	156825	154692	146231	130038
Mean	128443	117660	99396	115842	116714	109232	108539	102289
SEM	25008	23311	24926	25596	25458	30121	26819	25898

Table 6. ATP consumption expressed as change of relative light units (**Δ**RLU) by the basal P-gp ATPase activity in the treatment with verapamil or 600-HPTChC-1 (0.02% - 0.32% (w/v)).

	Control	Verapamil (μM)	600-HPTChC (%(w/v))				
Conc.	N /A		0.02	0.04	0.08	0.16	0.32
N1	6920	28018	13394	10241	27470	23096	29203
N2	13910	32329	13665	19118	22204	20193	16646
N3	11518	26795	10744	5828	7961	16422	32614
Mean	10782	29047	12601	11729	19211	19904	26154
SEM	2051	1679	932	3908	5827	1932	4855

VITA

Miss Ratjika Wongwanakul was born on May 21, 1984 in Bangkok, Thailand. She received her Bachelor's degree in Pharmacy from the Faculty of Pharmacy, Srinakharinwirot University, Bangkok, Thailand in 2008 and Master's degree in Pharmacology from the Faculty of Pharmaceutical Science at Chulalongkorn University in 2011. Then, she entered the Doctor of Philosophy program in Biopharmaceutical Sciences, the Faculty of Pharmaceutical Science at Chulalongkorn University in 2012 and got the educational grant supporting the 3 years PhD study by Thailand Graduate Institute of Science and Technology (TGIST). She also was supported by the research grants from Ratchadaphiseksomphot Endowment Fund of Chulalongkorn University (RES 560530026-AS), the 90th Anniversary of Chulalongkorn University (Ratchadaphiseksomphot Endowment Fund, GCUGR1125582018D) and others joined with NANOTEC.

During her PhD study, she attended and presented a poster twice. Firstly, the poster was presented at the 4th Thailand International Nanotechnology Conference, November 26-28, 2014 at Thailand Science Park, Pathumthani, Thailand in the title "Effects of chitosan Quat-188, quaternized chitosan, on anti-proliferation and intestinal differentiation in Caco-2 cell model". The manuscript from this presentation was published in Journal of Bioactive and Compatible Polymers (2016) in the topic of "Biocompatibility study of quaternized chitosan on the proliferation and differentiation of Caco-2 cells as an in vitro model of the intestinal barrier".

Secondly, the poster was presented at the 5th Thailand International Nanotechnology Conference, November 27-29, 2016 at the Greenery Resort Khao Yai, Nakhon Ratchasima, Thailand in the title "Enhancement of drug bioavailability of quaternized chitosan by dual synergistic mechanism through transcellular and paracellular transport in the intestinal cell monolayer using Caco-2 cell model". At her second attention, she got the honorable student poster presentation award. In addition, she got the overseas research experience scholarship for graduate student of Graduate School and Faculty of Pharmaceutical Science from Chulalongkorn University to have the good opportunity and great research experience for 5 months between Feburary 6, 2016 to June 30 2016 at the Laboratory of Pharmacology and Toxicology, Faculty of Pharmaceutical Sciences, Chiba University, Japan.